ProQuest Number: 10290062

ProQuest 10290062

ProQuest LLC.
789 East Eisenhower Parkway
P.O. Box 1346
Ann Arbor, MI 48106 – 1346

ELECTRO-MECHANICAL WEAR IN OVERHEAD CURRENT

COLLECTION SYSTEMS OF RAILWAYS

Peter Robert Evison

being a thesis submitted to the
Council for National Academic Awards
for the degree of

Master of Philosophy

in collaboration with British Railways Board
Research and Development Divison

Department of Electrical and

Electronic Engineering

Trent Polytechnic

Nottingham   February 1989

ABSTRACT

Electro-mechanical wear in overhead current collection systems of railways

The effect of the increase in line speeds on the overhead current collection system is a matter of concern for British Rail, particularly in terms of the quality of current collection and the wear of both the overhead wire and the carbon collector strips. This project is concerned with an investigation into the wear performance of existing collector materials, by the refinement of an existing wear machine used to simulate railway conditions for the contact materials. The development of a data logger and a high resolution method of measuring copper wear for the wear machine are described, and the results of the contact strip wear tests are presented and discussed. Also included is a survey of the recent developments that have been made in the field of current collection, with particular emphasis on railway practice.

ACKNOWLEDGEMENTS

LIST OF FIGURES

Page

ABBREVIATIONS

APT(P)	Advanced Passenger Train (prototype)
DB	Deutsche Bundesbahn (German Federal Railways)
EMI	Electromagnetic interference
EMU	Electric multiple unit
ICE	Inter City Experimental (German high speed train)
JNR	Japan National Railways
LVDT	Linear variable differential transformer
NWR	Normal Wear Rate
OHLE	Overhead line equipment
PSD	Position sensitive detector
PWR	Prime wear rate
S&E	Schunke and Ebe
SNCF	Societe Nationale de Chemin de Fer Francais
TGV	Train à Grande Vitesse

CHAPTER 1

INTRODUCTION

With the trend in modern railway systems towards low maintenance energy-efficient high speed electric trains, the use of lightweight high voltage overhead line equipment has become widespread. The evolution of such equipment has a long history, and is based upon service experience and field trials. More recently, the application of computer modelling to the design of the system as a whole, namely the OHLE (overhead line equipment) and the pantograph, taking into account the stability of the vehicle and the aerodynamic effects, has played a crucial role in the development of efficient high speed systems.

In contrast, the materials used for the current collection system have seen little development in recent years. Hard drawn solid copper wire, of varying cross-sections, is used almost exclusively world-wide, although research into other wire materials is in progress. The development of new collector materials could involve their selection as a pair as there is obviously some inter-dependence between the wear properties of the contact strip and the contact wire. However, the selection of the overhead wire is also affected by such factors as tensile strength, electrical conductivity, corrosion resistance and cost, and as existing copper wire has a very long lifetime (perhaps 60 years) and would be very expensive to replace, then other than further improvements to the mechanical arrangements of the overhead line equipment, the emphasis is on improving the performance of the collector strips.

British Rail have used a metal impregnated carbon strip, Morganite MY7D grade, since the inception of its 25kV AC overhead system in the mid 1960s, having previously used heavier duty metallic strips on its now non-existent 1500V DC overhead systems. The main requirements of the collector strip are that they should provide reliable current collection whilst being economically efficient, in terms of replacement and labour costs and costs incurred by holding vehicles out of service. To fulfil these requirements they should :

- be lightweight, to reduce the dynamic forces between the pantograph and the wire and thus help maintain contact and reduce wire deflections;

- be mechanically robust, to reduce their susceptibility to shock loads and thereby improve reliability;

- have high electrical and thermal conductivity, to reduce the temperatures on the sliding surfaces and the resultant wear;

- be generally wear resistant with a low coefficient of friction, and should not cause undue wear or erosion of the overhead wire - particularly important as the replacement of the wire is expensive and causes disruption to services.

The collector strips can be regarded as being sacrificial in that they are relatively cheap, and easy to replace. They can be classified as either carbon based or metallic, and because of the predominance of the former, and the fact that they cannot easily be mixed on the same system (both on the laboratory simulator and in the field, for reasons given in sec. 2.2.1), carbon based types only have been tested. Because of the variety of ingredients and the complicated manufacturing techniques involved, for the purposes of this study attention is restricted to the range of commercially available collector strips as supplied via British Rail's

2

Railway Technical Centre at Derby, and by Morganite Electrical Carbon Ltd. These types basically consist of base carbons fired at different temperatures (to give differing degrees of graphicity), and base carbons impregnated with one or more different metals (to improve impact strength and reduce resistivity). Full details of the materials tested are given in Chapter 5 and Appendix A.

The purpose of this thesis is to examine the performance of some existing contact materials using a laboratory simulator (hereafter referred to as a "wear machine"), and to bring together recent work from published material. This review of the literature is presented in Chapter 2, which includes an outline of the historical developments in the overhead system design and the materials used.

The wear of the contact wire is discussed in Chapter 3, and considers in particular oxidational wear.

Extensive testing of MY7D grade carbon strips has already been completed [1,2]. Copper wear rates are of the order of 0.1 to 1.0µm/hr, and with a measurement resolution of several µm, the duration of each test may of necessity be up to several days. As testing is required over a range of speed, current and load (contact force) conditions, the original test program stretched to 2 years in duration. To test the complete range of strip materials listed in appendix A, some improvement is required in the copper measurement resolution in order to enable more numerous but shorter tests to be carried out. Other improvements to the wear machine have been made principally to improve the quality of the simulation and the general safety of operation. The monitoring and recording of the test conditions has also been accomplished by the provision of a data logger. All these developments to the experimental apparatus are described in Chapter 4.

The remainder of the thesis is concerned with the results and discussion, followed by a brief summary.

3

Units of measurement

Wear rates for the collector strips are quoted in terms of "normal wear rate" (NWR), where:

$$(1) \quad NWR = \frac{\text{volume of strip material worn away}}{\text{sliding distance}} \quad mm^3/m$$

For the measurement of copper wear, the "prime wear rate" (PWR) is quoted. This is, in the context of railway operation, the wire worn depth per pantograph pass, or, in the case of the wear machine, worn depth of the disc per contact make.

CHAPTER 2

THE OVERHEAD CURRENT COLLECTION SYSTEM

This chapter outlines the developments in the design of the overhead current collection system and the materials used, and their performance in service.

The use of an overhead wire and pantograph for the transmission of power in railway systems dates back to the turn of the century. Generally speaking, copper was used for the overhead wire, and metal strips mounted on one or more "diamond frame" type pantographs on the vehicle roof collected the current. Early overhead electric railway systems were relatively low voltage, typically 1500V dc (and as a result two pantographs were required to satisfy the heavy current demand), and the line speeds were also fairly low. Current collection with multiple pantograph operation was satisfactory until average train speeds were increased, with a resultant increase in current levels and disturbance of the sliding contacts due to dynamic interaction. This disturbance has the effect of inducing arcing and heavy wear [3]. This was one of the factors that led to the adoption of higher voltage equipment, enabling the less onerous current collection requirement to be provided by a single pantograph.

2.1 SYSTEM COMPONENTS

2.1.1 Overhead line equipment (OHLE)

The gradual evolution of the OHLE or fixed equipment design
has been forced by the requirements of higher speed and
power demands, reduced installation and maintenance costs,
and improved reliability and safety [4,5,6]. The
application of the computer has played an important role in
this development; its use has now spread beyond the
simulation of dynamic behaviour of proposed designs to the
actual detailed planning stages of particular projects
[7,8]. This section gives a brief overview of the
milestones in this development.

Low voltage dc equipment was originally used as this voltage
could be supplied directly to the dc traction motors
connected in series or parallel (or a combination of both).
The current requirements were correspondingly high, with
typical equipment ratings of well over 1000A. This
necessitated the use of expensive heavy-duty OHLE, and
closely spaced feeder stations because of the high
transmission losses.

The limitations of these systems prompted the French railway
administration to experiment with high voltage ac equipment.
The construction and maintenance cost savings together with
the improved energy efficiency, the higher quality of
current collection obtained (measured in terms of the degree
of arcing, wire disturbance and wear rates of strip and
wire), and the potential for the operation of higher powered
trains more than outweighed the increased costs of
insulation, maintaining clearances, and complexity of
locomotive equipment. As a result, in 1956 the 25kV ac
system was adopted by BR as the future standard [4], and
after successful evaluation in service trials was first used
in a major scheme on the West Coast Main Line in the mid

6

1960s. The majority of the equipment installed was of the mark I compound type, originally rated at 145km/h, with the stranded cadmium copper main and auxiliary catenary wires supporting the solid cadmium copper contact wire via vertical droppers. Fig (2.1) shows this and subsequent designs.

The horizontal stagger, necessary to give even wear across the width of the collector strips and prolong their life, was nominally +/- 228mm on straight track. This design was similar to the old low voltage dc equipment. But the high current rating of this type was not really required for use with 25kV, as had been recognised by other European railways where a more cost effective simple OHLE with a single catenary wire had been in use early on. BR subsequently adopted the use of simple OHLE with the addition of pre-sag, where a controlled amount of mid-span sag was allowed so that the compliance profile was more uniform [4,6,9,10], the advantage of this being that the pantograph trajectory is more level.

This mark II equipment, which used hard drawn copper instead of cadmium copper, was first installed in Glasgow in 1966. In subsequent schemes, the catenary wire was changed to aluminium, and later the wire tensions were increased to further improve the dynamic stability of the wire. The wires are auto-tensioned using weights and pulleys except where complex trackwork doesn't allow this. The present mark IIIb equipment represents a considerably cheaper and technically superior design to the mark I type and is rated at 160km/h, or 200km/h when used with a high speed pantograph. The reduced costs have been an important factor in justifying the investment of electrification of routes which may not otherwise have been considered. One potential improvement to the simple OHLE that may yet be introduced by BR is the addition of a stitch wire at the registration arms. This gives a further improvement to the compliance profile, but requires careful setting up.

7

In contrast to modern European practice, JNR use a complex form of damped compound catenary on its 250km/h Shinkansen routes [11]. This was considered necessary because of the use of high speed multiple-pantograph trains - for example a 16 coach formation uses 8 pantographs. Even so, the degree of arcing is frequently excessive, and has been the subject of further alterations to the design.

In France the clean sheet approach to the design of the LGV (Ligne à Grande Vitesse) has meant that the lack of level crossings and the provision of bridges and tunnels with adequate clearances have enabled the use of a constant height contact wire [9,12]. This reduces the required range of the pantograph reach, over which it must maintain a uniform uplift force, from perhaps 2.5m to less than 0.5m, allowing the use of a simplified low-mass design with superior dynamic performance at high speeds. This practice has also been adopted by DB in Germany for the electric Inter City Experimental railway [13], on which a world speed record of 406km/h was recently set up. Both systems use simple stitched equipment, with high wire tension.

There has also recently been a trend towards even higher voltage equipment, notably the 50kV systems used in North America and South Africa [14]. The choice of this higher voltage was probably influenced by the transmission problems due to the lack of reliable power supplies for railways in remote regions.

2.1.2 Pantographs

The "open ended" or "single arm" pantograph for the high voltage, low current systems first appeared in the mid 1950s in France. The main advantage of this type was that it had a lower mass, very important to the dynamic performance of the system. A lower mass design allows the pantograph to

react more quickly to vertical movements in the wire and thus maintain satisfactory contact. Later modifications were the fitting of dampers to reduce resonance effects [11], and the further reductions in the mass, particularly that of the pan head, whilst maintaining sufficient flexual and lateral rigidity. To improve the ability of the pan head to follow any vertical deviations of the wire relative to the vehicle roof, secondary suspension was added between the pan and the main frame. Wind tunnel experiments were used to improve the aerodynamics of the pantograph, to prevent excessive variations of contact force at different speeds and in all possible combinations of wind speed and direction. Also in this respect the layout of all the roof equipment is an important consideration.

British Practice

Three types of 25kV ac pantograph are used by BR. The original was the Stone-Faiveley AMBR mark I, introduced in 1960, which was a modified French design. It used MY7D strips instead of steel. This type was further modified by strengthening the top half of the frame to improve the lateral rigidity, and by fitting secondary suspension to the pan head. It is still in general use in this form. As with virtually all other pantograph types, the pan head is fitted with two parallel collector strips although a short additional strip was added to the centre of the pan on some 112km/h EMU pantographs, giving a much improved strip life [15].

A second type of pantograph used on BR was the GEC "crossed arm" type, now no longer being fitted. This was based upon the diamond frame pantograph, but modified to reduce the amount of vehicle roof space it required [15].

The third and most recent design of BR pantograph is the BR-Brecknell, Willis "Highspeed" [16,17], originally developed for the APT-P from the "Highreach" design. This is now used

9

where running speeds of greater than 160km/h are required. It is an open-ended design of lightweight construction with single box section frame arms, low friction joints, pneumatic suspension for maintaining a constant uplift force (90N +/- 20N) at all wire heights, and torsion bar spring head suspension. Aerofoils are fitted to counteract the asymmetry of the single arm design, to maintain the uplift force steady at all speeds and in both directions of travel. Satisfactory performance under mark IIIb OHLE has been achieved at 250km/h. This type of pantograph is also in use in the USA.

Continental Developments

One of the functions of the pantograph is to provide a nominally constant force for a wide range of wire heights. Although very small variations in relative wire height can be allowed for by the pan head suspension, medium amplitude variations must be taken up by the main frame suspension. As the frame has comparatively high inertia the response time may be inadequate to maintain contact. A solution to this is the two stage pantograph, which is in effect a low mass miniature pantograph mounted on top of a conventional frame [12,18]. The high inertia of the bottom frame is no longer so critical as it is only required to react to the large variations in wire height, such as on the approach to a level crossing or a low bridge, where the wire gradients are gradual. The SNCF uses a two stage pantograph, the AMDE, on the original 270km/h TGV-SE, whereas the new 300km/h TGV-A will use the GPU which is a simple open-ended type with a single plunger secondary suspension supporting the head [19,20]. On the high speed sections of the TGV routes the wire height is nominally constant, making the task of the pantograph less onerous. Elsewhere in France the most common type of pantograph is the AM18 [9,20], based upon the same Faiveley original as BR's Stone-Faiveley units. Steel strips are used almost exclusively by the SNCF (see next section).

10

Other high speed railways, in Italy, Germany and Japan, all had to have new pantographs capable of providing adequate current collection at speed. However there is little published information available on these types. The 250km/h German ICE uses an open-ended pantograph with a stainless steel frame for strength, and other aluminium parts for lightness [21].

2.2 CONTACT MATERIALS

2.2.1 Metal Strips versus Carbons

The materials used for pantograph collector strips can be broadly classified as metal types and carbon-based types. Although the use of carbon for current transfer in electrical rotating machines has become almost universal because of its excellent friction and wear properties, its use as a pantograph collector strip material was limited due to its inferior mechanical strength and current carrying ability relative to the metal strips. It has frequently been recorded that the wear of carbon is principally electrical rather than mechanical, and that wear increases with current (see later). With subsequent improvements in the electrical and mechanical design of the OHLE, and the development of more suitable carbon-based materials, the use of carbon in this application has become widespread.

The two key factors that have brought about this change were the adoption of high voltage (low current) lightweight systems, and the improvement of the strength of the carbons by the addition of various metals. The latter process is carried out by the vacuum impregnation of the carbon with metals in their molten state. The effect of impregnation is to increase the strength (in compression and bending) approximately 3 fold, but at the penalty of increased cost and weight [22,23,24]. Impregnation also gives a large

11

increase in thermal and electrical conductivity, allowing an increased current rating. The increase in the system voltage, 16 fold in the case of BR, provided a corresponding decrease in required current rating for both the strip and the fixed equipment. The reduced current requirement allows the use of cheaper light-weight OHLE, this beneficial mass reduction limiting the dynamic forces experienced by the collector strips.

Where railway administrations have changed over from metal to carbon strips, dramatic improvements in both strip and wire lifetimes have been recorded [20,22,23,25,26,27,28]. Other benefits that have been noted have been the reduction in the emission of electromagnetic interference (EMI)[15,29], and the reduction in arcing in cold weather conditions due to lower adherence of ice to the smoother sliding surface on the wire [3,26]. This smooth wire surface and the accompanying build-up of a carbon film is a vital feature of successful operation with carbons. Where employed, carbon strips should be used exclusively as metal strips disrupt the surface films, and any changeover from metal to carbon should be carried out in as short a time as is feasible. Another factor in favour of carbon strips is that their optimum contact force, in terms of wear performance, is greater than that of metal strips. This is more compatible with the dynamic force variations found in service [23], and as a result better contact is maintained, with less arcing.

Although the continued use by BR of Morganite MY7D, a copper/lead impregnated carbon, has established reliable current collection and very low wire wear, problems did occur when speeds were increased above 160 km/h [17,30,31]. Chipping and cracking of strips due to abnormal shock loads, in particular at neutral sections, occurred during the initial high speed runs associated with the APT development program [30]. The use of a copper coating on the sides of the strips to increase immunity to hard spots has been used in the past, and was in fact recommended by the ORE in 1971

12

[22], following problems experienced by OBB (Austria) and the SNCB (Belgium) with strip cracking and dislocation. This type of strip will suffer a weight penalty though, and may not he suitable for high speed operation. In Britain the problem of impact damage to strips has been tackled by enhancements in the design of the overhead equipment, rather than by any strengthening of the strips, although work is in progress to improve them by the possible use of resilient coatings on the leading faces or by chamfering the leading edge [17]. To help prevent serious damage to the OHLE due to strip break-up, a pneumatically operated automatic dropping device causes the pantograph to be lowered clear of the wire should a strip become dislodged [15].

There are still circumstances where the use of metallic strips is considered more appropriate. In France, the SNCF uses steel strips, sometimes without lubrication, most notably on the 270km/h TGV. However, it is suspected that wire wear rates are relatively high (although this is not officially admitted), and an investigation into the use of carbon strips has been carried out [20]. Carbon has been used successfully on Paris suburban electrical multiple units, with low strip wear rates. The changeover to carbon for the TGV has apparently been deferred as it is believed that satisfactory operation isn't possible until the wire has an adequate flat worn upon it.

In Japan, JNR use sintered iron or sintered copper/iron strips on their Shinkansen routes [32], operating at up to 250km/h. It is reported that high wire and strip wear rates occur [25], and there has been a thorough investigation into the use of alternative materials [32] and lubricants [33,34] to try and reduce these rates. The problems experienced using lubricants with metal strips are that it is difficult to obtain an even supply of lubricant to the wire, and should the lubricant fail heavy wear may result, perhaps increasing by a factor of 10 [35]. Also, the lubricant may attract abrasive particles.

13

More recently, there has been a JNR research program involving a laboratory simulator to compare the wear rates and contact losses at up to 200km/h of the BC16 sintered copper/iron strips, with and without lubricant, and of a carbon strip [36]. Although the carbon wear rates were much lower, it was stated that the impact strength would need to be improved before the materials would be suitable for service use.

The collector strip materials tested in this present work are listed in appendix A, along with their physical properties where known. The selection is restricted to carbon types only as these are the most prominent, and it was considered impractical to mix types on the wear machine. Details of the composition and the manufacturing processes of carbon brush materials can be found in the literature [24,37,38], and specifically for MY7D in Dixon [23].

The fundamental process in the sliding of carbon-graphite materials on copper or other metals is the transfer of a film of graphite, in the form of aligned platelets, onto the surface of the copper on top of any surface layer of metallic oxides that may be present [39,24,40,41,42, 43,44,45]. It has even been reported that the existence of the copper oxide film may aid the formation of a graphite film [46]. The presence of water vapour very much reduces the surface energy of the graphite platelets [47], giving a low shear modulus. The result is a stable, low friction sliding couple with very low metallic wear.

2.2.2 Wear Characteristics in Service

It is known that the wear of both carbon-based and metallic strips is predominantly electrical [15,22,23,28,29,36], as is the case for brush/slip-ring systems [48,49,50]. Ferguson [28] quotes the example of a test with MY7D by BR

14

on a multiple unit train where one pantograph was electrically isolated whilst the other collected current as normal. When the strip on the current carrying pantograph had been worn down by 13mm and was thus life expired, the strip on the isolated pantograph, which had merely been subject to mechanical wear, had only worn down by 2.6mm. Because of this dependence of wear on current, it has been found that the total strip consumption per train is nearly independent of the number of pantographs in use on that train as, with an increased number of pantographs, the current collected per strip decreases in proportion, and therefore the wear of each strip decreases in a similar manner.

Kasperowski [29], who divides the total strip wear into two components, electrical and mechanical, states that the increase in strip wear with current is more than proportional. Arcing contributes significantly to the electrical wear of the strips [51,36,52], and it may be surmised that the combination of heavy currents and high contact losses results in short strip lifetimes. The two principle causes of arcing are poor dynamic performance and adverse weather conditions. Dixon [53] reports that wet conditions cause increased wear, possibly as a result of electrolytic action, and that in winter the icing of the wire and pantograph can induce heavy strip wear due to arcing. Similar seasonal effects have been reported elsewhere [22,29], with strip wear in winter estimated to be double the summer values. The effect of environmental pollution on strip wear has also been observed [3,15,29], in particular where steam locomotives used to operate under the wires. It is also possible that the exhaust fumes from diesel locomotives may also increase the corrosion of the strips (and the contact wire). The best conditions for corrosive attack are the combined presence of atmospheric pollution and water vapour [54]; it is known that the levels of both are significantly higher in winter [55], resulting in increased levels of chemical attack in that season.

The Contact Wire

Unlike strip wear, and slip-ring wear in rotating machines
[48], wire wear rates do not appear to be affected by the
levels of current flow. Evidence from BR for this is
derived from wire wear measurements taken at three features
([3], and a series of more recent measurements as yet
unpublished):

i)   at the approach to neutral sections, where wire wear is
      the same before and after the track magnets (ie the
      point where the vehicle circuit breakers are operated
      to interrupt the current flow);

ii)   on adjoining sections of 25kV and the now defunct
      6.25kV, where currents will differ by a factor of 4,
      there was no increase in wire wear in the low voltage
      sections;

iii) on steep gradients where the currents drawn by climbing
      trains will be much higher than trains travelling down
      grade; there is no significant difference in wire wear
      for the two directions, although some earlier
      measurements for BR by Yang [56] indicate wear
      increased by a factor of 33% to 50% on the up-grade
      wire.

Williamson [57], using BR's push-pull wear simulator (see
sec. 2.3) also concluded that there was no strong
relationship between wire wear and current levels. However,
Kasperowski [29] does report a current dependence in railway
service, although this is based upon a comparison between
the wear of low voltage dc wires and high voltage ac wires,
and if the OHLE and pantograph design and the collector
strip type were not the same for both, then the comparison
is an unfair one. One type of location where heavy current
demand could possibly be the cause of high wire wear is in
station areas [3,56,58]. This may be due to the combination
of heavy current flow and low speed generating higher

surface temperatures on the wire, leading to increased rates of oxidation and softening of the copper. It is known that the lubricating effect of graphite falls off at temperatures above about 500°C.

The use of lightweight equipment will also ease the problems of transient wear at 'hard spots', eg registration arms. This is a very important factor as it is the wear at these locations that effectively determines the lifetime of the whole wire. Oda [36] reports that for JNR the wear rates at hard spots are up to 20nm/pan passage. This is about ten times the typical open-route mid-span values, and reduces the lifetime of the wire on routes where there is very heavy traffic to as little as 1 to 3 years. In Britain where, in contrast to Japan, carbon-based strips are used in conjunction with low mass OHLE, Betts et al [51] estimate that the wear rate at hard spots is only twice the in-span value. They also state that the area of maximum wear is at the approach to a hard spot where there is a clearly defined, highly polished wear band with no evidence of arcing, suggesting that the wear is purely mechanical. Measured in-span wear is typically 2nm/pan passage on BR, not much lower than the Japanese figures for the faster Shinkansen routes of 2.3nm/pan passage quoted by Oda [36], and 5nm/pan passage assumed by Kamiya [59]. However, because the Shinkansen trains are multiple-pantograph, the wear per train passage is considerably higher.

Kinking of the contact wire, usually as a result of the mishandling of the wire on installation, can also promote high local wear. Yang [56] reports that wear at kinks is approximately 80% higher than normal, and also quotes German research which identified kinking as being responsible for 64% of all contact losses.

A new type of contact wire developed by JNR has been tested with promising results [60]. The wire is aluminium with a steel core, and is lighter than its copper equivalent and allows the application of a more controllable degree of sag,

important for even compliance. The wire and strip wear are
significantly lower, with reductions in wire uplift, arcing
and emission of EMI. The explanation given for the lower
disturbance levels in the wire is that its density is 25%
less than an equivalent copper wire. This elevates the wave
propagation velocity giving improved dynamic performance at
high operating speeds.

The use of an aluminium contact wire has also been
investigated in the USA [61], where various strip materials
including carbon based types were tested on hard alloy
aluminium wire in a laboratory simulation. The principle
advantage of the material over copper is stated as being its
lower cost. No results appear to have been published.

2.3 PREVIOUS SIMULATIONS

There have been several investigations of wear in overhead
electric railway systems that have involved laboratory
simulations. Examples of such apparatus found in a search
of the literature are listed below, although in some cases
the available information is very sketchy.

i)   W Cramp, 1936 [62]
      1.4m flanged wheel with helical coil of tensioned wire;
      low operating speed (typically 32km/h); wire wear
      measured by micrometer, strip wear by weighing.

ii)   ORE, 1958 [27]
      Vertical axis machine with strips carried on a rotating
      arm, fixed wire; 160km/h.

iii) M Iwase, 1960 [33,63]
      A rotating 2m ring, vertical axis, onto which wire is
      wound; reciprocating strip; 120km/h.

iv) C Pritchard, 1974 [64]
     Push-pull machine, 15cm sample of straight contact wire
     moved across a stationary strip in a longitudinal back
     and forth manner; low speed ie 1.8km/h; enclosed within
     a perspex environmental chamber; capable of dwell mode
     operation.

v)   ORE, 1976 [58]
     30m section of wire, propelled trolley mounted
     pantograph; used for determining static/starting
     current ratings.

vi) L E Carlson et al, 1981 [61]
     Wire mounted on 5.5m wheel, stationary strips.

vii) O Oda, 1984 [36]
     Pantograph mounted under 2m disc, 50-200km/h, 40-80N,
     0-200A

In addition Morganite Electrical Carbon have developed a
wear simulator, but no published information is available.
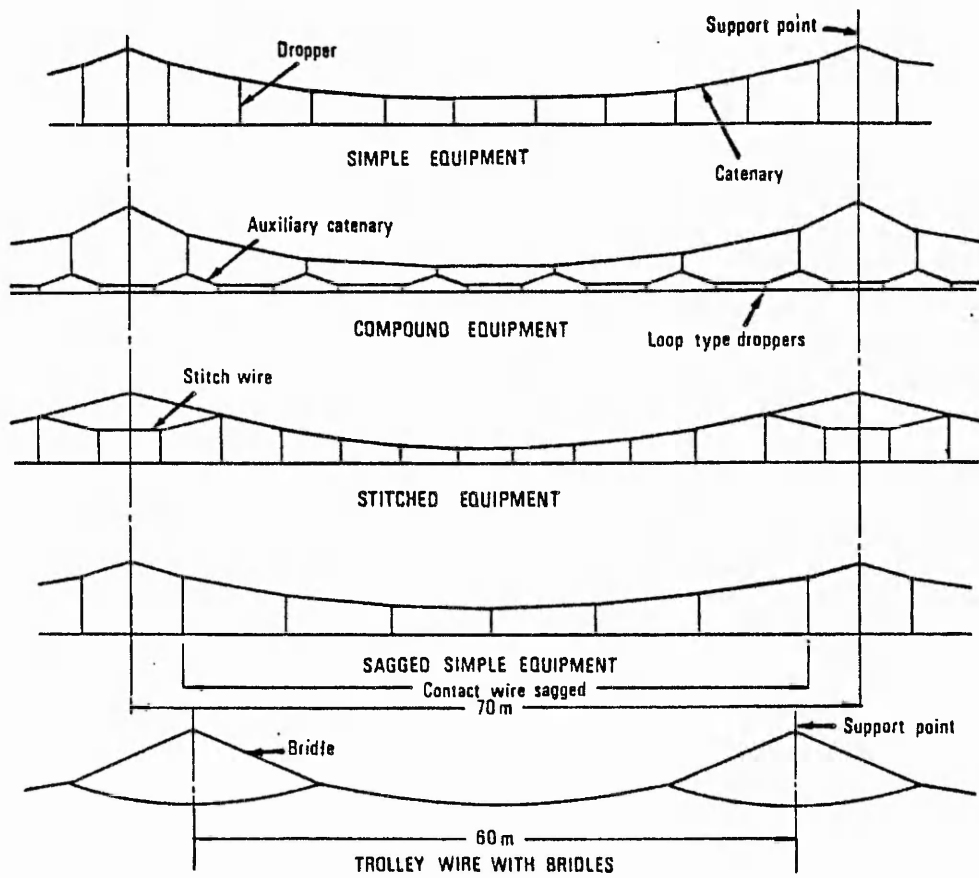
Fig. (2.1) Types of overhead line equipment (OHLE) in use on British Rail

CHAPTER 3

CONTACT WIRE WEAR

The process of sliding wear is highly complex, with several different regimes identified. The principle mechanisms are: abrasive, adhesive, corrosive (including oxidational) and sub-surface fatigue. Unfortunately, from the point of view of analysis and prediction, the wear process is usually an interactive combination of two or more of these, and in the case of the contact wire it is further complicated by the passage of current and exposure to the environment.

A feature of railway current collection that differs from current collection in rotating machines is that there is a relatively long dwell time between passes of the carbon. This type of operation can be simulated by the wear machine and is referred to as "dwell mode", whilst the very short intervals between passes of the brush over the copper, as found in rotating machines, is referred to as operating in the "continuous mode".

It was hoped to determine the dwell mode wear rates for copper with the different collector strip materials using the wear machine, but unfortunately this has not been possible within the time available due to the failure of the taper-roller bearings of the wear machine. Although the bearings were replaced, it was found that the radial lead-out of the new bearings was about 25μm, with a period of 2.33 revolutions (the shaft must rotate 2.33 times for the roller race to complete one revolution). This eccentricity has a serious effect on the accuracy of the disc wear measurements, and increases the instability of the sliding contact at higher speeds. However, although no experimental data was obtained, a discussion of results from earlier work

on wire wear and related matters is included here.

The basis of the original wear model [2] is that the removal of copper takes place in two stages: oxidation of the surface copper, and its subsequent dislocation by the collector strip. Experimental evidence supporting this as the principal wear mechanism is presented by Klapas et al [2] in his fig. 17, reproduced in fig. (3.1), which shows the disc wear rate increasing by approximately 2 orders of magnitude as the dwell time is increased from about 0.07s to 1 minute, after which it levels out. This agrees with railway service experience; a corresponding difference in wear rates is encountered between contact wire wear and the wear of slip rings of a similar duty. If significant oxidation of the copper occurs during this dwell time, it appears likely that oxidational wear is occurring. The first step in an analysis is to examine the nature of the oxide growth.

3.1 THE OXIDATION OF COPPER

There have been numerous studies on the oxidation of copper, and the effect of time and temperature on the rate of oxidation. In an early review, Rönnquist and Fischmeister brought together the results from 17 such investigations [65]. The two principle methods of measurement employed were gravimetric and coulometric; a summary of these and other techniques can be found in Evans [66].

Copper readily oxidizes in air at room temperatures and above. Reaction between copper and oxygen generates a surface film which becomes protective by providing a physical barrier between the copper and the atmosphere, tending to limit further oxidation. The Pilling-Bedworth test [66] states that for oxides with a ratio of oxide volume to volume of metal displaced of greater than one, the

film is protective, whereas if the ratio is less than one the film is discontinuous and areas of fresh metal are still directly exposed to oxygen. The ratio for copper is 1.68. This is not the only requirement for a protective oxide however [67], as the film must also have:

i)   low electrical conductivity or low diffusion coefficient for metal ions (see later)

ii) a high melting point and a low vapour pressure,

iii) a coefficient of expansion approximately the same as that of the base metal,

iv) good adherence,

v)   good high temperature plasticity, to resist fracture,

vi) a Pilling-Bedworth volume ratio of slightly more than unity, not too high in order to avoid compressive stresses in the oxide.

The last four conditions are relevant to the hypothesis of oxide removal, discussed in the next section.

There is general agreement that the electrochemical process of oxidation for copper is as follows. There is a net outward diffusion of copper ions from the base metal through the oxide film due to the ion concentration gradient. Ions at or approaching the interface with the atmosphere combine with the oxygen ions to form fresh oxide on the surface; the reaction occurs near the surface as the relatively heavy oxygen ions do not diffuse readily into the oxide lattice. The outward flux of copper ions therefore determines the rate of oxidation, and the latter is said to be diffusion dependent. As the film grows in thickness the diffusion flux decreases, fewer copper ions reach the surface, and the oxidation rate slows.

23

The collection of experimental results presented by Rönnquist and Fischmeister indicate an initial near linear growth of oxide with time, followed by a transition into a more gradual parabolic rate, as given by:

(3.1) $y^2 = kt + A$ where y = mass of oxide
                                       t = time
                                       k = parabolic rate constant
                                       A = constant

from which: $dy/dt = 0.5k/y$,

ie the oxidation rate is inversely proportional to the film thickness, which supports the theory of ionic diffusion dependence.

It has been suggested elsewhere by Rönnquist [68] that the transition between these rates may coincide with a reduction in the levels of inherent compressive stresses within the oxide due to the formation of stress induced cavities. If the film is highly stressed, the copper ion diffusion rate may be enhanced by the high density of lattice dislocations (this may also be the case with films on abraded surfaces). When de-stressed by the formation of internal voids, the diffusion rate reduces and the oxidation rate becomes parabolic.

Cavities have also been observed between the oxide film and the base copper, although the interface itself is reported by Evans [69] and Rönnquist [68] to be indistinct, with a gradual transition from pure metal to relatively pure oxide. These cavities are thought to be the result of the coalescence of copper ion vacancies that are generated by the outward diffusion flux. This could cause a weakening of the oxide film, especially when there is stressing or flexing of the substrate metal, or temperature cycling. However, Russell et al [70], and Spry and Scherer [45] both state that in the case of copper slip rings, the oxide film is firmly bonded to the base metal. Spry based this

24

conclusion on the fact that there is no change in film thickness when an increasing load is applied to the film.

One final but important observation on the growth and stability of copper oxide films, made by Rönnquist [68], is that films are rarely parallel, especially in the case of films on copper exposed to typical polluted environments. For this reason the quantity of an oxide is normally quoted in terms of the mass per unit area ($\mu g/cm^2$) rather than oxide depth. Factors that can affect local film growth are surface roughness, grain size and orientation, surface contamination, wear damage, and localized heating.

Temperature Dependence

The rate constant k increases exponentially with temperature, as indicated by the diffusion equation [66]:

$$(3.2) \qquad k = k_1 \exp\{-W/RT\}$$

where k_1 is a constant, W is the activation energy for ion migration, R is the gas constant, and T is the temperature in degrees Kelvin. Where there is a temperature gradient across the film, for instance in the case of frictional heating of the surface induced by sliding contact, the effective temperature determining the copper ion diffusion rate will lie between the temperatures on the surface and at the base of the film.

As previously mentioned, voiding may occur within the oxide or at the interface between the oxide and the base copper. This mainly occurs when the oxide temperature is below about 500°C, ie within its brittle range. These cavities, as well as de-stabilizing the film, may obstruct the outward diffusion of copper ions, thus the oxidation rate decreases to a quasi logarithmic rate at these lower temperatures. In contrast, at temperatures above about 800°C the oxide is in its plastic state and there is little tendency for cavities

25

to occur.   Mathematical models predicting the occurrence of
the parabolic (high temperature), and the logarithmic (low
temperature) rates have been developed by Evans [66].

The composition of the oxide film also appears to be
temperature dependent.   Cuprous oxide (Cu_2O) is known to
predominate at temperatures below about 250°C, and above
750°C, whilst in the intermediate range cupric oxide (CuO)
is more likely to be present but only on films thicker than
about 60nm.   Generally, where a layer of CuO does exist, it
usually forms at the surface, overlaying a film of Cu_2O,
although the adherence is said to be poor.   It is rarely
thicker than about 15nm [65,71].

3.1.1 The Oxidation of the Contact Wire

Most of the experimental work on copper is carried out on
carefully cleaned samples in strictly controlled
environments.   In an industrial environment, surface films
have been found to be more complex, containing oxide,
hydroxide, sulphide, sulphate, chloride, nitrate, soot,
dust, oil, water and ammonia compounds [72].   Kasperowski
[29] reports that an examination of the film on the contact
wire revealed brake and ballast dust.   The overall effect of
atmospheric pollution is, in general, to increase the rate
of growth of the film.   Vernon [73] and Shreir [55] report
that the presence together of sulphur dioxide and water
vapour (above a critical level of relative humidity, about
70%) profoundly affect the corrosion of the wire.   In such a
case, the films are very thick and adhere very poorly, and
severe erosion occurs even on the non-sliding surfaces [15].

Kasperowski [29] also describes problems with excessive
electromagnetic interference (EMI) due to film growth.   On
track where traffic is very light, for instance in sidings,
the build up of the film on the wire results in large

26

fluctuations in contact voltage accompanied by EMI. Problems have even been experienced on routes in regular use but where current consumption and speeds were low, despite the fact that the sliding surface of the contact wire appears smooth and polished. Cleaning with steel brushes almost eradicated the EMI initially, but the film soon built up again.

3.2 OXIDATIONAL WEAR MODELS

Most studies of wear concentrate on the cases of rotating or reciprocating components, where in general there is little time for oxidation between passes and other wear mechanisms predominate. In the case of the contact wire, single pass wear is more relevant because of the relatively long dwell times. There are however some cases of multiple pass sliding where oxidational wear is thought to predominate and published work relevant to this is summarized here.

Stott et al [74], and Batchelor et al [75] have produced comprehensive reviews of the literature on the oxidational wear of metals. The latter authors describe and compare the models of Quinn [76] and Wilson et al [77]. Quinn, who considers the mild wear of smooth unlubricated metals, produces the equation for the normal wear rate of a metal disc on a pin and disc machine:

$$(3.3) \qquad NWR = \frac{d \, A_r \, A_p \exp\{-W/RT_0\}}{\varepsilon^2 \, p_0{}^2 \, f^2 \, v} \qquad m^3/m$$

where d = sliding distance at a given asperity contact
A_r = real area of contact
A_p = Arrhenius constant for parabolic oxidation
W = activation energy for parabolic oxidation
R = gas constant

27

T_0 = oxidation temperature

ε = critical film thickness at which detachment occurs

p_0 = average oxide density

v = velocity of sliding

f = mass fraction of oxide which is oxygen

Unfortunately, this equation is not easily tested as it contains too many unknowns, namely the oxidizing temperature and the critical film thickness before rupture, and even W, the activation energy. Quinn and Sullivan [78] present evidence that the effective oxidizing temperature is the contact (or flash) temperature, which is that attained by the asperities during actual sliding contact. Quinn suggests that the wear process starts with an initial period of severe wear as oxide films on the disc are destroyed. This is followed by a mild wear regime, where thick oxide layers build on the asperities only, fracturing at a critical thickness. Once stripped of its oxide covering, the asperity becomes non load bearing. Wilson et al [77] present a similar picture, with severe wear initially, but subdivide the types of asperity contacts into 3 classes:

i)   thick oxide covered asperity against the same

ii) as above but one asperity uncovered

iii) uncovered asperity against the same

Sullivan and Hodgson [79] experimented with dry sliding steel at low velocities (less than 1m/s). They develop an equation for normal wear rate for their pin and disc experiments, similar to Quinn's:

$$(3.4) \qquad \qquad NWR = (k \pi A_r)/(f p_0 v) \quad m^3/m$$

where A_r, f, p_0, and v have the same meanings as in equation (3.3), and k is the oxidational growth constant given in equation (3.2), which will include the temperature dependence. Inspection of both equations shows that the wear rate is predicted to be inversely proportional to sliding speed. This is because the oxide growth on the disc

wear track occurs during the time between passes of the pin, and thus the higher the velocity, the lower the time available for oxide growth and therefore the lower the wear per unit distance of sliding. In the case of the contact wire however, the dwell time is independent of the velocity, and both of these factors would be included in the oxidation rate constant.

Both of these mathematical models are more general than that originally developed for the contact wire by Klapas et al [2]; they make no attempt to define the real area of contact or the effective oxidation temperature. They also refer only to the case of metal to metal sliding with no current flow. With reference to the oxidational wear model for the contact wire mentioned above, an examination of the films existing on the surface of the wire before and after a sliding pass would be helpful.

3.3 THE OXIDATIONAL WEAR OF COPPER

Oxidational wear is known to occur on copper in sliding carbon - copper electric contacts. Spry and Scherer [45] experimented with initially clean slip rings and found that the film gradually increased in thickness over many hours of use, with a current density of 19A/cm^2 and a brush pressure of 0.21kg/cm^2, although the limiting thickness (5 to 35nm) was generally a function of brush grade and polarity. They did however find agreement between the wear of the copper and the expected oxidation rate, using data from other sources, provided the bulk rather than the flash temperature was used in the determination of the latter. They also specify three contact area types, of which the first two are electrically conducting, and the last is load bearing only:

i) major 'a' (carbon-molten copper)
ii) 'a' (carbon-copper)
iii) 'b' (carbon-cuprous oxide)

29

There is other evidence that in the steady state oxidational wear predominates; Failkov et al [80] identified a correlation between the oxidation rate of different copper alloy slip ring materials and the wear rate. The materials with inherently lower rates of oxidation also had lower wear rates. There is therefore evidence of oxidational wear in brush/slip-ring systems.

Lancaster [81] measured a decrease in oxide film thickness with sliding time, though only when current and contact pressure levels were high. He also states that the thickness of the overlying graphite layer increases as the oxide film thickness decreases. The decrease in oxide thickness indicates oxidational wear that is at least transient in nature is occurring.

3.4 THE WEAR OF THE CONTACT WIRE

There are obvious differences between the dynamics and physical characteristics of brush/slip-ring and railway overhead contact systems. In the latter case linear sliding occurs, with fairly frequent contact breaks and a certain amount of flexing of both the wire and the collector strips; also the wire is under high tension (about $10^4 N$). All the components are fully exposed to the environment, often damp in Britain. The current density on a collector strip may frequently exceed $10^6 A/m$, about an order of magnitude greater than brush current densities on large electrical machines. Contact pressures used for railway current collection are greater, with very high transient peaks [29,51]. Dwell times in railway operation are orders of magnitude greater than for a slip-ring, ranging from about two minutes to a few hours, with an overall average of about 17 minutes on the busier routes [82].

The large difference between wear per pass on a slip ring and on a wire must be explained in terms of a combination of some or all of these factors. The experimental evidence obtained in laboratory simulations suggests that dwell time is the most influential parameter [2,57]. With reference to figs. (3.1) and (3.2), after Klapas et al [2], the wear rate increases with dwell mode operation but still falls some way short of railway figures (it is felt that the results after Yang plotted on fig. (3.2) are artificially low due to an over estimation of the density of traffic, 50,000 against about 30,000 quoted by Holmes [82]). The arcing that occurs at contact make/break with dwell mode operation of the wear machine may also have artificially enhanced the disc wear rates; Williamson [57] carried out dwell tests without current and at low speed (1.8km/h) and found a weaker dependence of copper wear on dwell time. However, the wear rates were high, ranging from 0.14nm/pass for a 15s dwell time, to 0.62nm/pass for a 60s dwell time, which are difficult to explain in terms of pure oxidational wear, especially as the test conditions were not likely to induce high surface temperatures. More likely, there is significant oxidation and subsequent oxide removal together with increased abrasion by the oxide wear debris. The contact force used by Williamson was 11.6kg, more than twice that used by Klapas, and could account for the increased abrasion.

It does seem therefore that oxidational wear is the most significant wear mechanism on the contact wire, although from the evidence stated above the effect of dwell time may not be so significant as has previously been suggested. The estimated surface temperatures on the wire that occur at the instant of the passing of a collector strip will result in the generation of a significant quantity of fresh oxide, but subsequent cooling to near average wire temperatures must occur almost immediately [83]. Results from Rönnquist and Fischmeister [65] suggest that the increase in oxide thickness (converted from mass gain by assuming a parallel film) over a period equal to the average dwell time is very

31

much less than 1nm even at temperatures over 100°C, although this is under laboratory conditions. But as the wear rate of the contact wire is typically 2nm per pass, it is difficult to see how the oxidation occurring during the dwell time could account for the very large increase in the wear rate relative to slip ring values.

It may be that the oxidation occurs mainly at the instant of sliding but that the film contains cavities and is brittle, with imperfect adherence, due to the aforementioned environmental factors and the high stressing of the wire. This would result in a moderate increase in oxidation during the dwell time, and more effective removal of the film by successive collector strip passes. Kasperowski [29], who reports on an analysis of these films, states that film removal is very irregular and inconsistent even over short distances. There may also be some abrasive wear of the copper, as copper fragments were noticed in the surface of some of the collector strip samples after use in the wear machine (see next chapter), and Williamson [57] noticed a similar effect with samples used on the push-pull rig.

With reference to the high wire wear rates noticed in station areas, mentioned in section 2.2.2, this may be due to the elevated surface temperatures that occur when heavy starting currents are drawn at low speeds [58]. Accelerated oxidation would result, leading to increased wear.

Wire wear at hard spots may be approximately double typical mid-span values, as noted in section 2.2.2, and coincides with transient increases in the contact force. This high wear is probably due to three factors, all related to the contact force: higher friction induced surface temperatures leading to increased oxidation, more effective oxide removal, and increased wire abrasion. On this basis, and in order to limit the percentage contact losses and collector strip damage to acceptable levels, it would appear that the primary requirement for trouble free current collection is the reduction in the transient levels of contact force.
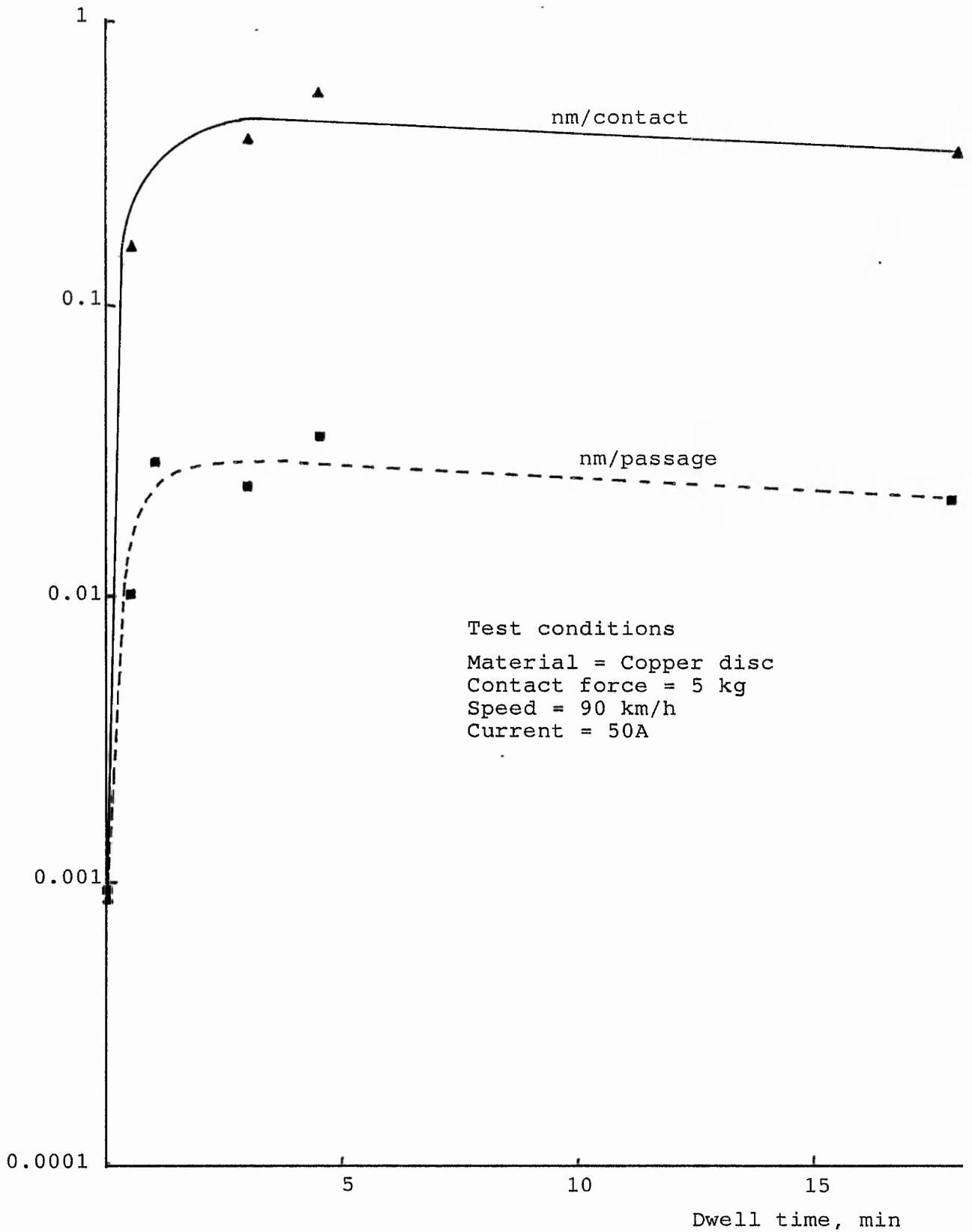
Fig. (3.1)   Worn depth as a function of
              dwell time (disc), after klapas et al [2].
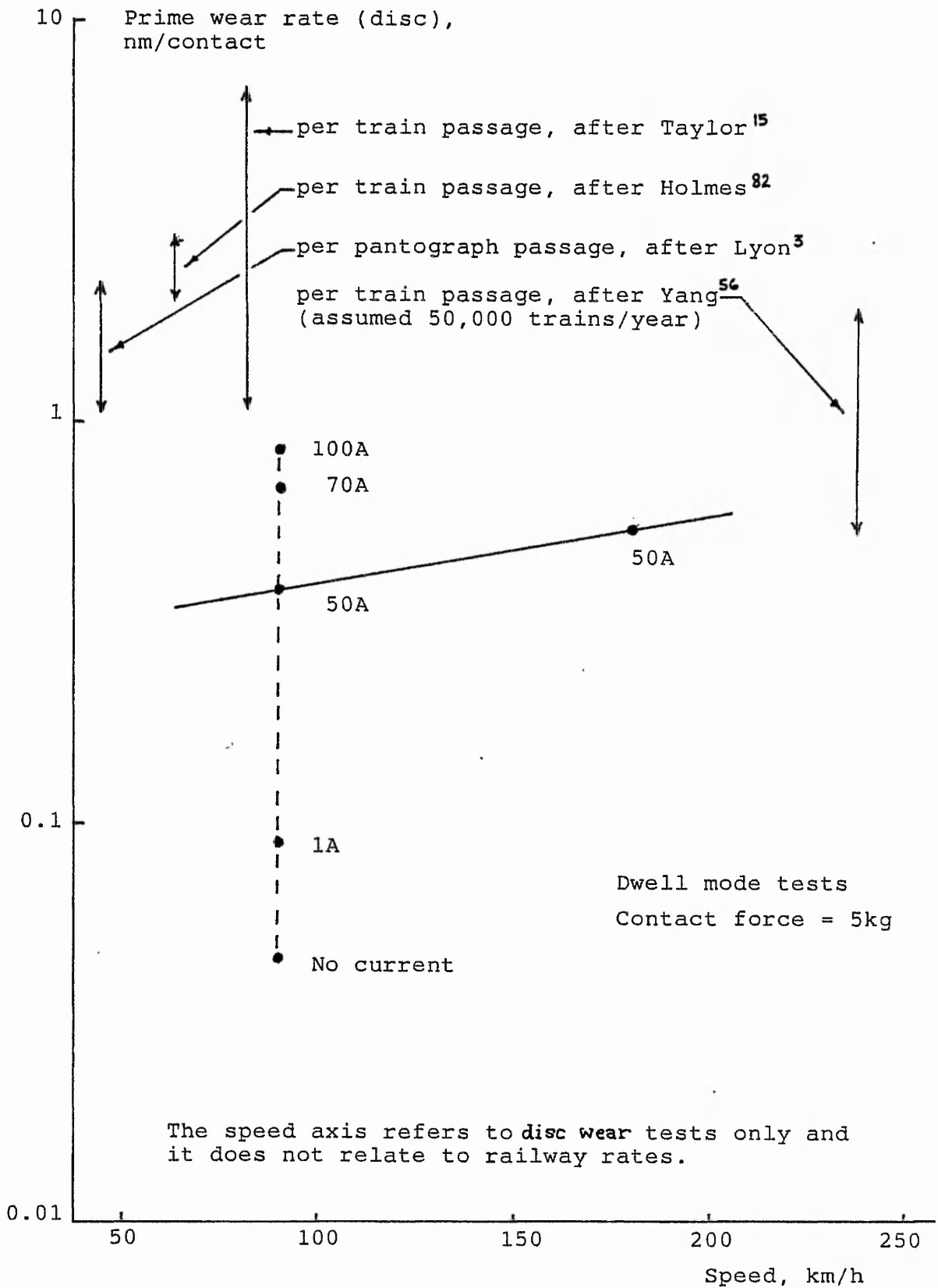
Fig. (3.2)   Comparison of wire wear in railways with disc
             wear in dwell mode tests, after Klapas et al [2].

34

CHAPTER 4

EXPERIMENTAL ARRANGEMENTS

4.1 WEAR MACHINE DESCRIPTION

A full description of the wear machine in its original form can be found in the literature [84]. Figs. (4.1) to (4.3), reproduced from Klapas et al [2], show the basic features. The principle additions to the experimental apparatus have been the data logger and the disc wear measuring system, and these are described later. Other modifications that have been considered or carried out are detailed below.

4.1.1 Dwell mode operation.

An air compressor has been added to power the strip raise/lower mechanism, replacing the N_2 cylinder, to enable longer test durations. A major problem experienced with dwell mode operation is the arcing that occurs when the strip is being raised or lowered. This arcing is undesirable as it alters the test conditions by causing a roughening of the sliding surfaces and the elevation of the surface temperatures. A dashpot damper has been fitted to the strip holder arm to control the lowering of the strip, and this has prevented the bouncing of the strip and arcing that accompanies it. The effect of the damper is shown in figs. (4.4) and (4.5). To eliminate the arcing on contact break, the current is broken remotely by a circuit breaker

immediately before the strip is raised. The period of sliding after the current has been interrupted and before the strip is raised is about 50 ms, see fig. (4.6), which is about one tenth of the total sliding time and is thought to be much less significant, in terms of affecting the sliding conditions, than the arcing that would otherwise occur.

4.1.2 Strip holder arrangement

The maximum operating speed of the simulator is in practice limited by the occurrence of arcing due to the dynamic instabilities of sliding which increase with speed. These instabilities set up resonant vibrations in the strip holder at a series of fixed frequencies unrelated to the disc rotation speed. The strip holder is mounted on linear bearings, which permit strip traversing, below long horizontal arms connected to the machine frame by roller bearings, to permit vertical freedom of motion of the collector strip. Play in these two sets of bearings, together with resonant vibration in the arms, affects the stability of the strip.

The amplitude of the vibrations generally increases with speed, see fig. (4.7), and above 150-180 km/h the arcing is usually at an unacceptably high level. Strip vibrations are known to occur occasionally in railway service, usually with metal strips, and may even lead to the gradual formation of a corrugated wear pattern on the wire [29,85]. Improved design of the pantograph head is said to alleviate the problem.

There is some disagreement over the cause of these vibrations. Bowden and Tabor [86] argue that if the friction-velocity characteristic has a negative slope and the system is underdamped, then there will be an undulation in sliding velocity that will excite resonant vibrations in

36

the mechanical components. This is common at low sliding speeds, eg the stick-slip motion in a squeaking door hinge (this can be cured by lubrication which modifies the friction-velocity characteristic so that it has a positive slope). Shobert [50] however believes that the mode of vibration may not necessarily be in a plane parallel to the direction of sliding but is, more likely, normal to it, ie parallel to the brush axis. The brush reaction force may under certain conditions have a component acting against the direction of motion resulting in a "digging in" effect giving an undulating contact force. A solution to this is to design the brush holder so that it provides a trailing angle, ie the brush is inclined in a trailing direction [37,43,87,88,89].

Pedelty [48] believes that in the case of chatter in a brush/slip-ring system, running without current and thus with a low brush temperature may lead to high friction and frictional vibration. It may also lead to the "glazing" of the slip ring surface, ie the build up of a high resistance film. Passage of current across the sliding surface may provide a lubricating effect due to softening and melting at the asperities [29,35], accompanied by a decrease in copper wear [1,57] and friction [40]. Although the melting point of copper is 1083°C, softening occurs at down to a third of this value. A similar effect has also been noticed in the case of the sliding of metals without current where the wear rate has been known to *decrease* with an increase in speed, probably due to a melt lubrication process [79]. Lancaster and others have also noticed that the friction coefficient falls with current [40], and it has been proposed that this is due to either a reduction in shear strength, or a decrease in real contact area.

The passage of current can also improve the stability of sliding at high speeds on the wear machine. This is believed to be as a result of the reduction in the friction force due to micromelting or melt lubrication. Stable sliding can be achieved at 250km/h provided the current is

37

greater than about 100A and the traversing speed is low. High temperatures due to current constriction and frictional heating are generated resulting in a thermal bulge in the region where the density of 'a' spots (conducting asperities, see Holm [90]) is highest, leading to an even higher density and increased temperatures as the contact is confined to region of the bulge. This phenomenon is visible as a small region on the sliding surface of the strip, perhaps 2 to 3mm across, glowing red or yellow hot for a few seconds until it oxidizes and burns out, and a new contact region emerges elsewhere. The strip wear is very high under these circumstances. As stated, the traversing speed must be slow so that the thermal mound on the strip surface has time to develop; such a condition is not relevant to railway operation, except at very low train speeds where the traversing of the wire is slow. The phenomenon of brush thermal instability is also described by Williamson and Allen [91] though without mentioning a thermal bulge, and Marshall [92], whilst Chen and Burton [93] report that the height of thermal asperities can exceed by several times the initial roughness. Dow and Stockwell [94] also describe the phenomenon in mechanical systems, where friction is the sole source of heating. Barber et al [95] have detected these hot spots, or thermoelastic instabilities, on railway wheel treads where tread brakes are used.

Efforts were made to reduce the vibrations by placing resilient materials (various grades of synthetic rubber) and damping materials (lead sheet) under the strip or strip holder, and by altering the strip holder position so that the strip was effectively trailing by 12°, but were unsuccessful. Studies of the mechanics of brush holders indicate that a low mass strip holder would be required for vibration free running, with the contact force supplied by a spring rather than by dead-weights [50,96,97]. Cramp also experienced similar problems, and reduced the mass of his contact holder from 32kg down to 5kg to cure it [62]. To fit spring suspension to the contact holder would have meant major alterations to the wear machine so it was decided

instead to limit the maximum speed used for tests to 150 km/h, although higher speeds could be used on high current tests.

4.2 COPPER DISC WEAR MEASUREMENT

The major difficulty in measuring the wear on the copper disc is to obtain adequate resolution of measurement. This is necessary because the copper wear rates are relatively low, compared with the collector strip wear, therefore this resolution determines the test duration. Because of the large number of tests required to evaluate the performance of different collector strip samples over a range of sliding conditions, it is important that the test duration should be minimized. Assuming infinite copper wear resolution, a minimum test period is required to ensure that steady state conditions have occurred for a sufficient proportion of the test to dominate any initial transient effect in the calculation of the average wear from the "before and after" displacement measurements. Thus it is estimated that the ideal test duration should be of the order of one day. Based upon earlier copper wear measurements [2] this would require wear resolution to better than 1μm.

Several methods of measuring disc wear in situ were evaluated by Klapas et al [2]. These mostly involved making differential measurements between a point or small area on the sliding surface, and an adjacent location on a non-sliding surface or shoulder. Fig. (4.8) illustrates how this shoulder has been machined on the disc periphery. The capacitive method involved detecting the change in displacement for the sliding surface and the reference shoulder by measuring the capacitance between a fixed curved electrode and the disc surfaces. This arrangement suffered from poor repeatability due to thermal influences and other long term stability problems. A technique employing a pair

of "linear variable differential transformer" (LVDT) displacement transducers producing a differential measurement between the sliding surface and the reference shoulder at 4 equally spaced positions around the disc also suffered from poor repeatability, mainly due to sensitivity to imprecise relocation of the probe styli.

Consequently, the indentation method was chosen by Klapas. This involves making a spherical indentation in the sliding surface with a depth of approximately 50μm, and measuring the diameter of the indentation before and after the wear test using a travelling microscope, then calculating the worn depth.

In the present work three methods of copper wear measurement have been examined:

> 1. Indentation method
> 2. Optical lever technique
> 3. A dual LVDT multiple sampling system

4.2.1 Disc Wear Measurement : Indentation Method

The use of indenters is common practise in the measurement of material hardness. The Vickers hardness test uses a diamond pyramid which is slowly pressed onto the surface with a preset force. The Brinell hardness is determined in a similar way, but uses a spherical steel indenter. In both cases, the hardness is found from the indentation size, measured using a travelling microscope.

For the wear measurement application, the use of a spherical indentation is the most practical as it allows high gain, ie ratio of measured change in diameter to worn depth, and dimensionally accurate indenters of differing sizes are easily and cheaply produced by embedding a ball-bearing in

40

the end face of a punch.

The accuracy and resolution of the average worn depth measurement are generally determined by the following factors:

(a)   Distortion of the geometry of the indentation.   When the indentation is made by hitting the indenter, there is displacement of the material by plastic and elastic deformation.   When the indenter recoils after the impact, there is a limited amount of elastic relaxation resulting in an indentation of larger diameter than the indenter [90]. The plastic deformation pushes some material upward to form a ridge around the rim of the indentation.   This ridge is worn away after a few hours of sliding.   However, it may result in the formation of a lip extending over the edges of the indentation, making the measurement of the width, and therefore the worn depth, less precise.   This may be exacerbated by arcing damage around the periphery.   Fig. (4.9) shows a typical indentation where, although the reproduction quality is poor, the distortion and erosion of the edges due to sliding is visible.   With for example a 3.175mm ball bearing indenting to a depth of approximately 50μm, giving an initial indentation width of 0.5mm, if a decrease in width of 25μm (1 thou) could be detected this would imply a depth measurement resolution of 4μm.   The depth of the indentation should be shallow enough to give a large change in indentation width for a small worn depth, though not so shallow that the edges become indistinct.

(b)   There must be a limited number of indentations to make the method manageable, and to prevent interference with the tribological conditions.   As a result, a worn depth measurement may represent only localized values.   To obtain an average measure of the worn depth over the whole sliding surface, the wear test must be of long duration to reduce inaccuracies due to localized undulations in the wear rates.

Taking all these factors into account, it is estimated that

41

the resolution of wear measurement using the indentation
method is of the order of 2 to 3µm, based upon the
assumption that the diameter of the indentation could be
measured to a resolution of 12.5µm, determined by making
repeated measurements on an unworn indentation.

A possible method of improving the accuracy of the
indentation method is to record a video image of the
indentation with a video camera and use image processing
techniques to estimate the diameter, or to estimate the
change in diameter by superimposing images taken before and
after a wear test. These techniques were not followed up
because of the difficulties in obtaining accurate close-up
images (the magnification of each image must be highly
consistent) and in developing suitable image processing
hardware and software.

4.2.2 Disc Wear Measurement : Optical Lever Method

The principle of operation of this technique is shown in
fig. (4.10). A laser beam is directed onto the sliding
surface of the disc and is reflected onto a position
sensitive detector (PSD). From the diagram it can be seen
that any displacement of the sliding surface will give an
amplified deflection of the reflected beam incident on the
PSD. To compensate for the thermal expansion of the disc
(which would also cause the deflection of the reflected
beam) a reference beam is required. This would run parallel
to the working beam but would be reflected by the non-
wearing shoulder, and received by a second PSD adjacent to
the original device. Focusing lenses were required on both
incident and reflected beams to counteract the beam
divergence; each lens is common to both working and
reference beams.

A single channel prototype system, with no reference beam, was constructed using a 2mW He-Ne laser and a Hamamatsu S1543 PSD, see figs (4.11) and (4.12). The analogue signal processing circuitry, fig. (4.13), was based upon that suggested by Hamamatsu, and employs low offset drift op-amps. The principle of operation of the PSD is shown in fig. (4.14). With the reflected spot on the centre of the device, ie at x=0, the generated photocurrent I_0 divides equally to give $I_1 = I_2 = I_0/2$. If the spot moves a certain distance towards one terminal, the current out of that terminal increases proportionally (with a corresponding decrease in current from the other terminal), as shown on the graph. Given that the graph is nominally linear, of the form y=mx+c:

therefore: $I_1 = (-I_0/2L)x + I_0/2$

and using: $I_0 = I_1 + I_2$,

(4.1) $x/L = (I_2 - I_1)/(I_1 + I_2)$ - valid for $-L \leq x \leq L$

The arithmetic operation in equation (4.1) is carried out in the analogue circuitry using adding and subtracting amplifiers together with an analogue divider, and the output voltage V_0 is proportional to the off centre deflection of the reflected beam, x/L.

The main advantage of this system of in-situ wear measurement is that it allows continuous monitoring of the worn depth throughout the test. However, it suffered from lack of accuracy. A prototype single beam arrangement indicated a short term resolution of approximately 5μm, with a deterioration over longer term tests. A careful study indicated a number of sources of noise and drift, and these are dealt with in turn below:

(a) The variation in scatter from non-tangential surface undulations causes a random shifting of the reflected beam and therefore a false indication of surface displacement. This is caused by surface damage due to arcing and other surface irregularities visible through the microscope. With the disc rotating, the displacement signal varies at high frequencies about a correct mean level, though the limited frequency response of the PSD (quoted rise time 4μs) can give rise to a loss of resolution. The static resolution of the PSDs is quoted as 0.2μm for a 200μm spot size.

(b) The analogue signal processing circuitry has displayed two weaknesses, both as a result of variations in the total photocurrent I_0. I_0 is proportional to the reflectivity of the disc surface, laser output assumed constant, and has been shown to vary over an order of magnitude. Fig.(4.15) indicates the variation of reflectivity around the disc. High frequency noise on I_1 and I_2 can be reduced using matched low drift low pass filters. Firstly, all the amplifiers operate at unity gain, as set by 1% high stability resistors; any deviation from true unity gain will give rise to a noise output signal if the average photocurrent (I_0) varies. The worst case error with an order of magnitude variation in I_0 is equivalent to 50μm. This rise can be reduced by using a preselected combination of gain setting resistors.

Secondly, the analogue divider output doesn't stay constant (as it ideally should) when the average photocurrent I_0 is varied, with x_A constant. This non-linearity gives an effective output error from the divider of approximately 5μm. Fig.(4.16) shows the noise on the output, equivalent to a change of about 13μm in the disc radius, from a simulated input varying over an order of magnitude in amplitude (this type of input was used to enable the setting up of the analogue divider to be optimized). An alternative is to use

44

analogue to digital conversion of the $-I_1$ and $-I_2$ signals, and then carry out the division operation in equation (4.1) digitally. Assuming a constant photocurrent, 1µm resolution would require 11-bit accuracy. In practise this would need to be greater due to variation in the photocurrent. A method of improving the resolution of A to D conversion is to use multiple sampling/averaging [98]. The dual slope integration analogue-to-digital converter would be best suited to this application, as the integration period could be matched to a discrete number of disc rotations to eliminate noise due to periodic variations in reflectivity around the disc. However, long term variations in reflectivity would still affect the measurement resolution.

(c) Noise due to vibration and movement of the optical components relative to the disc. The movement is caused by the components not being sufficiently rigidly mounted, and by the thermal expansion of the materials involved. The error due to these effects can be reduced using a twin beam system where the additional beam uses the non-wearing shoulder of the disc as a reflecting surface and therefore acts as a reference; the difference in displacement being the worn depth. Any movement that is not equally applied to both the working beam and the reference beam will give an error in the in the worn depth measurement.

(d) Noise due to disc eccentricity. The eccentricity takes two forms. Firstly, there is a variation in the radius of the disc, which is typically 15µm. Using the two beam system, it is the difference in the radii of the reference shoulder and the sliding surfaces that are relevant, and this has been measured at 9µm using LVDT displacement transducers. The resultant noise signal is periodic with the disc rotation and low pass filtering of the PSD output signal will reduce this. The second type of eccentricity is due to the movement

45

of the axis of the disc relative to the machine frame and to the optical system. This is more complex in nature, the eccentricity having basic periods of 1 and 2.33 revolutions of the disc due to the characteristics of the roller bearings. Although there is no relative displacement of the sliding surface with respect to the reference surface, the absolute displacements cause errors due to the non linearity of the PSDs. This eccentricity is at present about 25μm peak-to-peak.

(e) Error due to the non-linearity of the PSD output characteristics. This is quoted as ±15μm to ±60μm. As this is a constant error, it may be reduced by separate calibration of both working and reference systems.

The effects of short term drift on the single channel system are shown for the disc both stationary (fig.4.17) and rotating (fig.4.18). These pen recordings plot the change in disc radius due to disc temperature variations, obtained from the strip LVDT and the optical system. Note that the vertical scales (estimated in the case of the optical system) are slightly dissimilar. Because of the short duration of these tests, it is assumed that there is negligible disc and strip wear in the test with the rotating disc.

In conclusion, the problems of the poor quality of beam reflection and the long term stability due to even microscopic movements of the optical components cast doubt over the feasibility of an economical and practically realizable system, and it was decided to look for an alternative method. This particular optical system may be better suited to determining an absolute displacement without the requirement of intermediate beam reflection.

4.2.3 Disc Wear Measurement : LVDT Multiple Sampling Method

With this method the worn depth is determined by measuring the height of the sliding surface above the adjacent reference shoulder before and after the wear test. The decrease in this height represents the depth worn away. The main improvement over the indentation method is that, instead of taking measurements at only four equally spaced positions around the disc, the sampling is carried out at several hundred locations. This provides a more accurate assessment of the wear all around the disc. In addition, because the apparatus in more compact and mechanically stable, it does not suffer as badly from the drift problems that afflicted the optical method. To produce a practical and consistent system, the operation is carried out automatically under the control of a BBC microcomputer, which controls the retraction and release of the LVDTs, the stepping of the disc and the logging of the measurement data. This data is analysed using additional software. Particular care was taken with the design of the LVDT signal processing circuits, to minimize noise and drift.

A prototype twin LVDT system was constructed and tested with one LVDT on the sliding surface, the other on the reference shoulder. The main improvements carried out after trials were in the mechanical arrangements. The LVDT styli are retracted to prevent damage to the copper surface and to avoid any non-axial forces on the LVDT styli and linear bearings. The original retraction mechanism was a solenoid but this was found to be too vigorous in its action. This was replaced by a servo motor driven rack and pinion system, with integral limit switches for pausing and motor reversal, see fig. (4.19). The mounting of the LVDTs must be very precise and steady in terms of position relative to disc. Any movement of these components relative to each other during a wear test will lead to errors. A slight drift in the recorded displacement difference signal is predominantly

47

due to temperature changes and is predictable; however, the mounting of the LVDTs was improved by replacing the traversing bed (originally used for disc machining purposes) with a set of fixed spacers. Fig. (4.20) shows the complete assembly in position on the wear machine, and fig. (4.21) shows the disc stepping mechanism. Another problem that was identified was that dust particles on the copper surface were causing false displacement readings. This was cured by blowing filtered air onto the disc surface before the styli were released by the retraction mechanism. In addition, both the copper surface and the styli were carefully cleaned beforehand with a soft clean cloth dampened with methylated spirit. During an actual wear test, the probe holder stays in place, only the styli are retracted clear of the disc, and the whole assembly is covered with cling-film to protect it from carbon dust. Originally , T shaped cylindrical LVDT styli were fitted to provide a line contact across the wear track, but due to difficulties in alignment, these were changed to a 3mm diameter spherical type, giving a point contact along the centre of the wear track.

Care was taken in designing the signal processing electronics to minimize the unwanted introduction of noise and drift. The two LVDT signals are fed via separate pre-amplifiers to a 2-way analogue switch followed by a common amplifier, demodulator and active filter so that any drift in these latter stages will affect both channels equally and thus cancel. OP07 and OP27 op-amps were used throughout for their low offset drift, and the overall drift introduced by the electronics was found to be negligible. Fig. (4.22) shows the circuit diagram, whilst the complete unit is depicted in fig. (4.23). The signal is then fed to the BBC's internal analogue-to-digital converter for sampling. The recorded displacement and temperature signals for each disc position are the average of 16 samples; this gives an improvement in resolution by a factor of 1/4 [98].

The entire system is under software control via the BBC's User Port to enable automatic operation. A set of

measurements for one disc revolution takes about one hour, and to further improve the resolution of the wear measurement, this is repeated for 4 or 5 complete disc revolutions. In practise the resolution is limited by the linearity and repeatability of the LVDTs, and the roughness of the copper surface. The LVDTs were calibrated in a jig and checked in situ by altering the temperature of the disc, whose radius varies by 4.5μm/deg.C, see fig. (4.24). Long term drift tests, with the styli resting undisturbed on the disc, have been carried out lasting several days and over a wide range of ambient temperatures. The results of one such test of 14 days duration are shown in fig. (4.25). Although this indicates a worst case error, for a constant temperature, of ˜0.65μm (or greater, as each plotted point was averaged over 100 samples), the error over the shorter duration of a typical wear test is expected to be less. In practice, the ambient temperature can be adjusted so that it is the same for the measurements taken both before and after a wear test. The estimated temperature error on the difference signal varies from -0.3μm/°C at around 16°C to +0.3μm/°C at around 21°C.

The drift of the signal processing electronics was tested using a high stability resistor network to simulate an LVDT input, and the ambient temperature within the equipment case was varied between 29 and 36°C over a 24 hour period. The worst case drift on the difference signal at single temperature was equivalent to 0.03μm, or 0.074μm over the complete temperature range. This indicates that the drift introduced by these circuits can be neglected.

An estimated overall wear measurement resolution of better than ± 2μm has been obtained. Fig. (4.26) shows a before and after profile for a wear test of 15 hours duration. The traces represent the surface-shoulder difference before (top trace) and after (bottom trace) the wear test, the difference between the traces thus representing the worn depth of copper for that test. In this example the average worn depth was 9.9μm, which compares with 6.4 and 8.9μm measured at two positions on the sliding surface using the old indentation method.

4.3 THE DATA LOGGER

The original series of strip wear tests were carried out with only the strip temperature and wear measurements being recorded, using a 2 channel pen recorder. To permit a more detailed analysis of the strip performance, it was decided to construct a data logger capable of recording analogue signals from additional sources [99].

It was decided to base an 8 channel data logger upon a micro-computer in order to provide a cost-effective and flexible system. Used in conjunction with a multi-pen X-Y plotter, it is possible to log the data, carry out any necessary signal processing and statistical calculations, plot each signal, and save the data to disc for a permanent record. A BBC Master microcomputer was chosen because of the ease of use of its I/O facilities.

4.3.1 Recorded Parameters

The data logger is required to record and display the following signals:

1. Wear machine frame temperature - this signal is derived from an LM35DZ semiconductor temperature sensor, and is used for the temperature compensation of the strip displacement signal.

2. Cooling water temperature - also uses an LM35DZ sensor. positioned within the output flow pipe. This signal provides the disc temperature information, and is also used for temperature compensation.

3. Carbon strip temperature - a type K thermocouple housed in a steel probe inserted into a hole in the carbon. The amplified output signal is relative to ambient temperature.

4. Drive motor load - this is a dc signal proportional to

the drive motor armature current, and provides an indication of the friction force between the carbon strip and the copper disc.

5. Strip displacement - an LVDT is in contact with the base of the strip holder, and after corrections (carried out in the software) to allow for the differential thermal expansion of the disc and the steel frame, the change in displacement is a measure of the wear of the strip only. This is because the disc wear is comparatively insignificant.

6. Arc light emission - a photodiode is mounted facing the trailing edge of the strip to give an indication of the presence of arcing.

7. Contact voltage - a secondary brush in contact with the side of the disc is used to obtain the voltage drop between the strip and the disc. This signal is fed to a high voltage isolating amplifier. A precision rectifier and filter are included to enable ac voltages to be recorded, as well as dc.

An eighth spare channel is available, in addition to the 4 channel analogue inputs that the BBC provides, to allow future expansion of the equipment.

The interfacing circuitry between the transducers and the BBC is contained in a single unit shown in fig. (4.27). See fig.(4.28) for the block diagram. The transducer signals are brought in on 2-core screened leads and are fed to the signal conditioning circuits, comprising instrumentation amplifiers and filters. Once the required input ranges of the measured parameters were decided upon, the amplifier gains were set to produce an output signal range of between 0 and 2.5V, the input range of the analogue-to-digital-converter (ADC). The filtering provides transient protection as well as 50Hz interference reduction. The multiplexer, under software control, selects each channel in

51

turn, passing the selected signal via a low pass filter to the ADC for sampling. The filter is an active 2-pole Bessel type, selected for its fast settling time, allowing faster sequential cycling through all the channels.

For the ADC, the successive approximation and the dual-slope integration types were considered. The latter has excellent noise rejection, as the integration time can be set so that it is equal to (or is a multiple of) the period of the interfering signal eg mains pick-up. However, the ZN448, an 8-bit successive approximation device, was chosen for its low conversion time ($9\mu s$) and its low cost. By using the 1MHz bus and an assembly language routine, sampling rates up to 16k samples/sec are possible. An 8-bit device was chosen as a compromise between optimum resolution, sampling speed and economy of disc storage space. Each sample is stored as a single 8-bit byte. The control section is based upon a decoder which produces the ADC and multiplexer control signals by decoding the addresses generated by the software.

In the continuous sliding mode, multiple sampling/averaging takes place continuously, with an averaged value for each channel stored, for example, every second. The data is also written to the screen after appropriate scaling.

In the dwell mode the carbon strip is only sliding on the disc for 0.4s , and is lifted clear for one minute during the intervening periods. The data logger is triggered by the passage of current operating a reed switch, so that sampling is carried out for the duration of the contact only. The ADC samples at its maximum rate, with only a single average value for each channel being recorded.

After completion of the test, the data may be retrieved off the disc, scaled as required, and then plotted using the X-Y recorder. Fig.(4.29) shows a typical plot for a continuous sliding test, some channels omitted for clarity. The strip wear rate can be calculated from the slope of the average strip displacement.

52
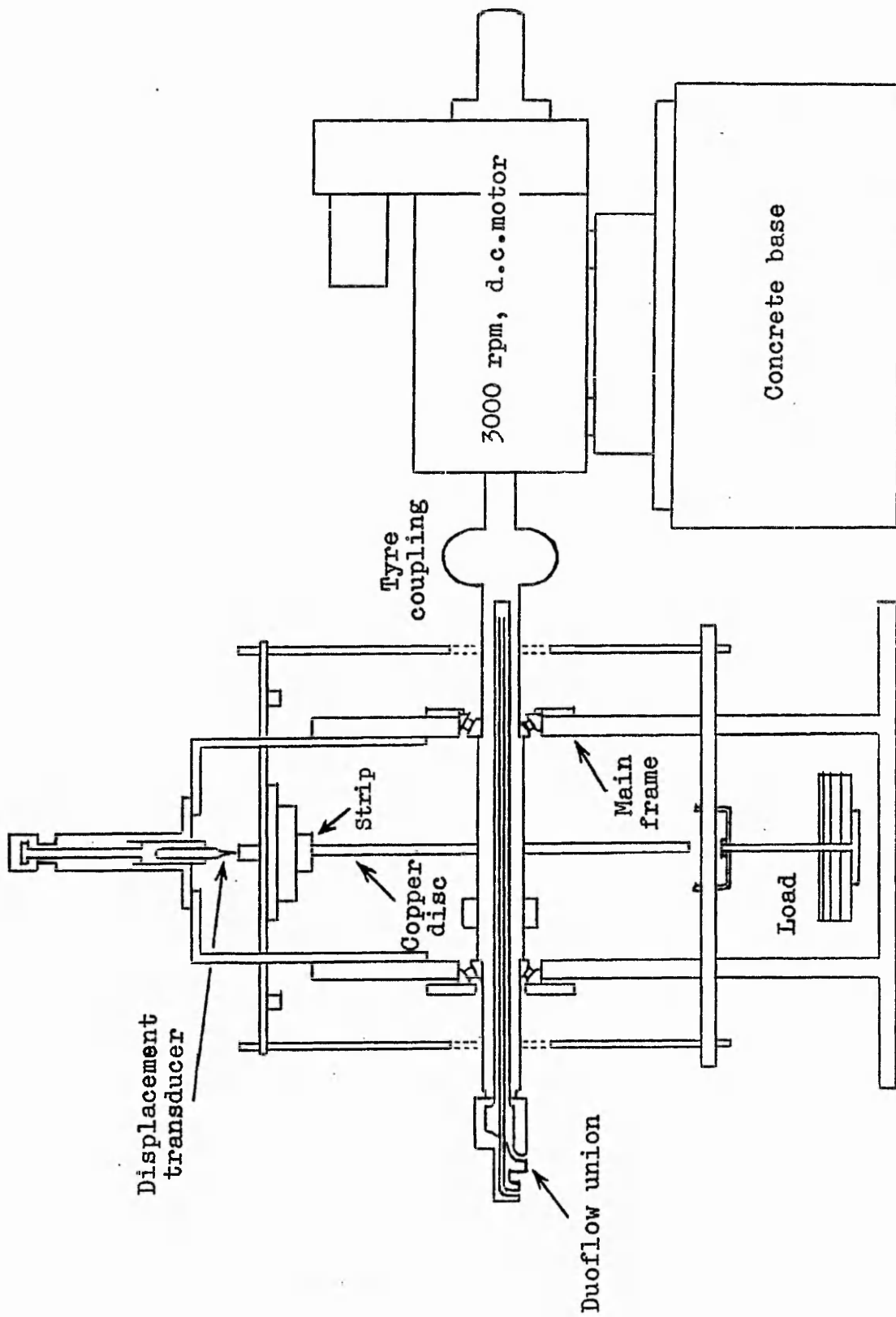
Fig. (4.1) Wear machine: front view (2)
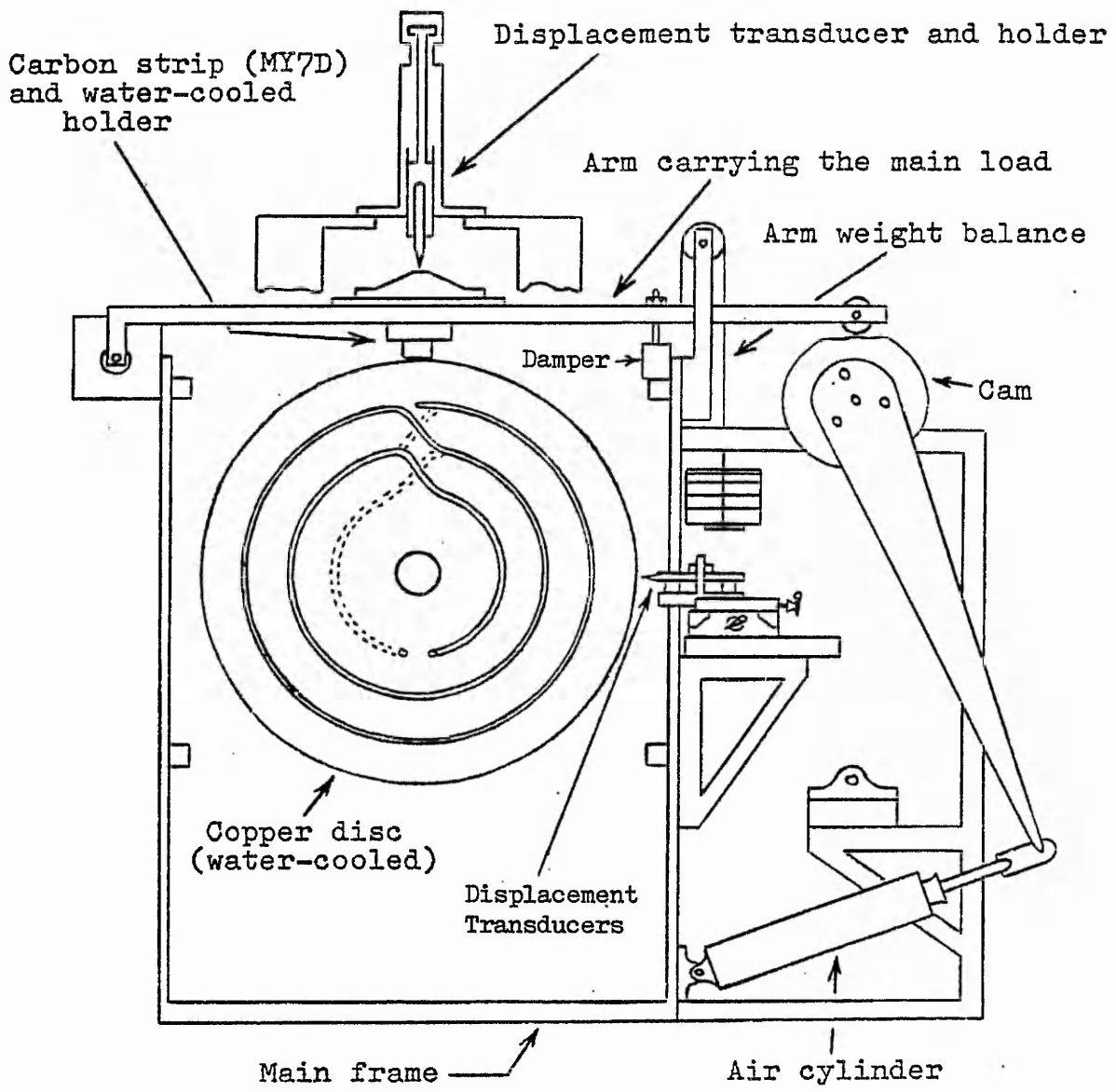
Fig. (4.2)   Wear machine: side view (2)
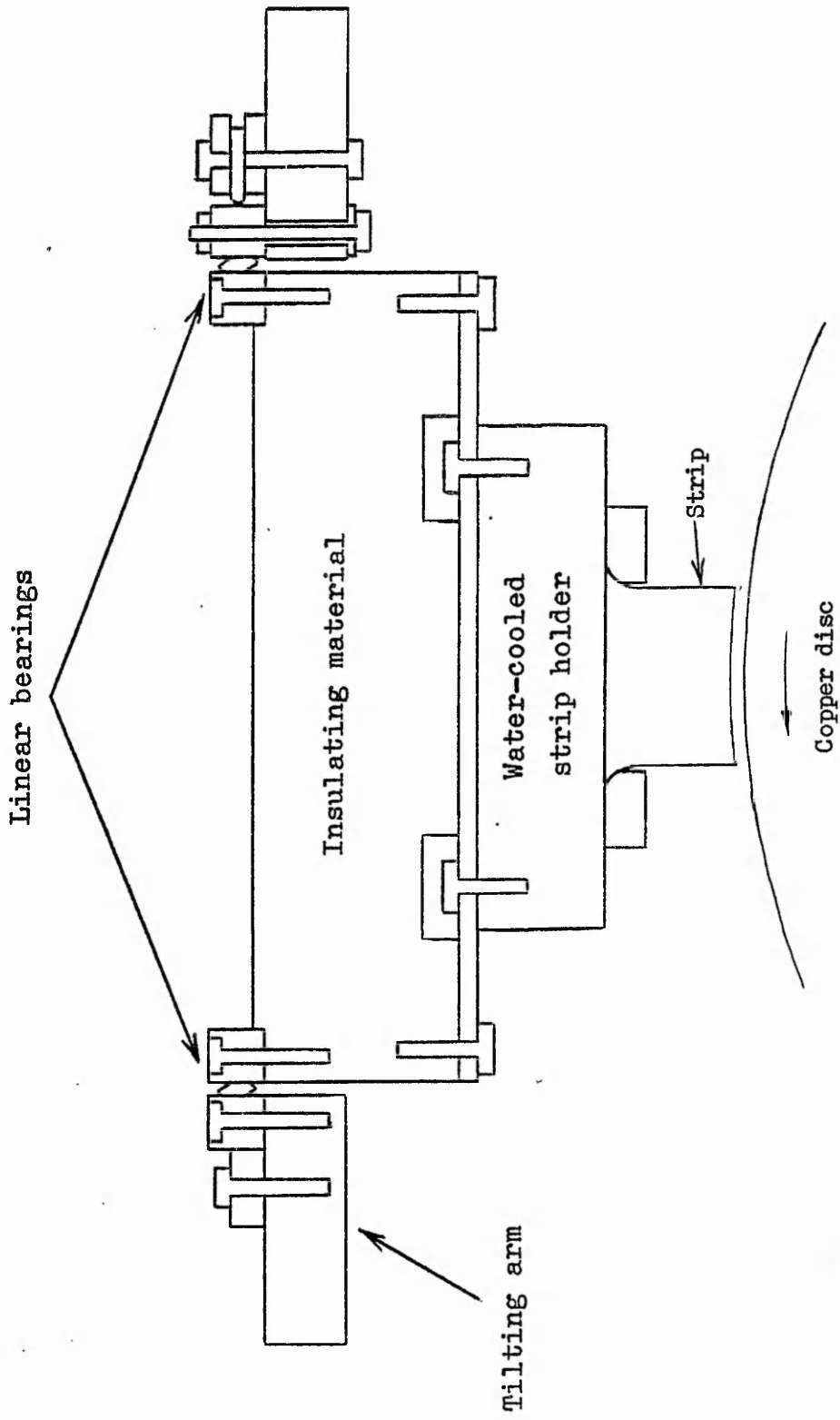
Fig. (4.3) Traversing contact strip holder. The traverse is parallel to disc axis (2)

55

(a)

no damper

0V

contact
voltage
-70V

strip holder
displacement
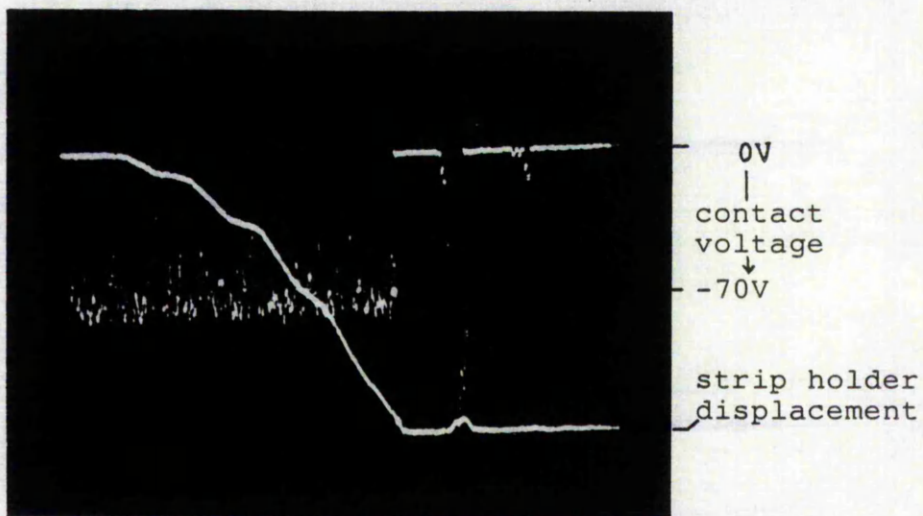
(b)

damper fitted
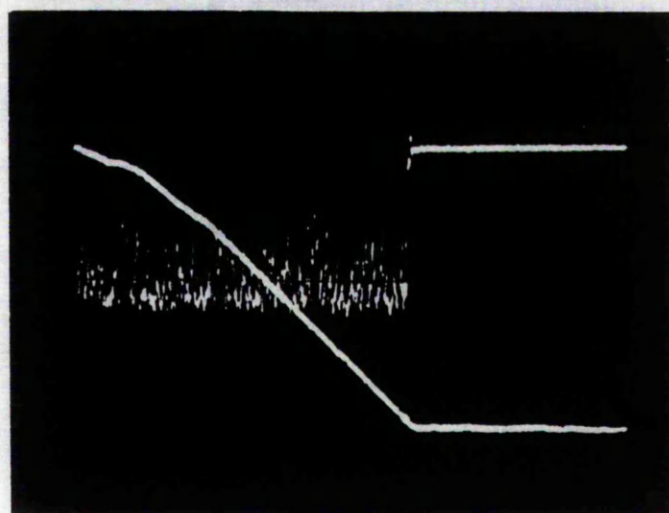
strip lowering,   contact
voltage o/c (-ve)   closed
←————— 0.5S —————→

Fig. (4.4) Effect of damping strip holder arm on contact-
make (dwell mode, V=60km/h, I=40Adc, L=50N). Contact gap
(open)   8mm.
(a) shows the contact bounce and the resultant arcing
    indicated by the contact voltage.
(b) shows the strip lowering more steadily, with no contact
    bounce when closing.

56

(a) no damper,
    no current
    interruption
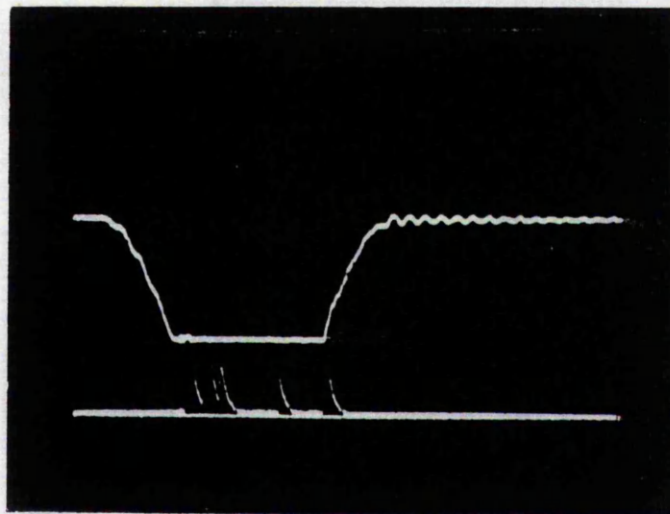
strip holder
displacement

arc light
emisssion

(b) damper
    fitted
    and current
    interruption
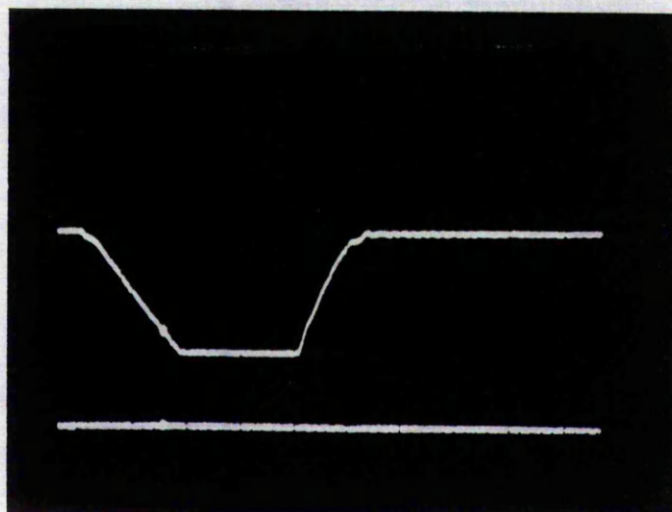
contact
make   break

←————————1.0s————————→

Fig. (4.5) Effect of damping strip holder arm, and of
remote current interruption before contact break (dwell
mode, V = 160 km/h, I = 40A dc, L = 5ON). Contact gap
(open)   8 mm.

(a) no damper or remote current interruption. Arcing
    due to contact bounce is evident, as well as at
    contact break.

(b) after modifications, arcing is effectively eliminated.

57
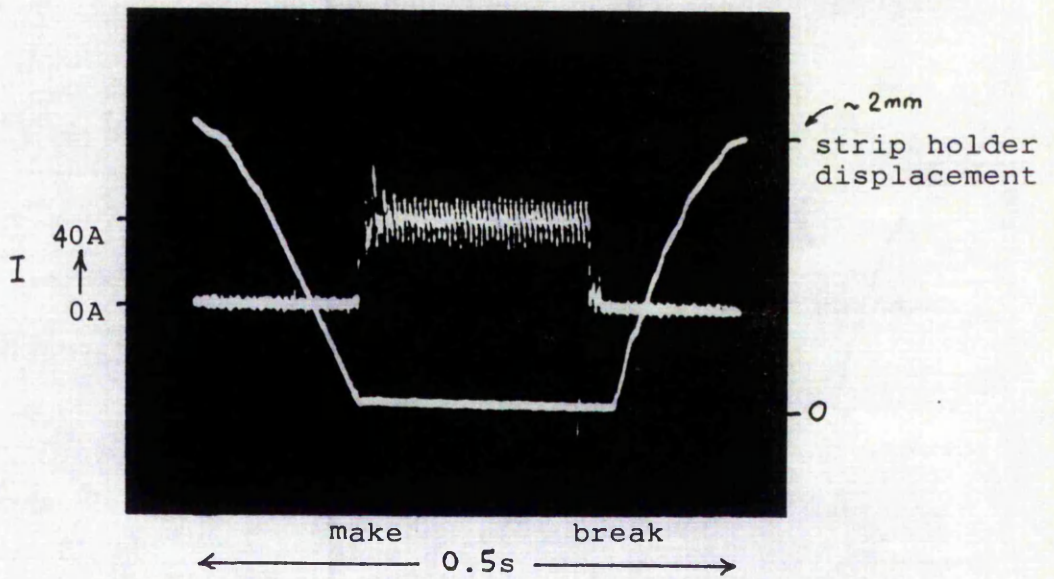
Fig. (4.6)   Effect of current interruption (by remote
             circuit breaker) before contact break, to
             reduce arcing. Sliding contact continues
             for approximately 50ms after current stops
             flowing.

             (dwell mode, V = 60 km/h, L = 50N, I = 40A dc)
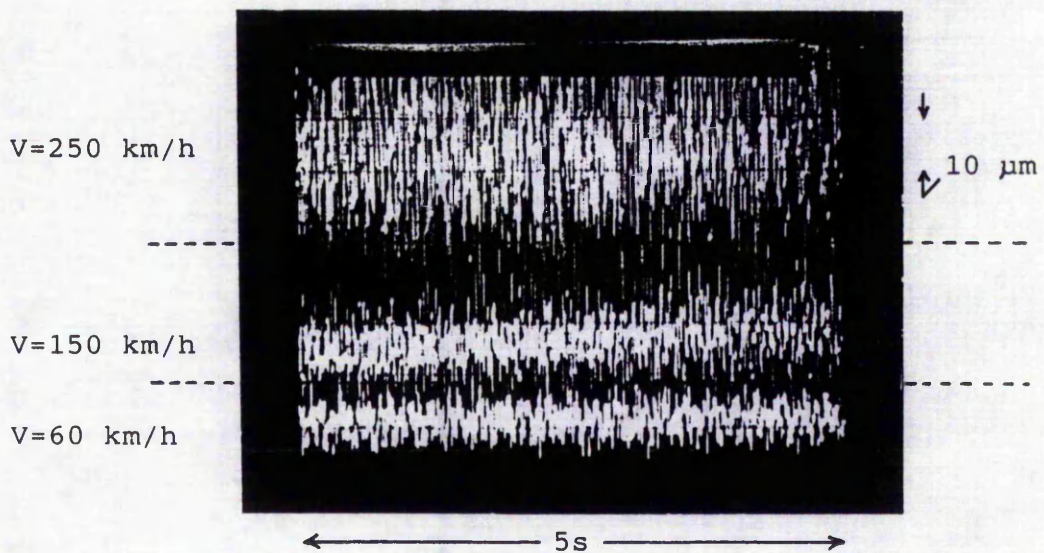
Fig. (4.7)   Contact vibration at various sliding speeds,
             measured by the strip displacement LVDT.

             (Continuous mode, I = 40A, L = 50N)
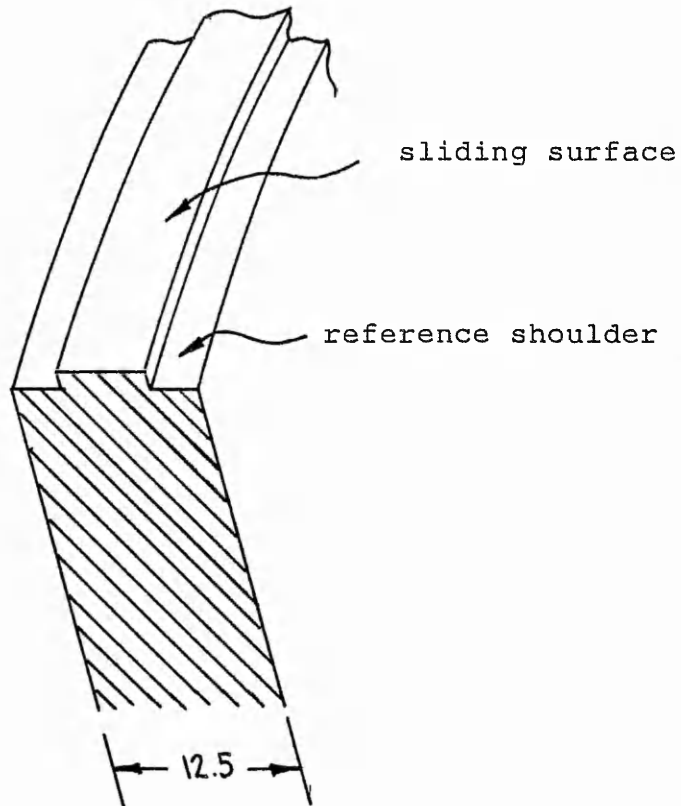
Fig. (4.8)   Profile of disc periphery.

The disc is 0.5m in diameter, 12.5mm thick overall, with sliding surface 6mm thick and either side a reference shoulder cut to a nominal depth of 1mm below the sliding surface.

direction of sliding
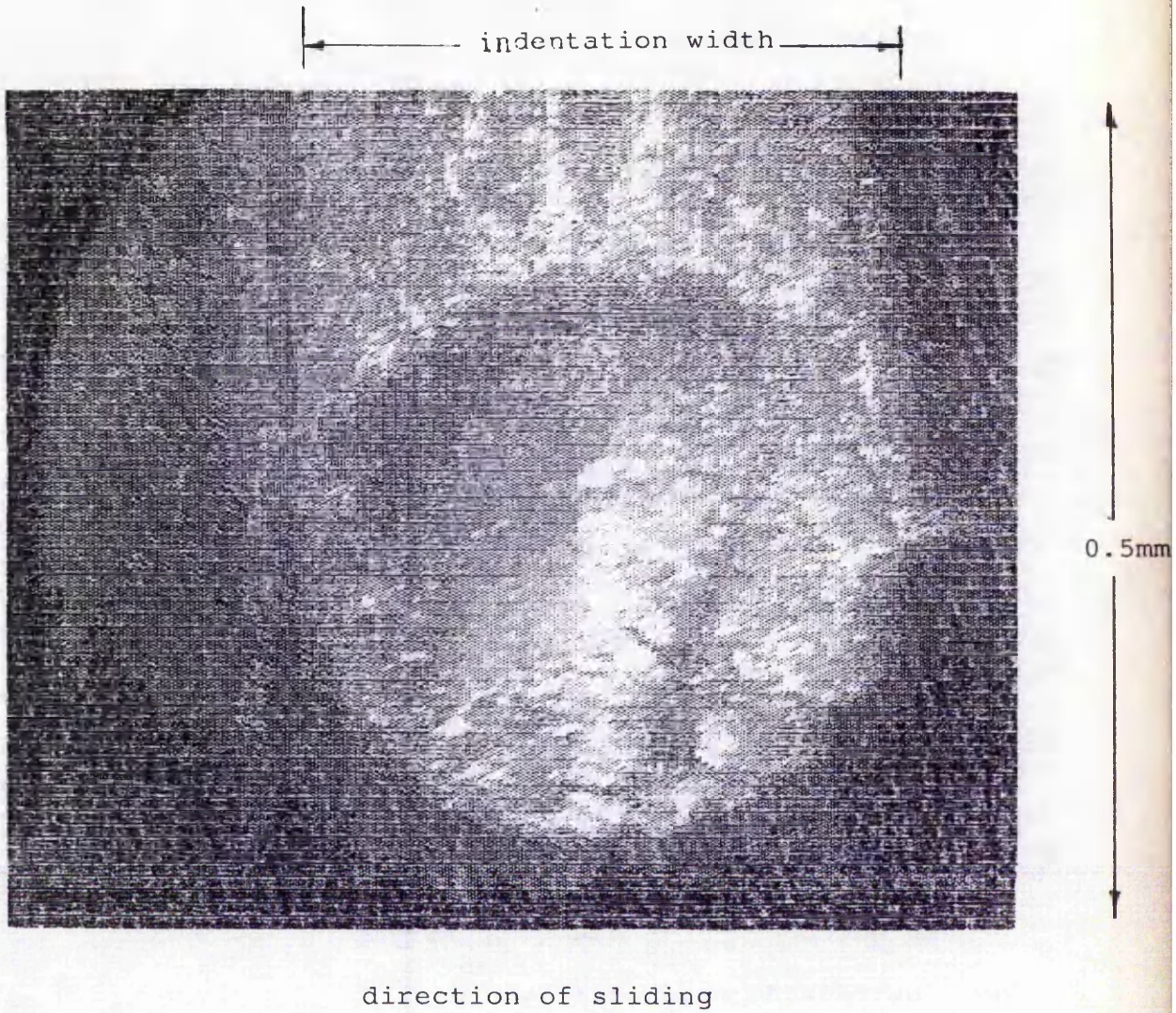
Fig. (4.9)   A reproduction of a video picture of an
             indentation in the copper surface, taken
             through a X20 microscope.
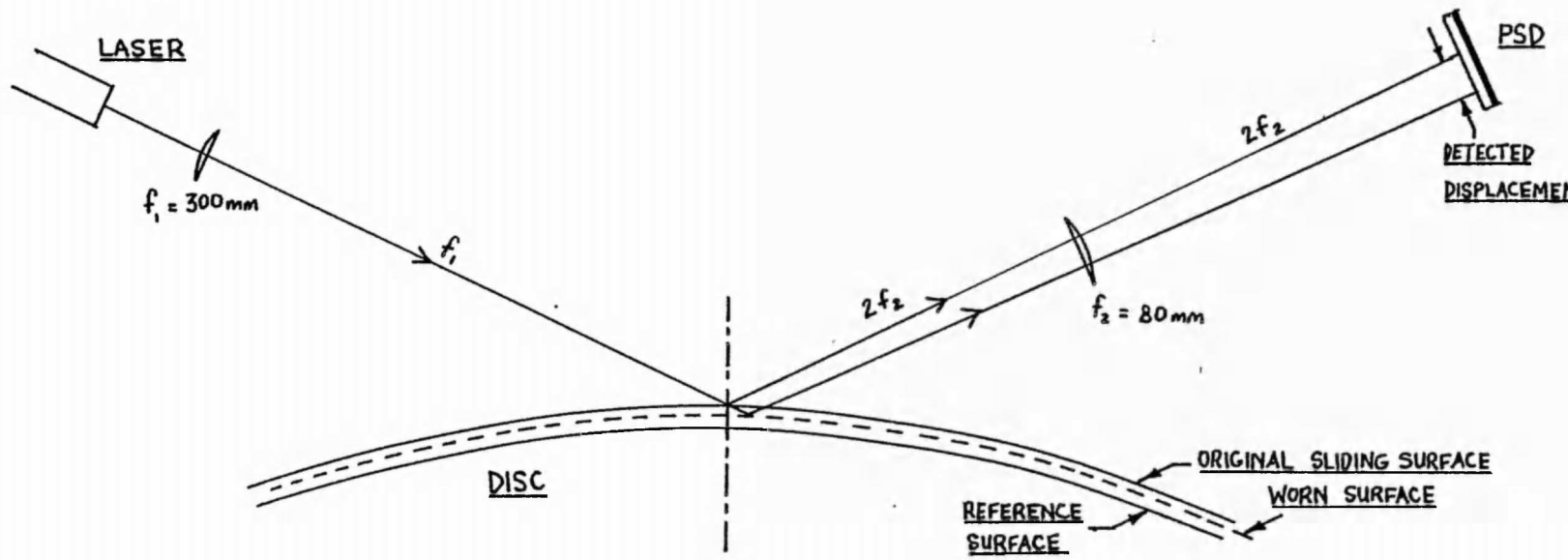
Fig. (4.10) Disc wear measurement, optical lever method (not to scale)

Fig. (4.11) Disc wear measurement using a laser and optical position sensitive detector. The laser and beam focusing lens are mounted on an optical bench in the foreground.
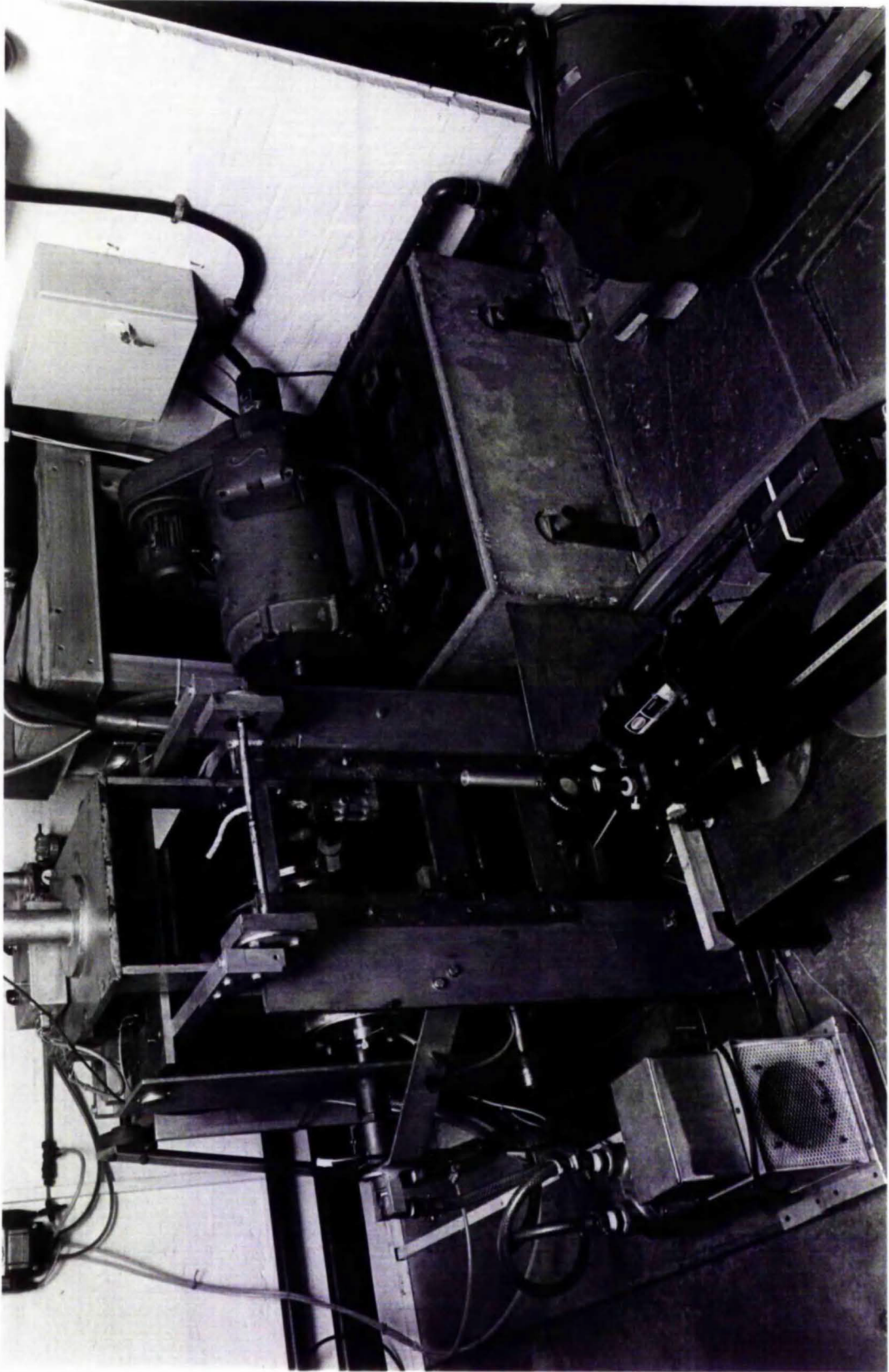
Fig. (4.12)   Close-up of the optical system for disc wear measurement. The output end of the laser is just visible on the right. Following the horizontal path of the beam, it is focussed onto the disc surface (the spot on the surface can be seen although the shape of the disc itself cannot be made out) where it is reflected vertically downward through another focussing lens onto the PSD, which is mounted on the base of the wear machine.
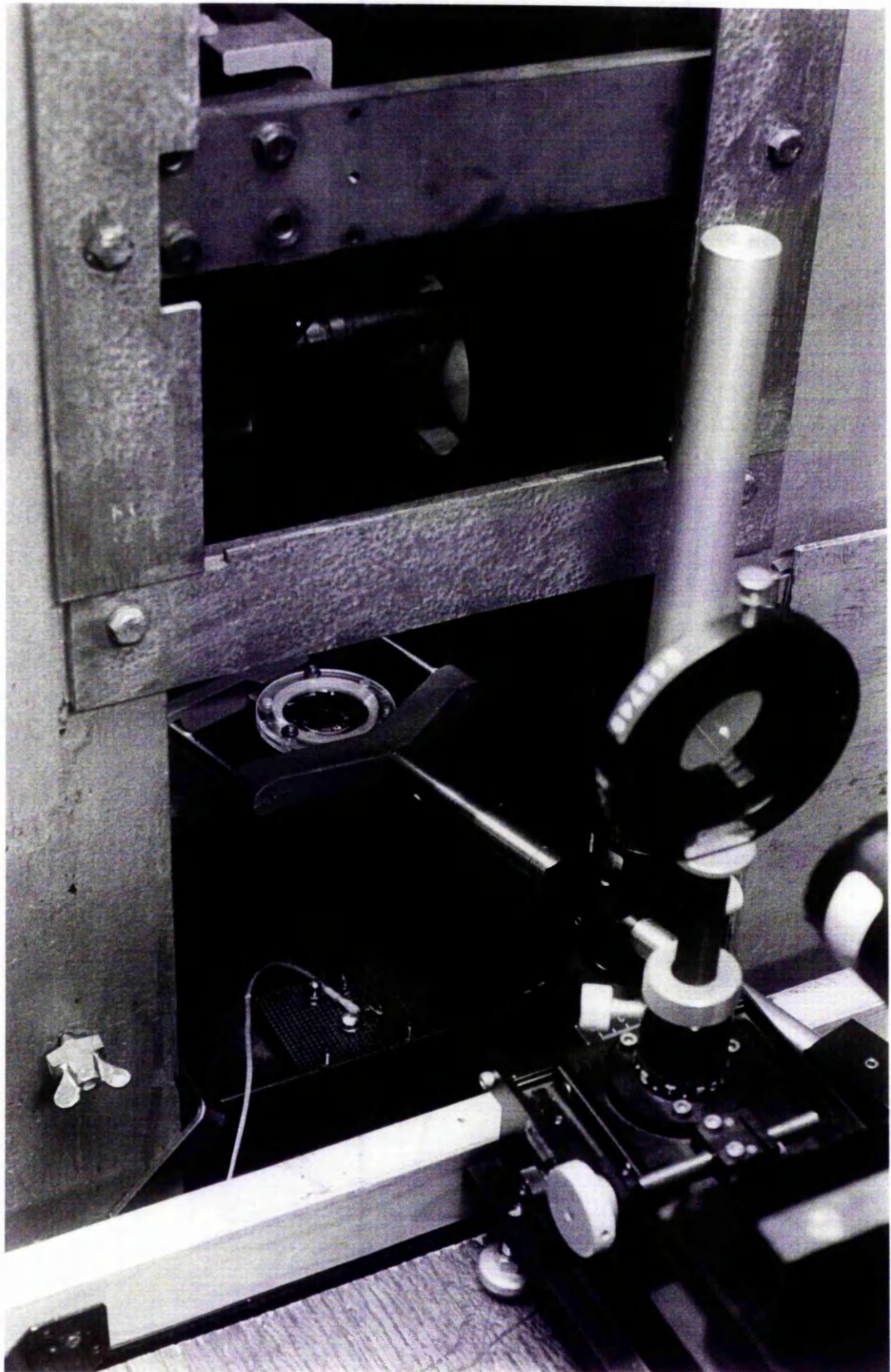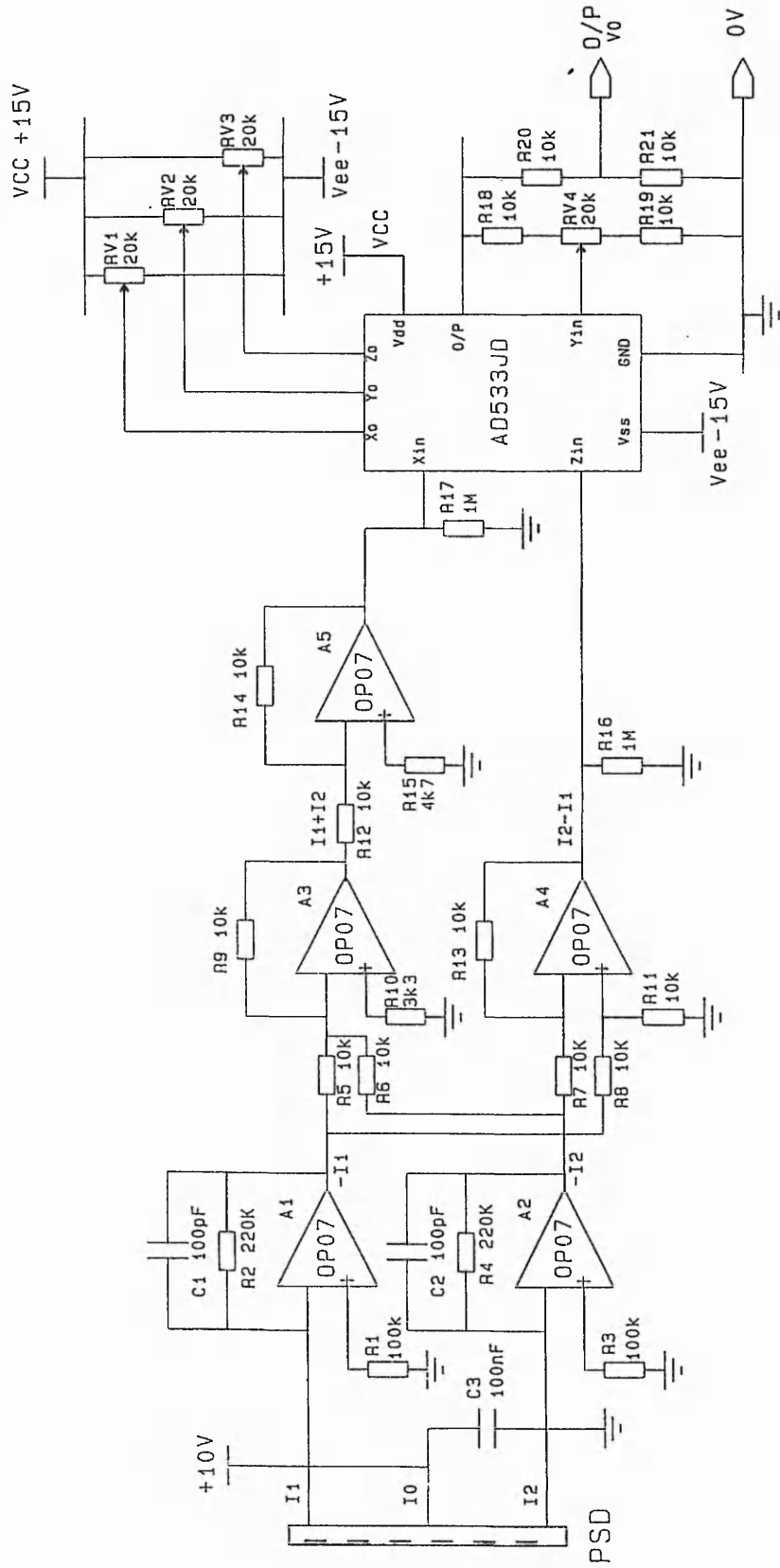
Fig. (4.13) Disc wear measurement, optical lever method. Circuit diagram of PSD decoding circuitry. AD533JD is an analogue divider i.c.

64
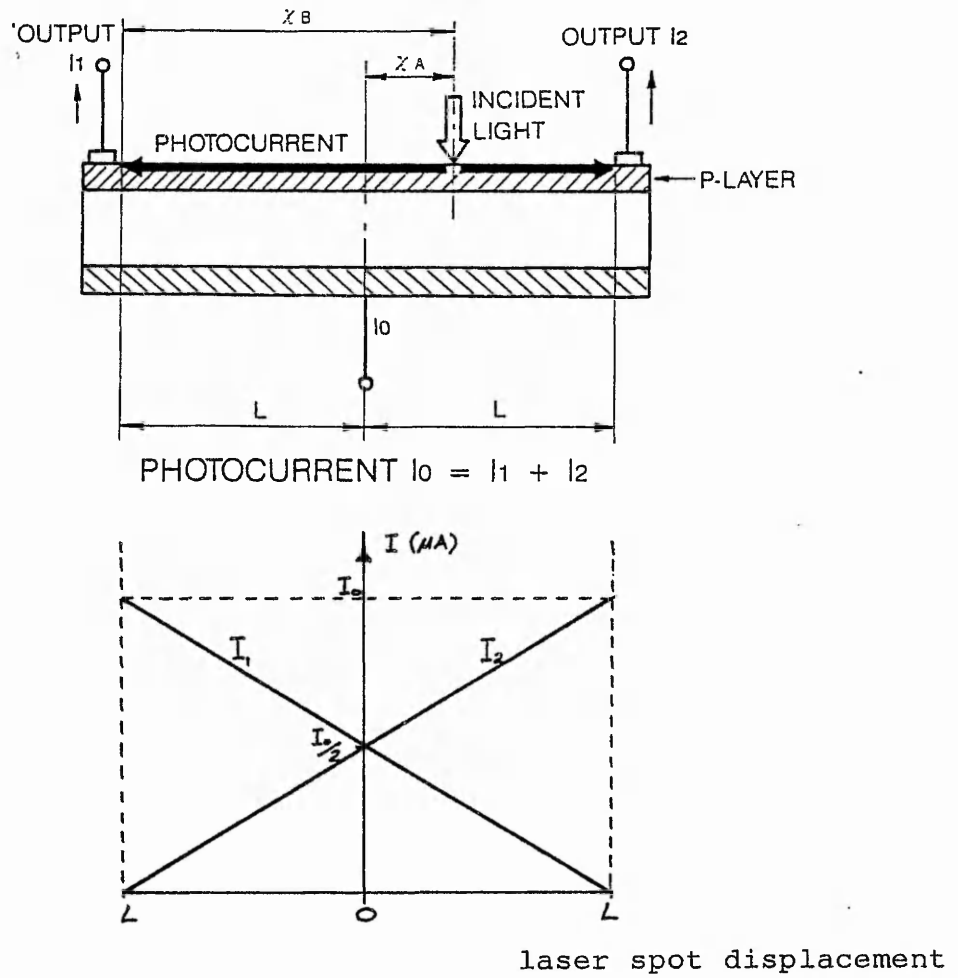
Fig. (4.14)   Operation of position sensitive
              detector (PSD) with output
              characteristic.

increasing
photocurrent

← ambient

←————————1 disc rev————————→
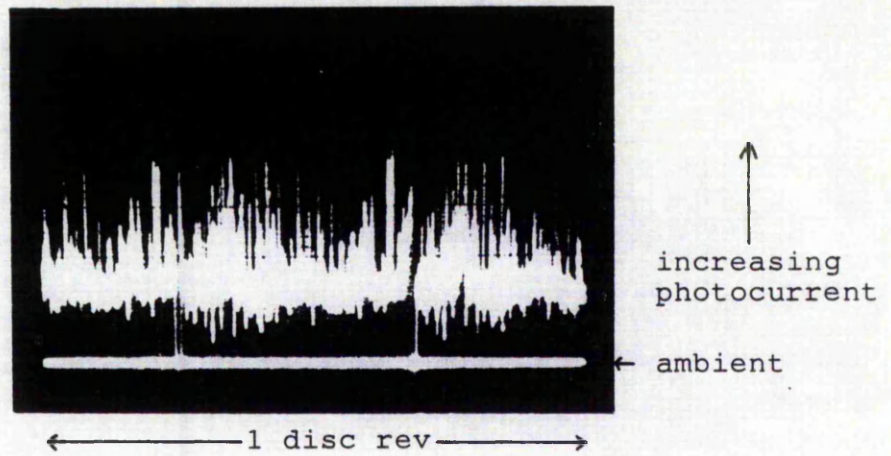
Fig. (4.15)   Variation in PSD photo-current as disc
               is revolved, indicating the change in
               reflectivity around the disc sliding
               surface (disc rotated at 0.1 rev/sec,
               laser spot size on disc 225µm).

├——— 1 ms ———┤

0

-0.5 mA

V_o (~100mV p-p)

I_1, I_2

+5 mA
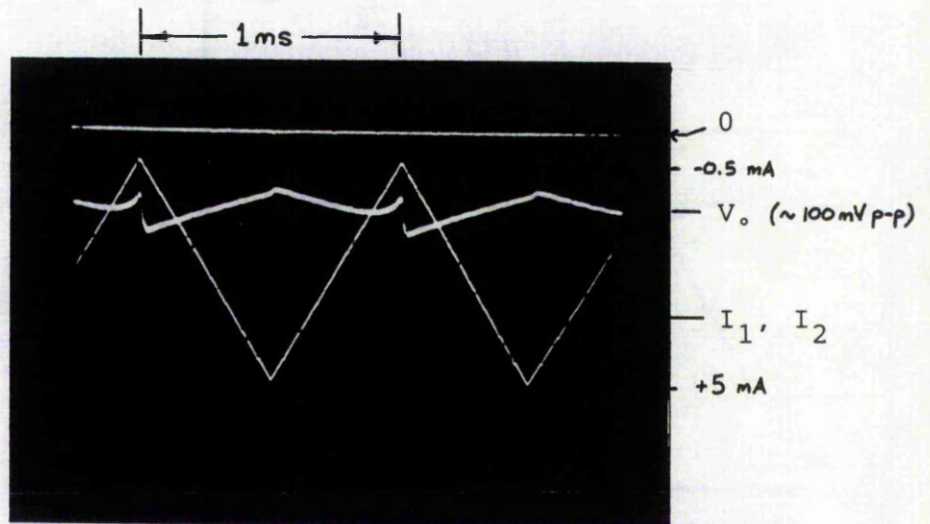
Fig. (4.16)   Noise on o/p signal V_o due to
               simulated variations in disc surface
               reflectivity, using a triangular wave-
               form from a signal generator feeding
               I_1 and I_2 together.
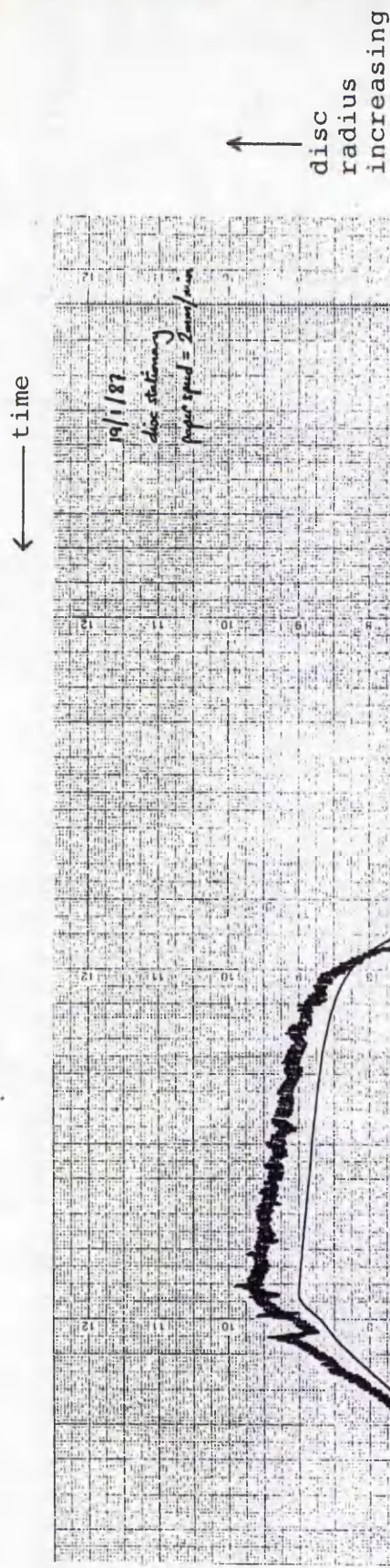
Fig. (4.17) Output signal of optical disc wear measurement system (V_o), with disc stationary and disc radius altered by adjusting disc temperature. A drift in V_o of about 10 μm, relative to the LVDT signal, occurs over the duration of the test.
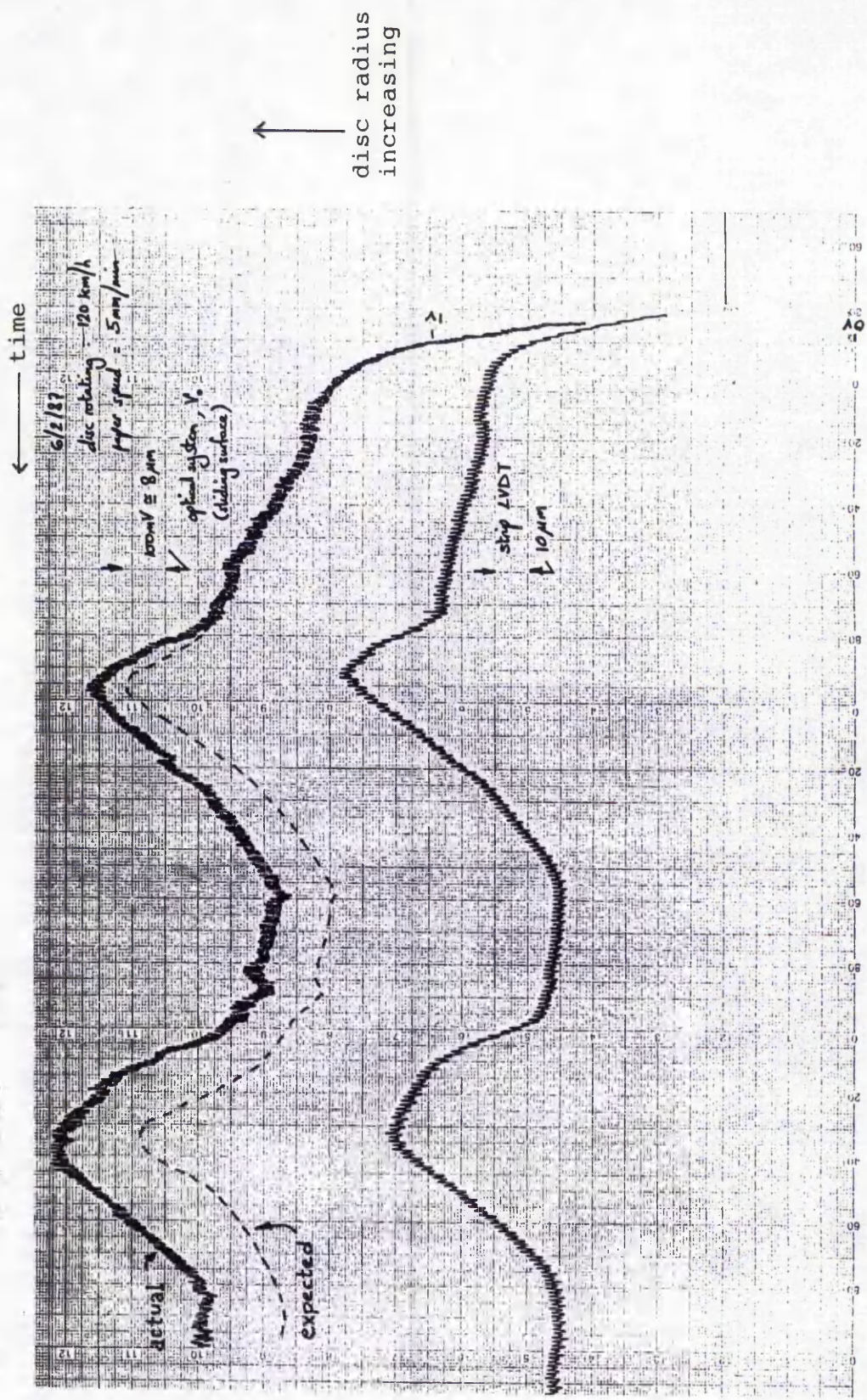
Fig. (4.18) Output signal of optical disc wear measurement system (V_o), disc rotating (V=120 km/h). As the disc temperature cycles, due to the characteristics of the cooling system, the disc radius also cycles. Drift in V_o is greater than 10 μm, over duration of test.

Fig. (4.19)   The modified LVDT holder assembly for the disc wear
measurement system, showing the retractor mechanism.
The two LVDT styli are shown in the retracted
position; the top stylus measures sliding surface
displacement, the bottom stylus performs the same
function on the reference shoulder. Limit switches
(out of sight) prevent over-travel of the retractor
mechanism.
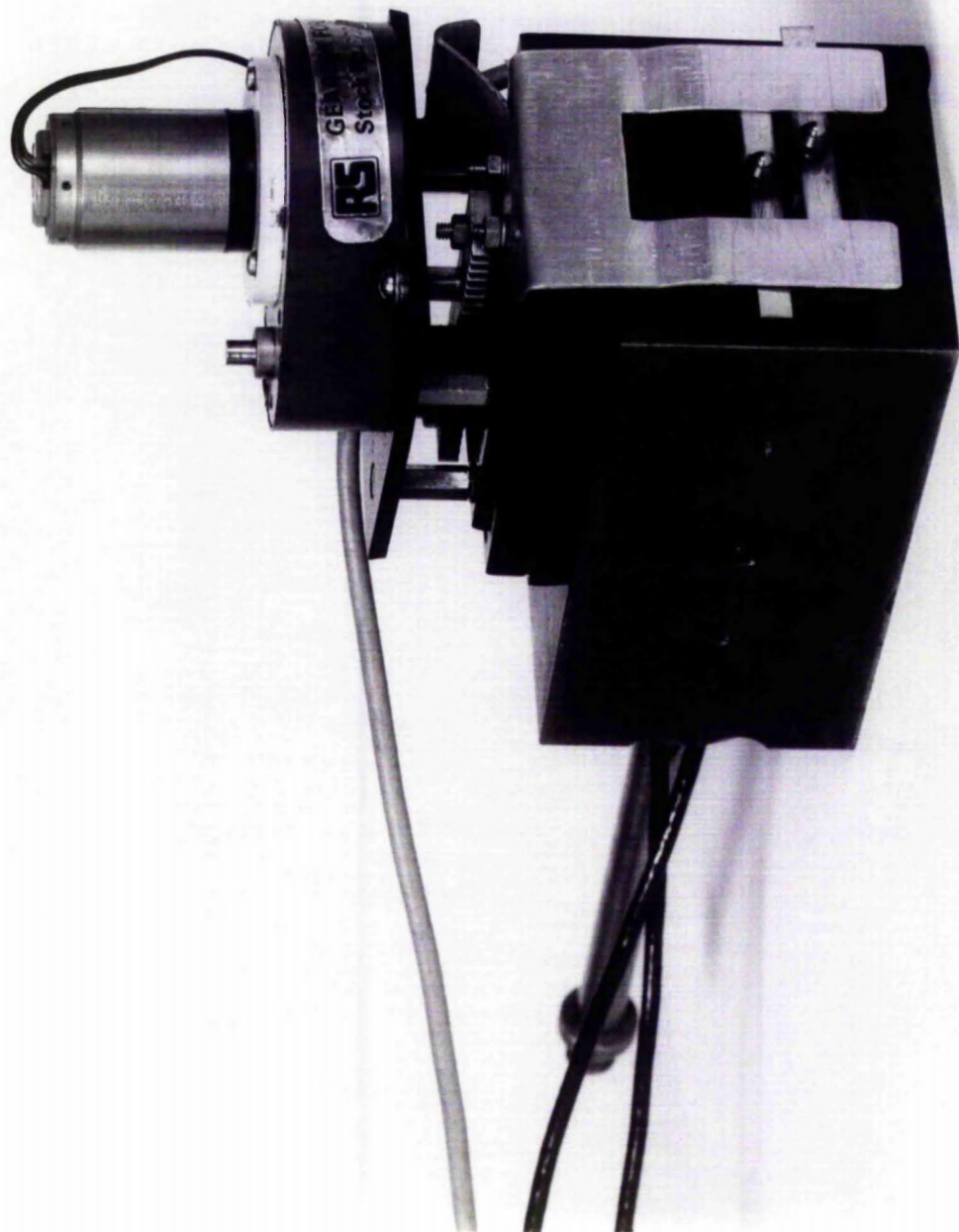
Fig. (4.20)   The LVDT holder assembly in position.   The disc sliding
surface can be seen behind the retractor drive motor.

70
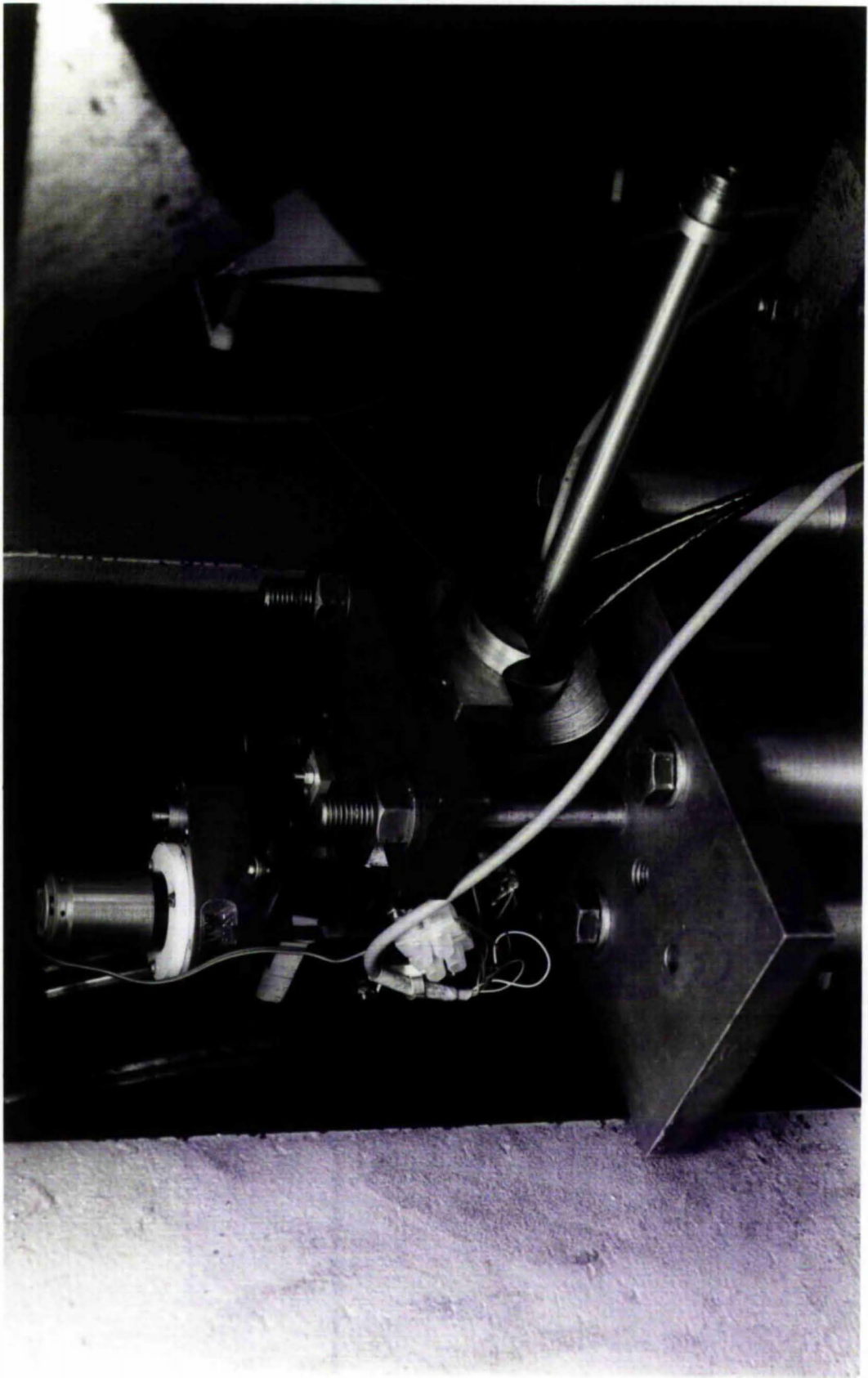
Fig. (4.21) Disc steeping mechanism for the LVDT disc wear measuring
system. The miniature synchronous motor drives the rubber
tyred capstan via a step down gearbox. The capstan is
held under spring tension against the side of the wear
machine disc, and rotates the disc in steps of approximately
1mm. The drive to the motor is controlled by the micro-
computer via a relay.
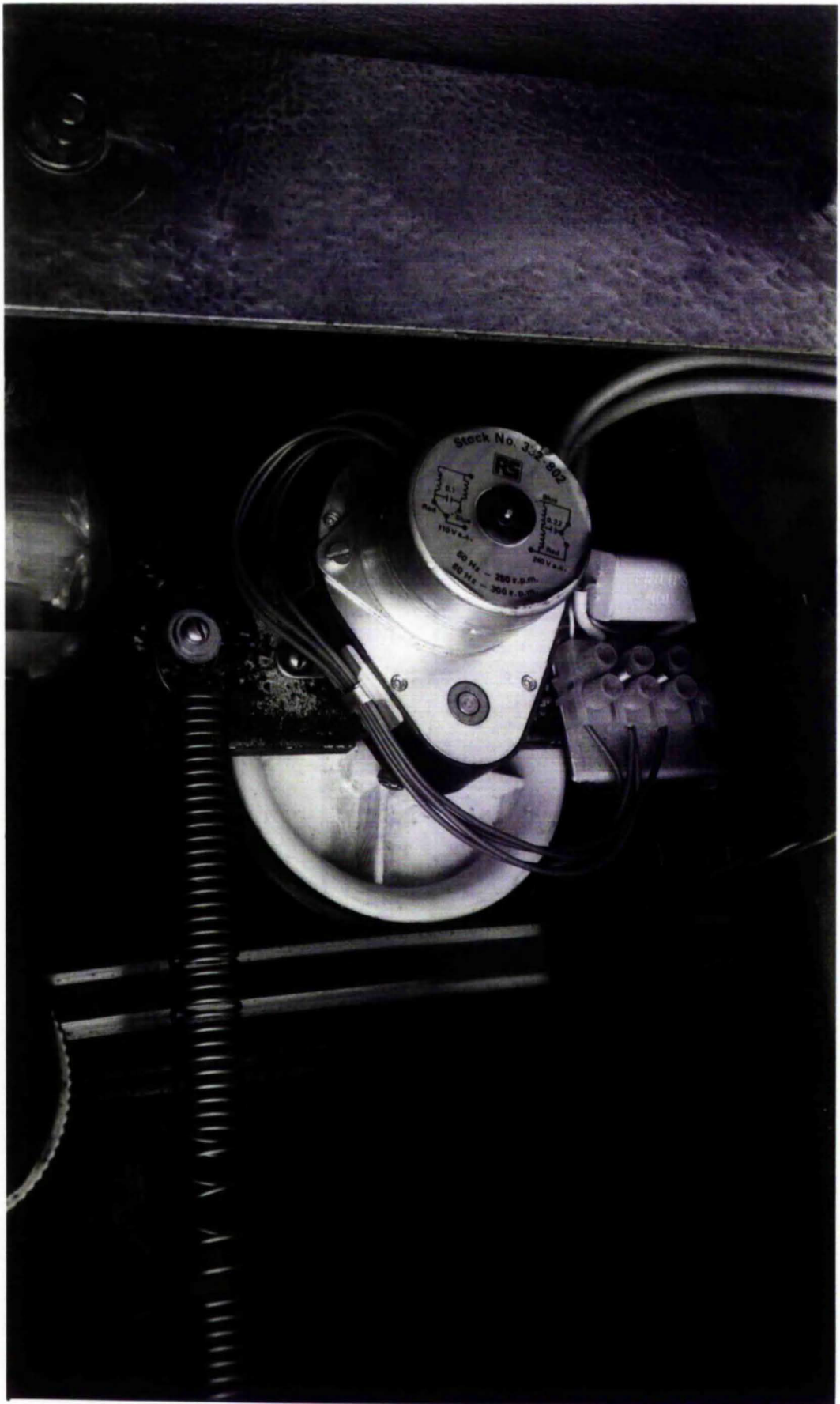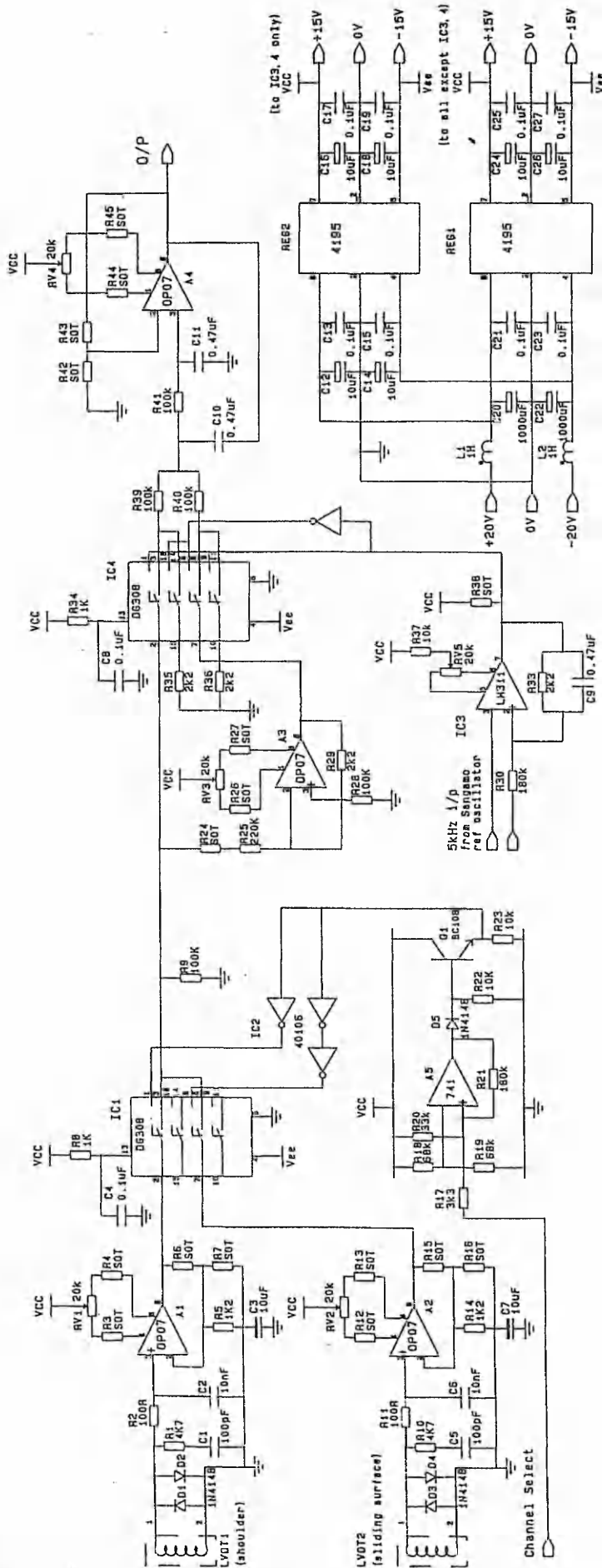
Fig. (4.22) Disc wear measurement, LVDT method. LVDT decoder/amplifier circuit. The channel amplifier/filters A1 and A2 feed the channel selector IC1. The selected channel is fed to the chopper demodulator circuit, A3 and IC4. The chopping signal is derived from the LVDT 5kHz oscillator. A4 is a 2 pole Bessel filter, which effectively removes any remaining 5kHz component in the signal. The dc output is proportional to the displacement of the selected channel LVDT and is fed to the A to D convertor in the BBC micro computer.

72

Fig. (4.23)   The complete signal processing unit for the LVDT disc

wear measuring system, based upon the Sangamo chassis.
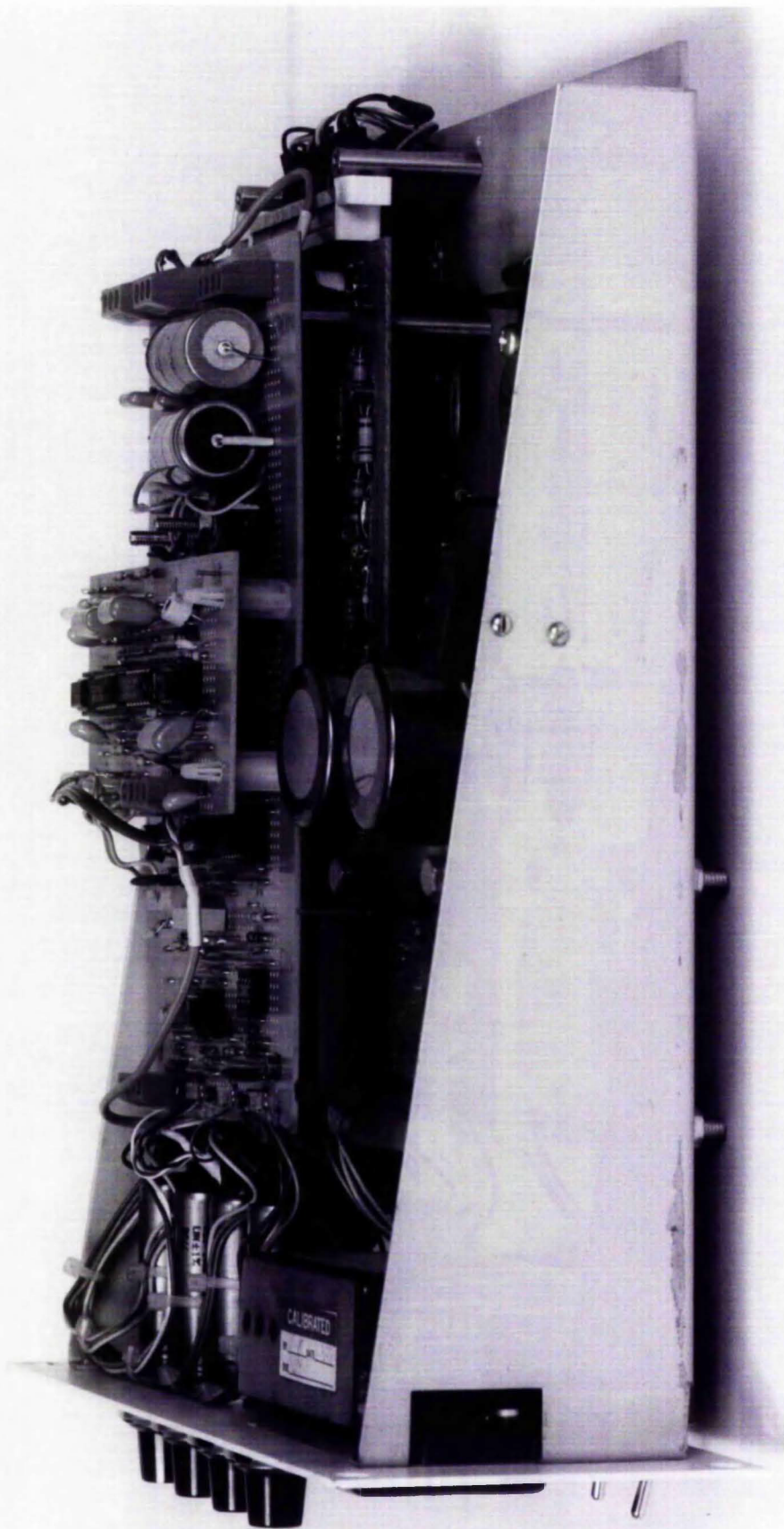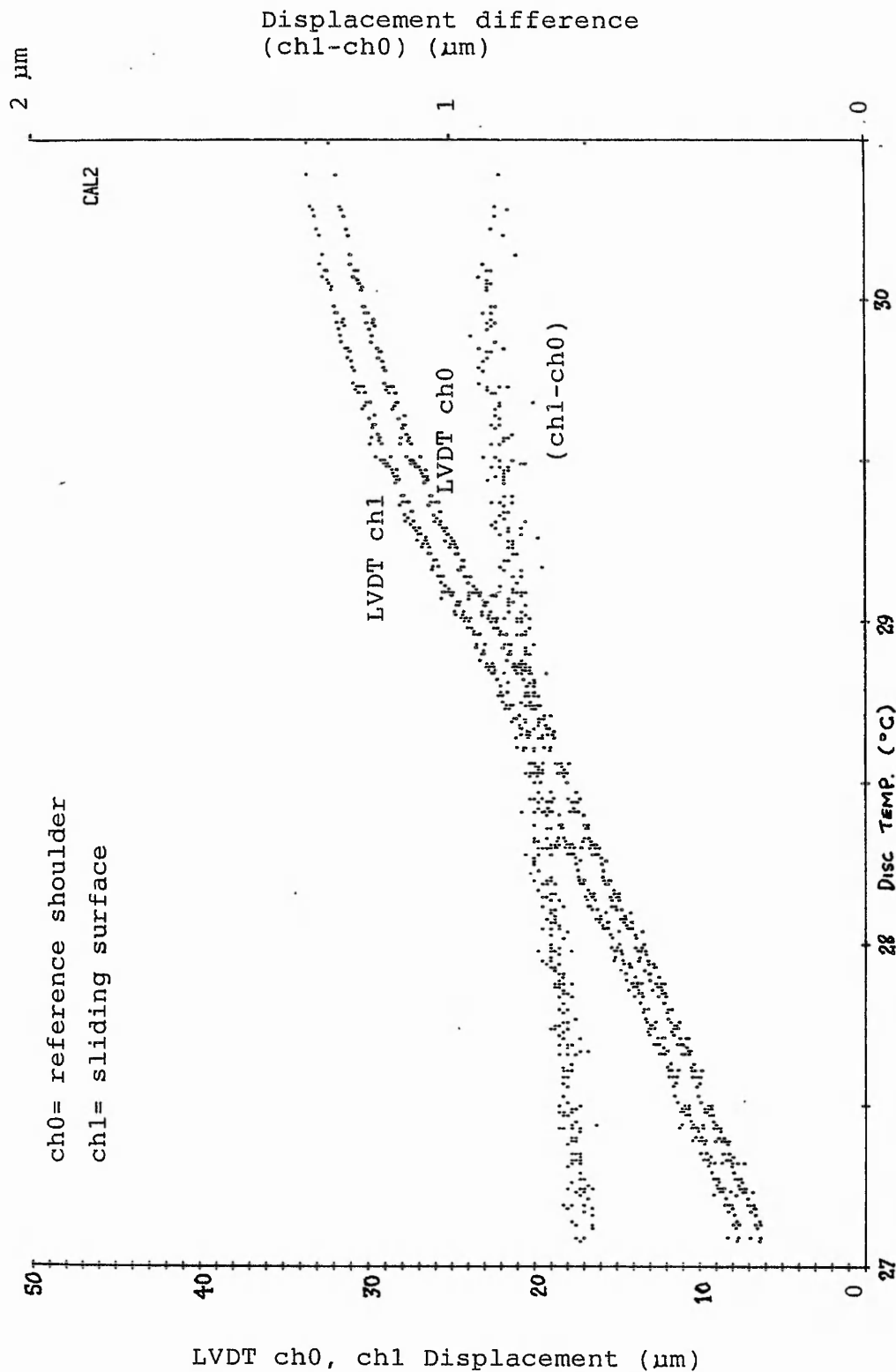
Fig. (4.24) LVDT calibration, scatter diagram. Ambient temperature constant, disc temperature varied to give a variation in disc radius over about 13 μm, temperature measured using a semiconductor sensor. The variation in the difference signal (shoulder displacement minus sliding surface displacement) is approximately 0.1 μm over this range.
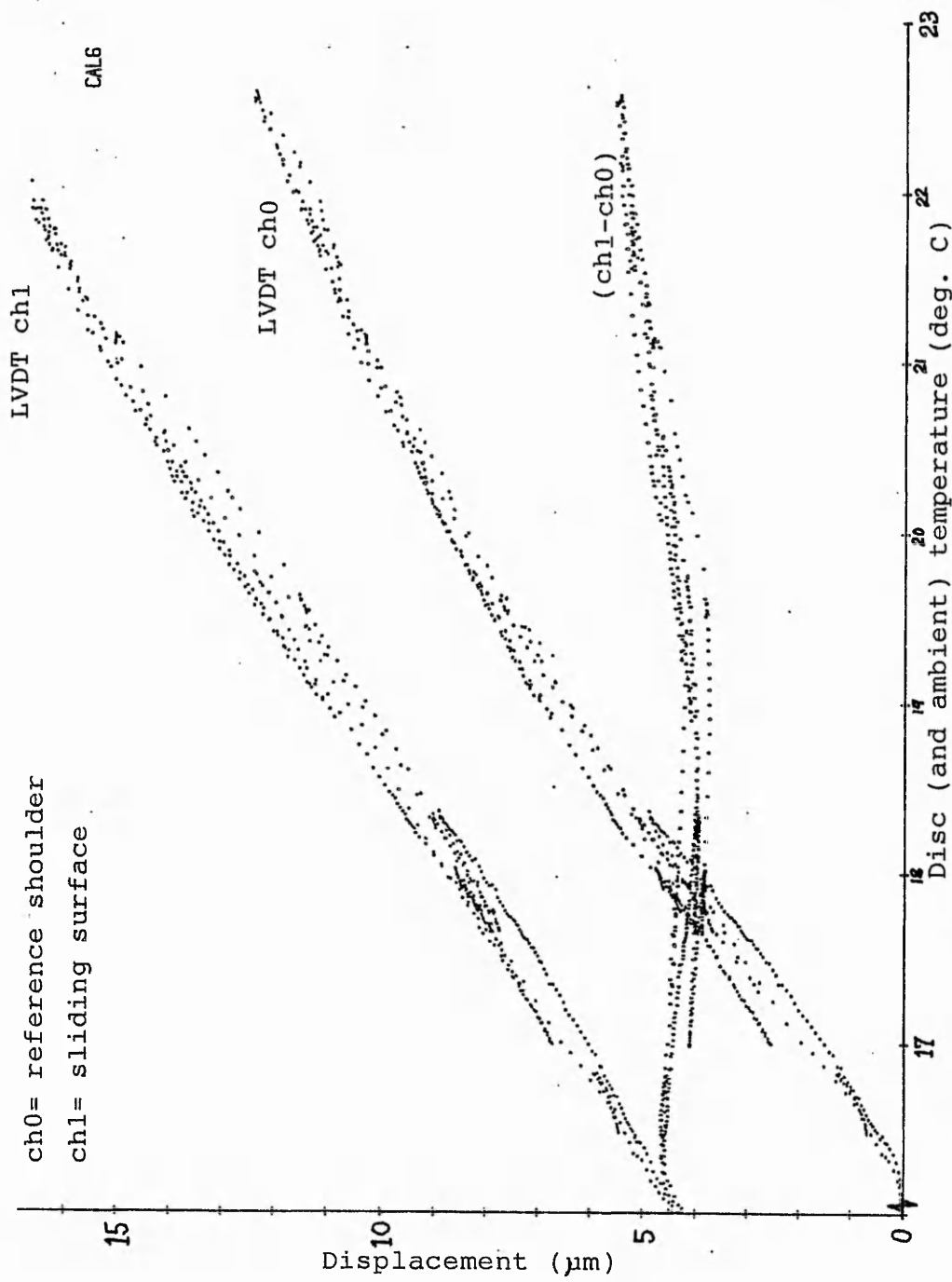
Fig. (4.25) Scatter diagram showing LVDT displacements, readings taken for cyclic temperatures over a 14 day period. All measurements were recorded using a BBC microcomputer, sampling every 20s, each plotted point calculated from the average of 100 recordings.

ch0= reference shoulder
ch1= sliding surface

LVDT ch1

LVDT ch0

(ch1-ch0)

CAL6

Displacement (μm)

Disc (and ambient) temperature (deg. C)

75
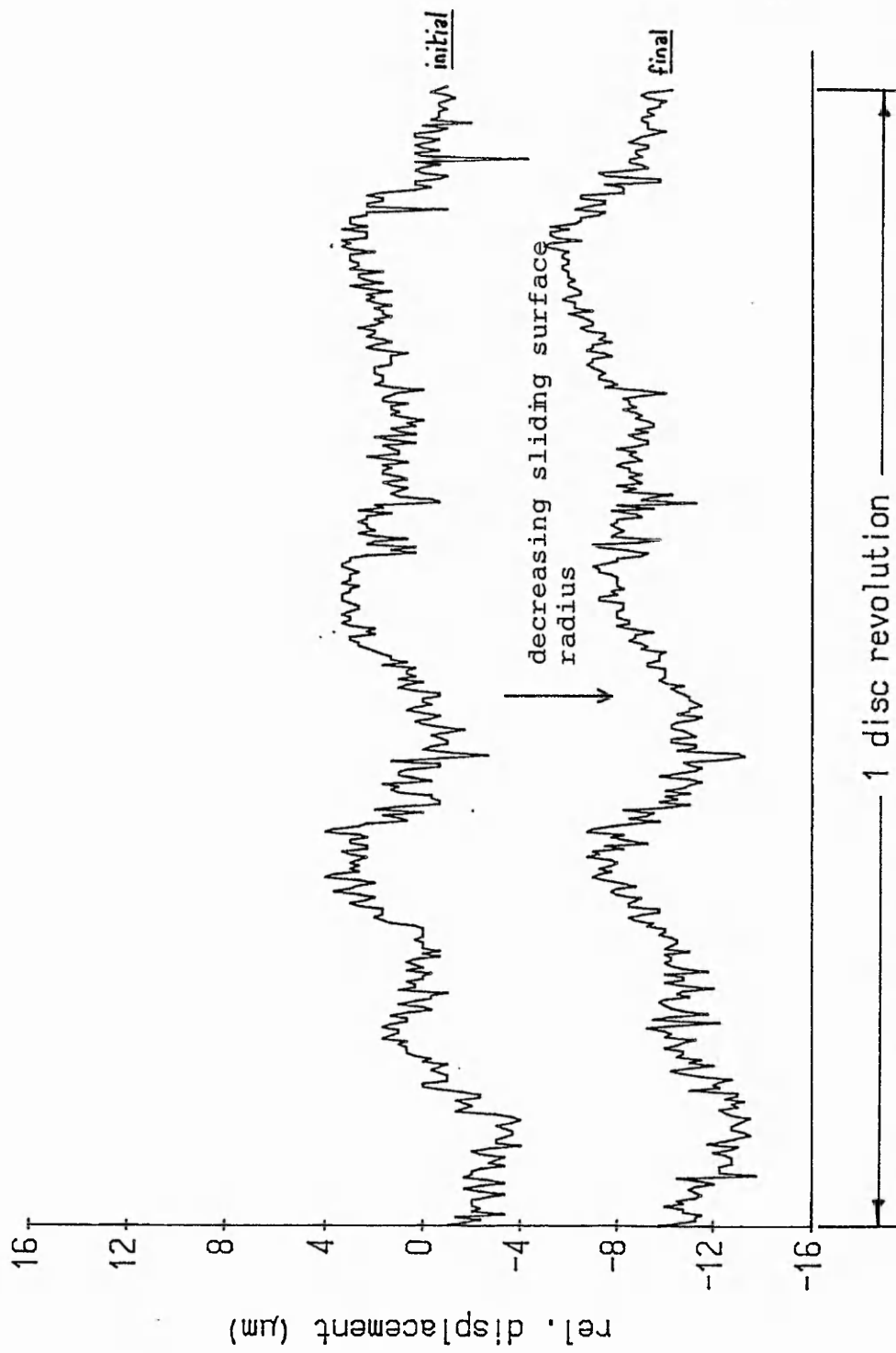
Fig. (4.26) Difference plots (sliding surface-reference shoulder) taken before and after a wear test (v=180 km/h, L=50N, I=50A dc, duration = 15 hours), representing an average wear of 9.9 μm.

Fig. (4.27) Data logger interface unit. The boards mounted on the door are the analogue signal conditioning circuits, whilst the analogue-to-digital converter and its associated digital circuitry are mounted in the back of the unit next to the power supply.
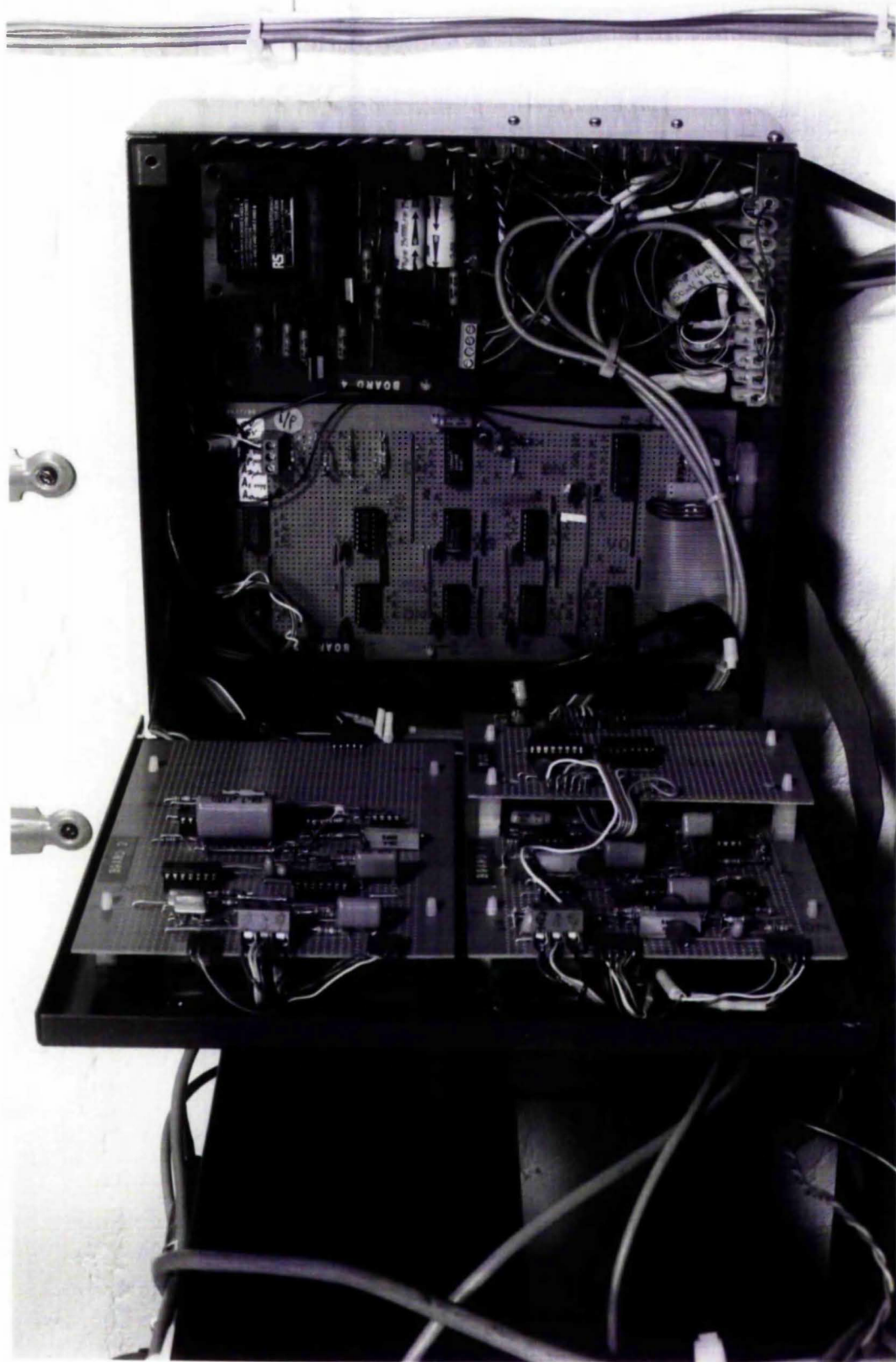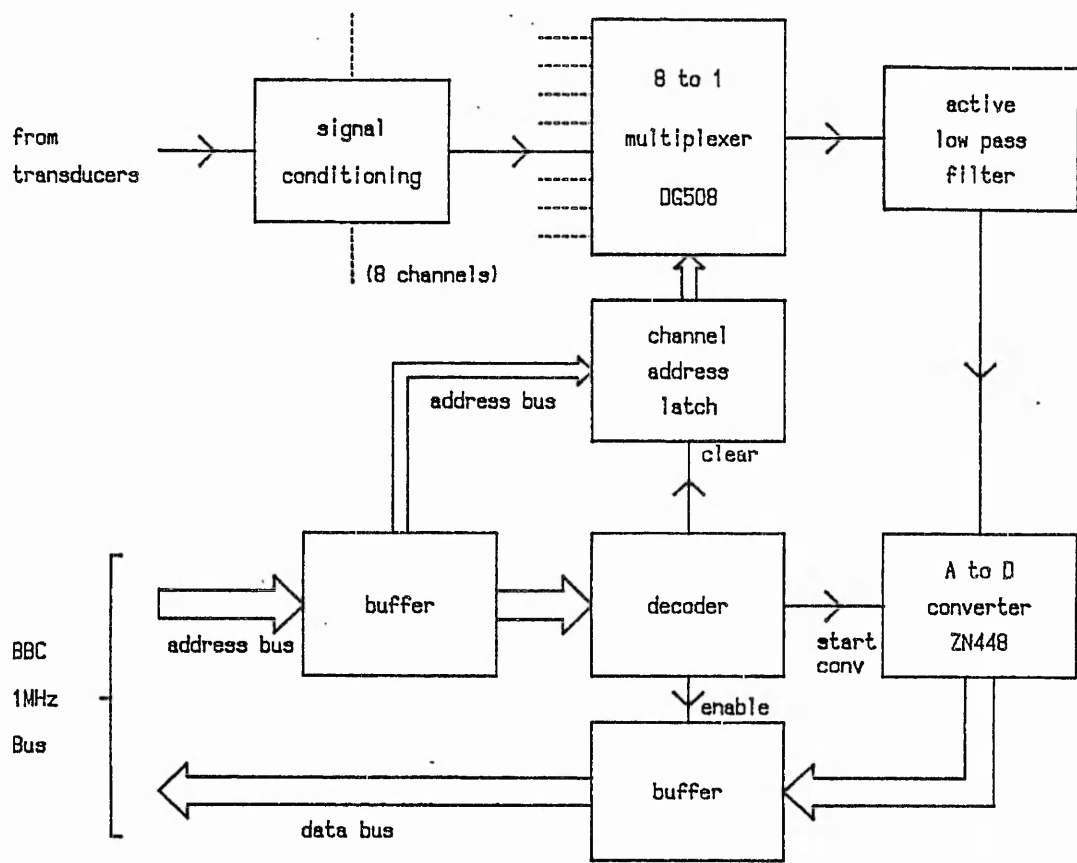
Fig. (4.28) Block diagram of interfacing circuitry
between analogue transducers and BBC Master micro-
computer.

WEAR TEST 21A1087

Speed	60 km/h	Mode	cont.
Load	50 N	T max	34 deg.C
Current	100 A dc	Traverse	off

each graduation = 10 mins   sample time = 2 secs

no. of samples = 4500

Time ⟶

150 mins

2	coolant temp. (deg.C)	50 deg.C
3	strip temp. (deg.C)	250 deg.C
4	drive motor load	arb. units
5	strip displacement (um)	250 um
6	light emission	arb.units
7	contact V (V)	1.25 V
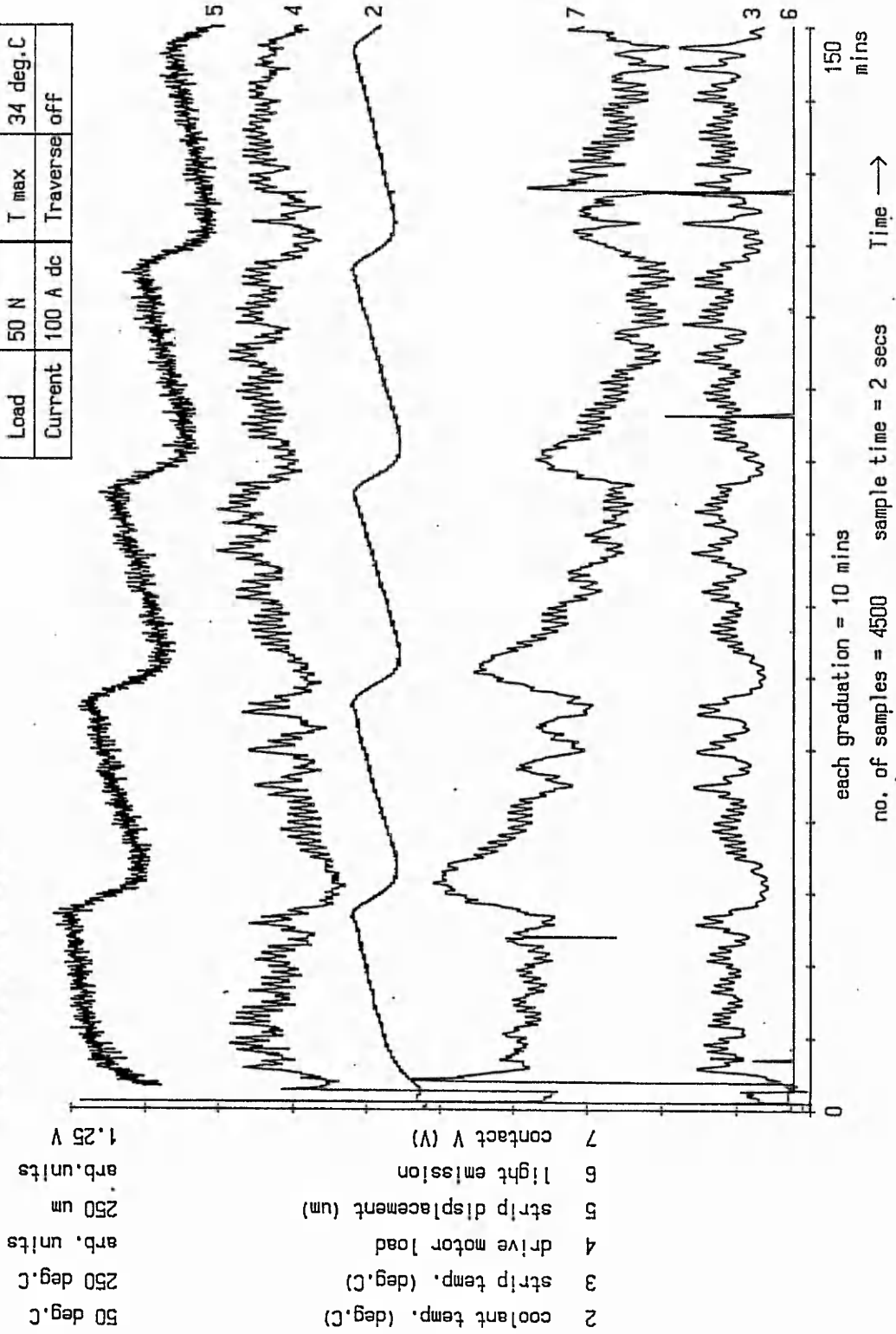
Fig. (4.29) Typical plotter output from data logger system. The original plot is in colour.

79

CHAPTER 5

RESULTS AND DISCUSSION

In this chapter the results of wear measurements on a range of carbon strip materials for a variety of sliding conditions are presented. The strip types are listed in table 5.1. Also presented are the results of copper wear measurements that were obtained using the indentation and LVDT methods. This present work is a development from an original investigation which was confined to MY7D collector strips only, for which the wear machine used here was developed [1,2]. The results of the earlier work, in summary, are that there is an optimum contact force for minimum wear of both the strip and the wire, and that both wear rates increase with speed and current, especially so for the strip.

5.1 STRIP WEAR

Information on the properties of the strip materials included in this present work, where known, can be found in appendix A. A particular range of materials were all based on the same CY3 base. This range includes J1A, J2A and J3A which were not impregnated, but were all heat treated to different temperatures (increasing in the order of listing); the higher the temperature, the higher the level of graphicity and homogeneity of the material. The other materials from this base were JCL, JCO and JAN, which were impregnated with copper-lead, copper, and antimony

80

respectively.   Although some continuous sliding tests   were
performed   at   speeds above 150km/h, the results   were   not
believed to be applicable to railway conditions for   reasons
explained in section 4.1.2.

The results of the wear tests for the strips listed in table
(5.1)   are plotted on logarithmic axes in fig (5.1), which
includes   the   results   for MY7D from the original   work   [2]
where   relevant.   All   the tests were with   a   50N   contact
force,   excepting   nickel-graphite.   One   of   the   most
noticeable   aspects of these results is the   variability   of
the   mean   strip   wear   rates.   One   explanation   for   this
inconsistency   is   the   inhomogeneity   of   carbon   based
materials,   especially after metal impregnation.   As all the
tests were of at least several hours in duration, presumably
ensuring   the attainment of steady state conditions,   it   is
difficult to identify any other cause.

It   was   noticed that wear across the width of   the   sliding
surface of the strip was not always even.   Indeed, some test
samples   had to be discarded as the difference in   thickness
across the strip increased above about 50µm.   It is believed
that   this   effect   may also have been   caused   by   the   non
uniformity of the properties across the strip.   Measurements
on   the   sliding surface of the copper disc, taken   with   a
traversing LVDT,   did not show any significant variations in
wear across the disc wear track.

The   base carbon JBC shows an increase in NWR   (normal   wear
rate,   ie worn volume per unit length of sliding, defined in
Chapter   1) with current,   ie doubling when I   is   increased
from   0 to 100A.   Similarly,   there is an increase in   wear
with speed,   with the NWR doubling as speed is doubled   from
60km/h to 120 km/h, at I=50A.   This increase is even   more
marked with no current,   suggesting that the increased   wear
isn't   due   to any speed induced arcing.   The   other   base
carbon materials J1A,   J2A and J3A,   all exhibited very   low
wear   rates   at   low   speed   and   current   (60km/h,   I=10A).
Unfortunately,   there   was insufficient opportunity to   test

81

these materials at higher speed and current, although a test with J2A at 60km/h, 50A showed virtually no change in wear, but when the speed was doubled to 120km/h the wear increased in a dramatic manner.

For the experimental impregnated materials the copper/lead impregnated strip JCL, which presumably should have shown wear rates similar to MY7D, performed poorly even at low speed. In general none of these materials, ie JCL, JCO and JAN, showed much promise, assuming the results quoted are representative.

The results from the tests with nickel-graphite, considered a "hopeful" by Williamson [100], were disappointing. Not only was the strip wear fairly high at low values of current, contact force and speed, but when the contact force was increased the wear became catastrophic on both the prepared samples. In addition the disc surface was so heavily scored on one occasion that it had to be re-machined, although when the heavily abraded strip surface was subsequently examined under a microscope there were no visible copper fragments as has been found with other strip materials. It could be that the results obtained by Williamson only appeared favourable because the material could only be tested then at very low speed. This material also has the disadvantage of being relatively heavy, with a density of 6.15g/cm^3 against an average figure of about 2.4g/cm^3 for MY7D.

The commercial copper/lead impregnated materials all performed equally satisfactorily, with the Ringsdorff and Schunke & Ebe (S & E) samples generally producing results within the band of MY7D wear rates. The one exception was the test at 120km/h, 50A for which the Ringsdorff sample exhibited above average wear. This result was the weighted average of two tests taken after 24 hours running-in at reduced speed; one of 4.2 hours duration (after a further 100 minutes running in at the rated conditions) followed immediately by a second of 13 hours. Again there was

82

insufficient time to prepare and test another sample from a different piece of this material, so again it is not known how representative of the material these wear rates are. Considering now the material currently used by BR, Morganite MY7D, it is obvious that there is a large variation in performance. For example, in the tests at v=60km/h, I=50A, L=50N, the batch 359Q sample ran for 38 hours with a average wear rate of less than $2x10^{-6}$ mm^3/m then ran for a further 13 hours at around $10x10^{-6}$ mm^3/m, with no interruption in sliding or change of parameters between these conditions. The wear rates of other MY7D samples with the same conditions were as low as $1x10^{-6}$ mm^3/m (a stable wear rate maintained during a 33 hour test), thus the total range of MY7D wear rates varied over an order of magnitude. The performance of batch 946P was consistently superior to that of batch 359Q in tests at higher current and higher speed, see fig (5.1). Whilst preparing the samples it was noticed that batch 946P was much harder to cut and grind than batch 359Q, and had a slightly higher density (see appendix A), suggesting that there is indeed a fair degree of variation in the carbon base.

From the point of view of the dynamic performance of the pantograph (see chapter 2), it is important that the weight of the strip should be minimized. It is interesting to note that the difference in density of the commercial strips is quite significant, ranging from 1.92g/cm^3 for the Ringsdorff sample, through 2.4 to 2.9g/cm^3 for MY7D, to 3.21g/cm^3 for the Schunke & Ebe strip, see appendix A.

Microscopic examination of the worn surfaces of collector strips has revealed some differences between those used in railway service and the samples from the wear machine, see figs (5.2) to (5.4). Most significantly, the wear machine samples show a relatively large number of metallic particles, apparently copper, embedded in the sliding surface. The size of these particles is typically 10μm across, though there are some much larger patches, and the density of cover of the surface of up to about 4%.

83

Particles of a similar size and density are also visible in non-impregnated strip samples used on the wear machine, indicating that the particles have been transferred from the copper surface, from where they have been dislodged, rather than being visible evidence of the impregnating metals. The test conditions prior to each strip being removed from the wear machine were not always identical, but were typically 60km/h, 50A, 50N. The used strips from railway service show very little evidence of this picking of the copper. However, Williamson [57] does report evidence of copper picking by the strip in his experiments with the push-pull test rig.

Heat treatment of carbon produces a more highly graphitized material, depending upon the kilning temperature [24]. The effect on the worn base carbon materials J1A, J2A and J3A is visible even by eye alone. Under the microscope, the worn surface of a sample of J1A, heat treated at only 1600°C, appears rough and multi-facetted compared with that of J2A and especially that of J3A, kilned at 2000°C and 2400°C respectively, see fig. (5.4). Heat treatment also has an effect on the hardness of the carbon; the higher the kilning temperature, the softer the material, see appendix A. The worn surface of the J3A sample is very smooth, with very little observable copper, whereas bright copper fragments up to 10μm across can be seen in J1A, and are estimated to cover about 2% of the total sliding surface. Obviously, there must have been some abrasive wear of the copper during the test run with this sample. The surface is quite heavily pitted, these regions being up to about 40μm across and 30μm deep. The surface of JBC, although cracked and pitted, appears more homogeneous in nature than J1A, though it still contains copper fragments.

There do seem to be visible differences between the sliding surfaces of the copper/lead impregnated strips when viewed under the microscope. The surfaces of MY7D batches 946P and 359Q are fairly similar, with a high instance of shallow cracking and pitting, but not much visible copper. The

Ringsdorff and S & E samples show the same features, although the latter has a noticeably higher quantity of copper fragments in the surface, see fig. (5.3). In contrast, the surfaces of the used strips supplied by BR, taken from a class 86 locomotive, appear much smoother with virtually no surface damage or visible copper, see fig. (5.2c).

However, the MY7D sample used in a wear machine dwell-mode test at 200A, 50N, 120km/h, see in fig. (5.3c), does appear more similar to the strip from railway service, except for some damage to the trailing edge, shown in fig. (5.3d), with patches of copper clearly visible. It does appear likely, therefore, that the sliding conditions with the wear machine operating in the dwell-mode are more prototypical than with continuous sliding, judging by the appearance of the strip, and by the fact that the dwell-mode strip wear results obtained by Klapas et al [2] are closer to the service values supplied by Dixon [23]. This may be due to the presence of an abrasive oxide layer on the disc surface in the dwell mode only, similar to that believed to exist on the contact wire, that is allowed to build up during the dwell time between strip passes. There is, however, still a discrepancy between the strip wear (where the increased level of arcing due to contact making and breaking may artificially increase the wear rate) in dwell mode and the those found in railway service. The higher wear found in service may be due to environmental factors, as mentioned in section 2.2.2.

5.2 COPPER WEAR

The wear of the copper wire, and its possible causes, is discussed in detail in Chapter 3. For reasons stated in Chapter 3, very few results for the wear of the copper disc were recorded. These were for MY7D only, and are not

considered significant enough to provide any deeper insight into wire wear than that already provided by Klapas et al [1,2]. They are however reproduced here for purposes of comparison and to provide an indication of the relative performance of the two techniques of measurement employed, namely the indentation and LVDT methods described in Chapter 4.

Table 5.2 lists all the recorded results using the LVDT method, and includes for purposes of comparison wear depth measurements taken using the indentation method where available. Not all the test conditions are supplied because the equipment was under test, and the conditions were being varied during some of the runs. As can be seen for the tests where figures are available, there was generally poor agreement between the two sets of measurements for the same test run. The results from one test where there was fair agreement, test 112, are given in detail in table 5.3. The plot of the LVDT measurements, averaged over all the readings given in table 5.3, can be seen in fig.(4.26). A particular distinguishing feature of the LVDT measurements taken after this test is that the standard devation of the measurements from the six revolutions was only 0.04μm, much lower than average, and seems to suggest that this set of results was not subject to the drift problems that may have affected some of the other tests.

All the indentation measurements taken during the tests are listed in table 5.4. As described in chapter 3, four indentations were made around the sliding surface at 90° intervals. In general, there is poor agreement between resultant worn depth measurements made at different indentation positions, which is believed to be due to the difficulty in determining the true diameter of the indentations after a test run.

SYMBOL (fig 5.1)	TYPE/BATCH	DESCRIPTION	ESTIMATED %Cu PICKUP
✳	JBC	Base carbon	1%
+	J1A	Base carbon/1600°C kilned	2%
X	J2A	Base carbon/2000°C kilned	0.1%
λ	J3A	Base carbon/2400°C kilned	0.4%
Y	JCO	Base carbon impregnated with copper	0.2%
□	JAN	Base carbon impregnated with antimony	not known
O	JCL	Base carbon impregnated with carbon & lead	2.5%
△	Nickel-Graphite	Experimental material supplied by BR	nil
▼	MY7A/316		0.2%
▲	MY7D/359Q	Commercial copper/lead impregnated carbon	0.2%
▼	MY7D/946P	" "	0.4%
◆	MY7D/316	" "	3%
✴	MY7D*/	" "	5%
✳	MY7D/Sheffield	" "	not known
●	Ringsdorff/ VH83N3	" "	0.2%
■	Schunke & Ebe	" "	1.5%

All samples. dimensions:

Length (in direction of sliding):   20 mm
Width   (transverse direction):   31 mm *except 19mm for
                                          MY7D (batch unknown)
Unworn thickness: ≈ 18 mm

TABLE (5.1)   COLLECTOR STRIP SAMPLES TESTED

87

Test No.	v (km/h)	I (A)	test duration (mins)	mean displacement shoulder (µm)	mean displacement surface (µm)	mean difference (µm)	SD	mean temp (°C)	mean wear LVDT method	mean wear indentation method
109	– running in –			10.27	16.65	6.38	0.26	19.28	0.22	
110	– running in –			31.98	26.1	-5.88	0.13	20.06		
111	120	120		16.14	8.29	-7.76	0.11	18.67	1.9	14.4
112	120	50	920	27.99	10.28	-17.68	0.04	19.54	9.9	7.5
113	150	50	– data corrupted on floppy disc (test abandoned) –					–		4.1
114	180	50	68	25.84	6.74	-19.07	0.3	18.51		-1.67
115	150	100	524	29.29	10.92	-18.32	0.13	18.28	-0.7	3.44
116	150	150	5	31.97	12.59	-19.34	0.25	19.12	1.1	-0.8
117	180	100	563	32.83	13.37	-19.42	0.2	19.95	0.1	0.37
118	250	100	219	24.95	43.05	18.1	0.98	18.44		
119	– running in –			21.22	26.98	5.62	0.25	19.33		6.3
120		50		24.12	33.99	9.42	0.48	20.71		0.7

Notes

1. displacement measurements are values taken after stated test

TABLE (5.2) DISC WEAR MEASUREMENTS – LVDT METHOD

88

| | shoulder | | surface | | mean | SD |
	mean displacement (μm)	SD (μm)	mean displacement (μm)	SD (μm)	difference (μm)	(μm)
PR112a	15.06	2.94	7.45	2.55	-7.6	1.86
PR112b	16.92	3.94	9.13	3.18	-7.8	1.84
PR112c	16.45	3.25	8.58	2.58	-7.87	2.06

(Test 112 run; v=120 km/h, I=50 A dc, L=5 kg, 920 mins)

PR113a	23.21	3.64	5.52	3.8	-17.6	2.02
PR113b	27.87	3.92	10.17	2.69	-17.7	2.07
PR113c	28.62	4.32	10.85	3.09	-17.7	1.99
PR113d	27.11	3.7	9.41	2.9	-17.7	1.97
PR113e	29.16	3.79	11.45	2.54	-17.7	1.97
PR113f	27.18	4.81	9.54	3.6	-17.6	1.96

Notes

1. Each line represents one disc revolution of measurements (at approximately 410 positions around disc).

2. Two sets of measurements are given: PR112a,b,c, taken before test 112, and PR113a,b,c,d,e,f, taken after test 112. The mean wear for that test was (using the averages of the mean difference readings):

$$17.67 - 7.76 = 9.91\mu\text{m}$$

This corresponds to a disc AWR of 38.4μm/hr

3. A plot of these measurements is shown in fig. (4.26)

TABLE (5.3)   EXAMPLE OF A SERIES OF LVDT MEASUREMENTS

Indentation nos.

Test no.	I		II		III		IV		mean
	δd	wear	δd	wear	δd	wear	δd	wear	wear
111	450	15.05					721	13.77	14.4
112	348	6.43	762		673		643	8.66	7.5
113	284	3.18	744	2.17	615	6.05	592	5.03	4.1
114	637		757	-1.5	638	-2.3	604	-1.2	-1.67
115	607	3.04	679	9.0	632	0.52	592	1.2	3.44
116	575	3.0	724	-5.02	652	-1.97	584	0.72	-0.8
117	578	-0.24	723	0.15	639	1.32	582	0.23	0.37
118	723		692		904		825		
119	632	10.6	625	7.15	875	4.27	785	5.33	6.8
120	613	2.53	618	0.6	881	-0.92	773	1.45	0.9
121	637	-2.43	664	-4.7	894	-1.85	772	0.15	-2.2

Notes

1. all dimensions in μm

2. indentations 90° apart around disc periphery

3. δd is indentation diameter, measured after each test

4. a line indicates a new indentation made at that position

TABLE (5.4) · DISC WEAR MEASUREMENTS : INDENTATION METHOD
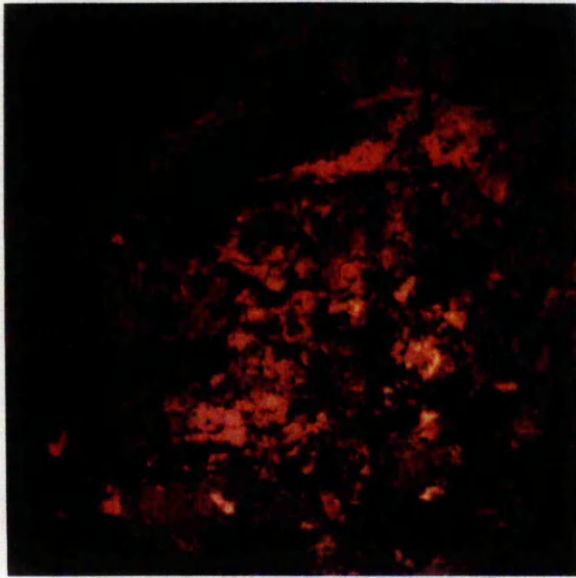
MY7D 946P
(continuous mode tests)

MY7D 359Q
(continuous mode tests)
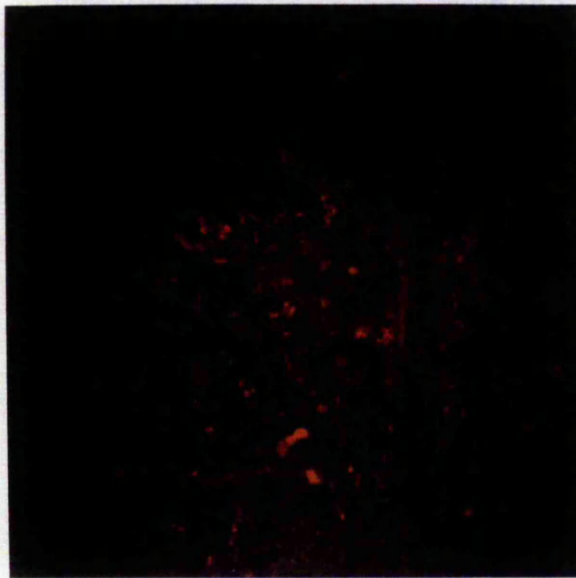
MY7D
(railway service)
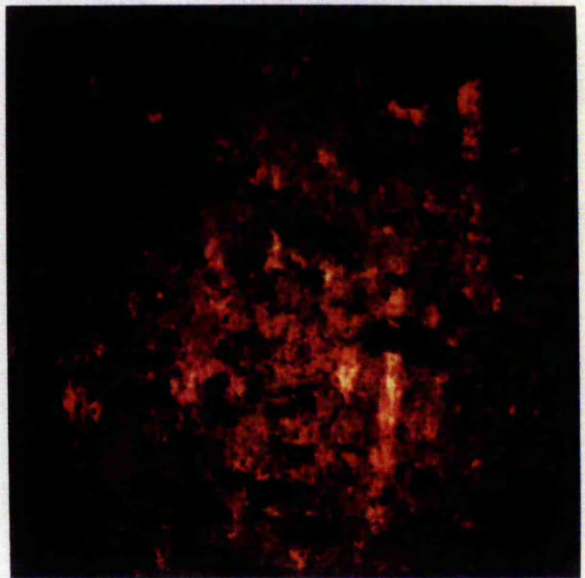
MY7D
(continuous mode tests)

Fig. (5.2)   Collector strip sliding surfaces (magnification x40)

S & E
(continuous mode tests)

Ringsdorff
(continuous mode tests)

MY7D
(dwell mode tests)
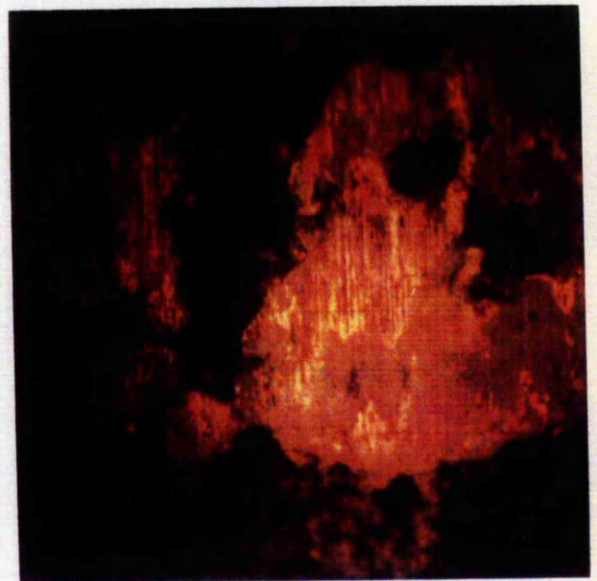
MY7D
(dwell mode tests)

Fig. (5.3)   Collector strip sliding surfaces (magnification x40)

J1A
(continuous mode tests)
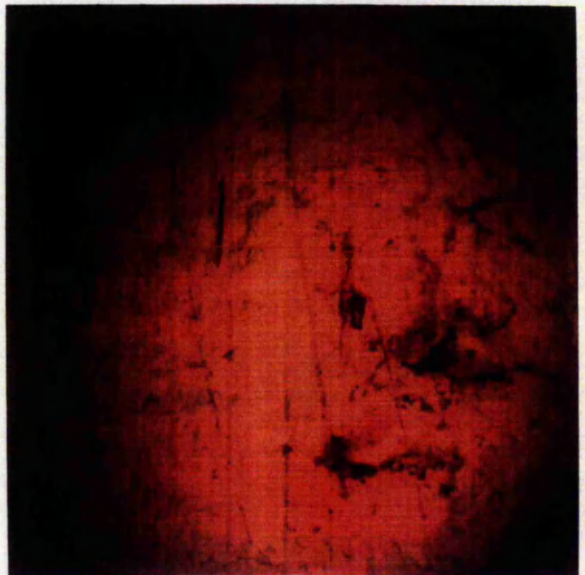
J3A
(continuous mode tests)

JBC
(continuous mode tests)

Nickel Graphite
(continuous mode tests)

Fig. (5.4)   Collector strip sliding surfaces (magnification x40)

CHAPTER 6

SUMMARY

This thesis describes an investigation into the electro-mechanical wear in the overhead current collection system. The contact materials are the copper overhead wire and the pantograph mounted collector strips. The main part of the work concerns the simulation of wear of the copper and a range of experimental carbon-based collector materials, and the dependence of the wear rate on sliding speed, contact force, and contact current. These materials include a range of base carbons fired at different temperatures to provide differing degrees of graphicity, and base carbons impregnated with a range of metals to improve their impact strength and increase their current ratings.

The developments in the design of the overhead line equipment and the nature of the contact materials have been presented as background information. The major advance in the design of this equipment was the replacement of low voltage (high current) systems by more economical light-weight high voltage equipment. This allowed the use of low wear carbon based collector strips in place of metal strips, not previously possible because of their inferior current rating and impact strength.

Although little experimental data on the wear of copper has been obtained, an examination of the nature of this wear has been carried out, based on the results from earlier measurements taken in the field and in laboratory simulations, and published information on the oxidation of copper. This has led to the suggestion that the wear of the copper wire is partly due to abrasion and partly due to

oxide removal, although the complex interaction of the different mechanisms of wear do not allow accurate prediction of wear performance. Exceptional circumstances may include the localized heavy wear found at "hard spots", accompanied by a peak in the contact force, where abrasive wear is thought to predominate, and the heavy wear found in some station areas, which may be predominantly oxidational as a result of the low train speeds (and therefore greater contact time) leading to higher wire surface temperatures.

To try and improve the simulation of collector strip wear and copper wear, certain improvements to the wear machine and the measuring systems have been carried out. Attempts to improve the performance at high speeds by reducing the vibration of the collector strip included the incorporation of resilient materials in the strip holder assembly, the replacement of damaged bearings in the strip holder arms, and the provision of a trailing angle to the strip relative to the sliding surface of the copper disc, but all were limited in their success. The cause of the problem was identified as being the resonant vibration at various discrete frequencies (independent of disc rotational speed) of the strip holder, probably excited by oscillating frictional forces at the sliding surface. This could be cured by providing a low mass strip holder with the contact force provided by a spring rather than a dead-weight, though this would require significant modifications to the wear machine and would make the preparation of the strip samples even more difficult, as they would have to be machined on all four sides as well as on the sliding surface.

Three methods of copper wear measurement were assessed: making indentations in the copper surface and noting the change in diameter after a wear test; using an optical lever technique; and finally, using multiple LVDT measurements. The latter two methods involved measuring the relative displacement between the wear track and an adjacent non-wearing shoulder. The LVDT technique was adopted as the most hopeful, although there was a significant deterioration

95

in resolution after the main bearings of the copper disc were replaced, due to the higher leadout (out of true) of the new bearings.

A micro-computer based data-logger was designed and constructed, enabling automatic recording of the temperatures of the wear machine frame, disc and strip, the strip displacement, the contact voltage, arc light emission, and the drive motor load (to give an indication of the frictional force).

The results of the wear tests on the range of collector materials are presented and discussed. Most strips produced time-varying wear rates under nominally constant operating conditions, presumably due to their inhomogeneous nature. The wear rates of different samples of MY7D grade (copper-lead impregnated) under the same conditions of sliding varied over more than an order of magnitude. No type of strip exhibited consistently superior wear performance over the range of sliding conditions. The nickel-graphite samples performed poorly, with severe wear occurring at even moderate levels of speed, contact force and current. There was visible evidence of copper "picking" by strips with the wear machine operating in the continuous sliding mode, though this effect was not apparent in the case of dwell mode (where the dwell time between train passes is simulated) test samples and a sample from railway service. It would appear that the wear of both the collector strip and the copper is best simulated in dwell mode tests, rather than continuous mode. The discrepancy between wear rates obtained using the wear machine and wear rates measured in service is still not fully explained, except in terms of environmental differences.

REFERENCES

1   Klapas D, Benson FA, Hackam R, Evison PR: Wear in simulated railway overhead current collection systems, *Wear,* **126,** 2,(1988), pp 167-190.

2   Klapas D, Benson FA: Wear of current-carrying conductors in relative motion. Final Report, The University of Sheffield, (December 1980).

3   Lyon EC: AC Suburban electrification - British Railways, Eastern Region, *J. Inst. Loco. Engr,* (1966), pp 585-672.

4   Sell RG: British Railways research on current collection, *The Railway Gazette,* **122,** (1966), pp 312-320.

5   Goldring AG, Suddards AD: Development of overhead equipment for British Railways 50Hz electrification since 1960, *Proc. IEE,* **118,** 8, (1971), pp 999-1011.

6   Sell RG, Prince GE, Twine D: An experimental study of the overhead contact system for electric traction at 25kV, *Proc. I Mech. E.,* **179,** 25(1), (1965), pp 765-781.

7   Gostling RJ, Hobbs AEW: The interacton of pantograph and overhead equipment: practical applications of a new theoretical technique, *Proc. Inst I Mech E,* **197C,** (1983), pp 61-69.

8   Heyda PG, Thackray GJ: Computer evaluation of electric railway catenary equipment by the method of normal modes, *IEEE Trans. Ind. Appl. (USA),* IA-17, 3, (May-June 1981), pp 321-329.

9   Boissonnade P, Dupont R: The electric traction fixed equipment and current collection, *French Railway Techniques,* (1978), pp 58-64.

10   Cronin JE, Waldrum JH: Great Northern suburban electrification Part 2: fixed equipment, *REJ,* (November 1974), pp 30-33.

11   Ebeling H: Current collection at high speeds. Problems of catenaries and pantographs. IRCA-UIC "High Speeds" Symp., Vienna (1968).

12   Boissonnade P, Dupont R: Current collection with two-stage pantographs on the Paris-Lyon line, *Rlwy Gaz. Int.,* **133** (10), (Oct. 1977) pp 392-395.

13   Rahn T, Spöhrer W: Development of new high-speed motor train units to be operated on the German Federal Railway Network, *Proc. Instn. Mech. Engrs.,* 202 (D2), pp 125-139.

14   Kendall PW, McNab IR, Wilkin GA: Recent developments in current collection, *Phys. in Technology,* (May 1975), pp 117-126.

15   Taylor K: British Railways' experience with pantographs for high-speed running, *J. I. Mech. E. Rlwy. Div.,* RDP 8/71, (1971) pp 349-373.

16   Coxon DJ, Gostling RJ, Whiteland KM: Evolution of a simple high-performance pantograph, *Rlwy. Gaz. Int.,* **136** (1), (1980), pp 44-47.

17   Betts AI, Gostling RJ, Hobbs AEW: Development of a pantograph for high speed running on economic overhead equipment. Int. Conf. on Electric Rlwy. Systems for a New Century, London 22-25 September 1987 IEE, pp 209-213.

18   Boissonnade P, Dupont R: Prospects for 300 km/h with 25kV 50Hz overhead line equipment, *Revue Générale des Chemins de Fer,* (September 1970), pp 492-505.

19   Coget G: New pantograph for TGV-Atlantique (300 km/h), *Rail Engineering International,* 3, (1986), p 16.

20   Daffos J, Gardou M: Recent research on SNCF pantographs, *Revue Générale des Chemins de Fer,* 105, (October 1986) pp 521-528.

21   Rahn T: The German Federal Railway High Speed Train, *Technica* (Switzerland), 35, 23, (5 Nov. 1986), pp 47-51.

22   O.R.E: Wear of contact strips and of the overhead equipment when using metallic or composite contact strips. Q A69, Rpt No 6 (final report), Utrecht, April 19971.

23   Dixon DL: Development with carbons for current collection, *I. Mech. E., REJ,* 2 (5), (September 1973), pp 46-59.

24   Lancaster JK: Dry bearings: a survey of materials and factors affecting their performance, *Tribology,* (December 1973), pp 219-251.

25   Souch DJW, Taylor G: The develpment of the pantograph for high-speed collection, *J. I. Mech. E. Rlwy. Div.,* **RDP 10/71,** (1971) pp 406-436.

26   Morganite Electrical Carbon Ltd: Carbon collectors for electric railways and trains, application data. Publicity document ADS 6, (mid. 1970's).

27   O.R.E: The effect of wear on pantograph contact strips and contact wires. Q A2. *Bull. O.R.E. Inst. Union of Rlwys.,* (July 1958), pp 11-14.

28   Ferguson IC (Morganite): Design of pantographs utilising carbon strips and survey of performance. Morganite Electrical Carbon Ltd. report L/80005/C (February 1980).

29   Kasperowski O: Contact materials for current collectors of electric motive power units, *Monthly Bullletin of IRCA*, **XV** (No 2), (1964), pp 47-69.

30   Jones CR: Beyond 200 km/h: Engineering options. Implications of increased speed for the design of overhead equipment. Railway Engineers Forum RD/CRJ/10.84.

31   Boocock D, King BL: The development of the prototype advanced passenger train, *Proc. Inst. Mech. Engrs. Rlwy. Div.*, **196**, (1982), issue 1, pp 20-31.

32   Iwase M, Saito T, Kokubu K: Pantograph contact strip (2) - development of new contact strip for the new Tokaido line, *Q. Rep. Railw. Tech. Res. Inst., Japan Nat. Rlwys*, 8 (3), (1967), pp 132-135.

33   Iwase M, Saito T, Kokubu K: Contact strip of pantograph for the new Tokaido line (Report 1) - problems and laboratory test, *Q. Rep. Railw. Tech. Res. Inst., Japan Nat. Rlwys.*, 5 (1), (1965), pp 5-10.

34   Teraoka T: Measurement of grease on the contact surface of overhead wires, *Q. Rep. Railw. Tech. Res. Inst., Japan Nat. Rlwys.*, **19** (3), (1978), pp 145-146.

35   Casstevens JM, Rylander HG, Eliezer Z: Influence of high velocities and high current densities on the friction and wear behaviour of copper-graphite brushes, *Wear*, **48**, (1978), pp 121-130.

36   Oda O: Wear of current collecting system in Shinkansen, *Q. Rep. Railw. Tech. Res. Inst., Japan Nat. Rlwys.*, **25** (2), (1984) pp 72-75.

37   Morganite Electrical Carbon Ltd.: Carbon Brushes and Electrical Machines, (Morganite Electrical Carbon Ltd., 1978).

38   Joglekar GD: Carbon brushes for rotating electrical machinery II., *ISI Bull.*, **24** (No 11), (November 1972), pp 481-486.

39   Savage RH: Graphite lubrication, *J. Appl. Phys.*, 19 (1), (January 1948), pp 1-10.

40   Lancaster JK: Carbons and graphite in tribology, *R.A.E. Tech. Memo MAT*, **198**, (October 1974) pp 1-25.

41   Deacon RF, Goodman JF: Lubrication by lamellar solids, *Proc. Roy. Soc.*, A 243, (1958) pp 464-482.

42   Shobert EI: Carbon brushes: the physics and chemistry of sliding contacts. (Chemical Publishing Co., New York, 1965).

43   Shobert EI: Carbon graphite and contacts. Proc. 1974 Holm Seminar on electrical contacts, pp 1-19.

44   Holm R: Electric Contacts Handbook. (Springer-Verlag, Berlin 1958).

45   Spry WJ, Scherer PM: Copper oxide film formation at a sliding carbon copper interface, *Wear*, 4, (1961), pp 137-149.

46   Lee PK: High current brush material development II. Metal-solid lubricant coated wires.   26th Ann. Holm Conference 1980.   *IEE Trans CHMT-4, 1*, (March 1981), pp 114-121.

47   Sims RF: The wear of carbon brushes at high altitudes, *Proc. IEE*, (Part 1), (1953), pp 183-188.

48   Pedelty JM: Carbon as a current collecting material, *Mining Technol. (GB)*, 57 (662), pp 470-472, 474, 476.

49   Markus A: Operating experience with the fringe fiber brush, *Wear*, 78 (1,2), (1982), pp 93-107.

50   Shobert EI: Carbon brush friction and chatter, *Trans. AIEE, Power. Apparatus & Syst.* (June 1957), pp 268-275.

51   Betts AI, Holmes R, Hall JH: Defining and measuring the quality of current collection on overhead electrified railways.   Int. conf. on electric railway systems for a new century, IEE London, 22-25 September 1987, 279, pp 214-217.

52   Lancaster JK: The influence of arcing on the wear of carbon brushes on copper, *Wear*, 6, (1963), pp 341-352.

53   Dixon DL: Wear associated with the collection of electric traction current from overhead systems. Symposium on Tribology in Railroads, (February 1969).

54   Evans UR: An introduction to metallic corrosion. (Edward Arnold, 3rd edition, 1981).

55   Shreir LL (ed):   Corrosion, Vol. 1 Metal/Environmental Reactions. (Newnes-Butterworths, 1976, 2nd edition).

56   Yang SJ: Contact wire wear measurement.   Tech. Note 1/71/OH (R), RTC Derby, British Railways, (July 1971), pp 1-15.

57   Williamson PK: The effect of current and dwell time on the low speed wear of copper overhead wire. Internal Memo IM TRIB25, RTC, Derby, British Railways, (July

1976), pp 1-5.

58   O.R.E: High power traction current collection at high
      speed. Q A129, Rpt I, (1976), pp 1-29.

59   Kamiya A: Measurement of contact wire wear by laser in
      the daytime, *Q. Rep. Railw. Tech. Res. Inst. Japan Nat.
      Rlwys.*, 20 (3). (1979), pp 117-121.

60   Fujii Y: Development of aluminium contact wire with
      steel-core, *Q. Rep. Railw. Tech. Res. Inst. Japan Nat.
      Rlwys.*, 27 (No 2), (1986), pp 61-65.

61   Carlson LE, Griggs GE: Hard alloy aluminum in contact
      wires - an engineering feasibility study. IEEE 1981
      Joint ASME/IEEE Railroad Conf.

62   Cramp W: The wear of trolley wires. ERA Rpt.,
      University of Birmingham, March 1934 - September 1936.

63   Iwase M: Current collection by the pantograph and its
      wear (Part I), *Q. Rep. Railw. Tech. Res. Inst., Japan
      Nat. Railways,* 1 (2), (1960), pp 29-32.

64   Pritchard C: Low speed wear of alternative pantograph
      collector materials.   Internal Memo IM TRIB 15, RTC
      Derby, British Railways, (November 1974), pp 1-17.

65   Rönnquist A, Fischmeister H: The oxidation of copper,
      J. Inst. Met., 89, (1960-61), pp 65-76.

66   Evans UR: An Introduction to Metallic Corrosion,
      (Edward Arnold, 3rd edition, 1981).

67   Fontana MG, Greene ND: Corrosion Engineering, (McGraw-
      Hill, 1978).

68   Rönnquist A: The oxidation of copper: A kinetic and
      morphological study of the initial stage, *J. Inst.
      Met.,* 91, (1962-63), pp 89-94.

69   Evans UR: The corrosion and oxidation of metals.
      (Arnold, 1960).

70   Russell JA, Burton RA, Ku PM: Atmospheric effects on
      friction and wear of oxidized copper, *Wear*, 8, (1965),
      pp 173-187.

71   Tylecote RF: Review of published information on the
      oxidation and scaling of copper and copper-base alloys,
      J. Inst. Met., 78, (1950-51), pp 259-300.

72   Campbell WE: The lubrication of electrical contacts,
      Proc. Holm Conf. on Electrical Contacts, 1977, pp 1-17.

73   Vernon WHJ: *J. Inst. Met.,* 49, (1932), p 153.

74   Stott FH,   Glascott J, Wood GC: Models for the

generation of oxides during sliding wear, *Proc. R. Soc.*, London, Ser. A, **402**, (1985), pp 167-186.

75   Batchelor AW, Stachowiak GW, Cameron A: The relationship between oxide films and the wear of steels, *Wear*, **113**, (1986), pp 203-223.

76   Quinn TFJ: Oxidational wear, *Wear*, **18**, (1971), pp 413-419.

77   Wilson JE, Stott FH, Wood GC: The development of wear protective oxides and their influence on sliding friction, *Proc. R. Soc.*, London, Ser. A, **369**, (1980), pp 557-574.

78   Quinn TFJ, Sullivan JL: A review of oxidational wear. Int. Conf. on Wear of Materials, St Louis, Missouri, April 25-28, 1977, ASME, pp 110-115.

79   Sullivan JL, Hodgson SG: A study of mild oxidational wear for conditions of low load and speed, *Wear*, **121** (1), (1988), pp 95-106.

80   Failkov AS, Tokarev BF, Zaichikov VG, Platov VS, Kozlov VV, Bugacheva NM, Skvortsov VV, Yaroshenko VI: Ways of improving the wear resistance of commutator copper with high current densities in metal-containing brushes, *Sov. Electr. Eng., (USA)*, **52** (11), (1981), pp 122-126.

81   Lancaster JK: The influence of the conditions of sliding on the wear of electrographite brushes, *Brit. J. Appl. Phys*, **13**, (1962), pp 468-477.

82   Holmes R, Thomas AL, Tansley J, Jenkins M: Wire wear measurements at Rugeley and Barking neutral sections. Tech. Memo TM ETR 125, RTC Derby, British Railways, March 1980.

83   Carslaw HS, Jaeger JC: Conduction of heat in solids (Oxford University Press, 1959).

84   Klapas D, Benson FA, Hackam R: Simulation of wear in overhead current collection systems, *Rev. Sci. Instrum.*, **56** (9), (September 1985), pp 1820-1828.

85   Manabe K, Morikawa T: Study on vibration phenomena of power collecting system with distributed parameter model, *Q. Rep. Railw. Tech. Res. Inst., Japan Nat. Rlwys.*, **22**, (2), (June 1981), pp 63-69.

86   Bowden FP, Tabor D: The friction and lubrication of solids (Part II). (Oxford University Press, 2nd edition 1971).

87   Dridzo ML, Pytkov Yu N: Vibration-resistant brush units for electric machines, *Sov. Electr. Eng. (USA)*, **51** (8), (1980), pp 31-34.

88   Joglekar GD: Rotating electrical machines and brush operation VII. Fictional characteristics of carbon brushes, *Electr. India,* 21 (9), (1981) pp 11-18.

89   G.E. Report: Power collection by sliding contact methods for high speed guided vehicles. US DoT Contract FR-9-0023, (August 1969), pp 1-64.

90   Holm R: Electric Contacts, Theory and Application. (Springer-Verlag, Berlin, 1967).

91   Williamson JBP, Allen N: Thermal stability in graphite contacts, *Wear,* 78, (1982), pp 39-48.

92   Marshall RA: The mechanisms of current transfer in high current sliding contacts, *Wear,* 37, (1976), pp 233-240.

93   Chen CP, Burton RA: Thermoelastic effects in brushes with high current and high sliding speeds. Proc. 9th Int. Conf. on Electrical Contacts, Chicago 11-15 September 1978, pp 571-575.

94   Dow TA, Stockwell RD: Experimental verification of thermoelastic instabilities in sliding contact, *J. of Lubrication Technol.,* (July 1977), pp 359-364.

95   Barber JR, Beamond TW, Waring JR, Pritchard C: Implications of thermoelastic instability for the design of brakes, *J. Tribol. Trans ASME,* 107 (2), (April 1985), pp 206-210.

96   Broniarek CA, Taylor OS: Mechanical stability of solid brush current collection systems, *IEEE Trans. Power Appar. & Syst. (USA),* PAS-99 (6), (November-December 1980), pp 2413-2421.

97   Reichner P: Brush contact on eccentric slip rings, *IEEE Trans. Power Appar. & Syst. (USA),* PAS-100 (1), (January 1981), pp 281-287.

98   Beverley P: How to get full 12-bit value from your ADC, *Acorn User,* (March 1984), pp 115-120.

99   Evison PR, Klapas D, Pratt JMK: Railway overhead current collection: a data logger for a wear simulator. 23rd UPEC Conference, Trent Polytechnic, 20-22 September 1988.

100   Williamson PK: Further developments of alternative pantograph collector materials. BRB R&D Div. Process Technol. Group, Int. Memo IM TRIB 34, January 1979.

APPENDIX A

Physical properties of collector strip materials

Bulk Density Measurments

Strip material	Bulk Density (g/cm³)
JBC	1.91
MY7D/316	2.4
MY7A/316	2.4
MY7D/359Q	2.7
MY7D/946P	2.9
Ni-graphite	6.15
Ringsdorff	1.92
S & E	3.21

Experimental Pantograph Materials. All based on LP71J(BK482/18)

Physical Properties

Material[1]	Treatment	Hardness[2]	Resistivity[3] (μΩm)	Bulk Density (g/cm³)	Bend-strength (kg/cm³)	Porosity (%)	Analysis (%) Cu	Pb	Sb
JBC	Nil	85/92	35/35	1.73	440/520	–			
J1A	hr, 1600°C	83/89	36/37	1.72	370/370	–			
J2A	hr, 2000°C	85/85	35/35	1.75	350/370	–			
J3A	hr, 2400°C	70/67	22/22	1.76	330/360	–			
JCL	Cu-Pb impreg.	87/90	5.5/5.6	2.34	930/880	0.26	19.0	7.3	
JCO	Cu impreg.	89/92	17/17	2.11	650/670	4.92	17.3		
JAN	Sb impreg.	97/94	11/11	2.22	1050/970	0.24	19.7		19.7

1. All CY3 base, no wax.

2. Scleriscope, modified hammer.

3. 4 point method.

RAILWAY OVERHEAD CURRENT COLLECTION :
A DATA LOGGER FOR A WEAR SIMULATOR

P R Evison, D Klapas, J M K Pratt
Department of Electrical and Electronic Engineering
Trent Polytechnic, Nottingham

INTRODUCTION

As part of a British Rail sponsored investigation into the wear characteristics of pantograph carbon strips and the overhead copper wire, a wear simulator has been constructed (1).

The wear rates of both the contact wire and the contact strips are simulated with a revolving copper disc (12.7 mm thick, 500 mm diameter) representing the contact wire, and a shaped contact strip which is held stationary against the periphery of the disc. The disc temperature is regulated by a water cooling system.

Originally only carbon strip measurements (temperature and wear) from the simulator were recorded, using a two channel plotter. In addition, copper wear was measured using a "before and after" indentation technique. Although this enabled the wear measurements to be carried out for various values of sliding speed, current and contact force, it did not provide sufficient data to allow a more detailed analysis and prediction of the performance of the range of carbon materials. An 8 channel data logger has been developed to extend the range of recorded data to include the contact voltage, contact friction and arc light emission. The system, based upon a BBC micro-computer, will allow relationships between the various measured signals to be examined both visually, using an X-Y plotter, and numerically using statistical analysis software.

As copper wear is generally very low (typically less than 1 um/hour) practical test durations can only be achieved if high resolution copper wear measurements can be made. A thorough investigation of practical copper wear measuring techniques has been carried out, and an LVDT (linear variable displacement transducer) multiple sampling system based upon the BBC micro-computer has been developed.

DATA LOGGER

This includes the analogue signal conditioning circuits for all 8 channels, providing all the necessary amplification and filtering, and the multiplexer and ADC (analogue-to-digital converter) together with its associated decoding and interfacing circuitry. Interfacing to the BBC is via the 1 MHz bus. See figure 1 for the block diagram.

Recorded Parameters

The data logger is required to record and display the following signals:

1. Wear simulator frame temperature - this signal is derived from an LM35DZ semiconductor temperature sensor, and is used for the temperature compensation of the strip displacement signal.

2. Cooling water temperature - also uses an LM35DZ sensor, positioned within the output flow pipe. This signal provides the disc temperature information, and is also used for temperature compensation.

3. Carbon strip temperature - a type K thermocouple housed in a steel probe inserted into a hole in the carbon. The amplified output signal is relative to ambient temperature.

4. Drive motor load - this is a dc signal proportional to the drive motor armature current, and provides an indication of the friction force between the carbon strip and the copper disc.

5. Strip displacement - an LVDT is in contact with the base of the strip holder, and after corrections (carried out in the software) to allow for the thermal expansion of the disc and the steel frame, the change in displacement is a measure of the wear of the strip only. This is because the disc wear is comparitively insignificant.

6. Arc light emission - a photodiode is mounted facing the trailing edge of the strip to give an indication of the prescence of arcing.

7. Contact voltage - a secondary brush is used to obtain the voltage drop between the strip and the disc. This signal is fed to a high voltage isolating amplifier (2). A precision rectifier and filter are included to enable ac voltages to be recorded, as well as dc.

An eighth spare channel is available, in addition to the 4 channel ADC inputs that the BBC provides, to allow future expansion of the equipment. The copper wear is determined using a "before and after" technique, rather than continuous monitoring (see later).

Circuit Description

The 7 input signals are low pass filtered and amplitude limited for transient suppression and are then amplified or attenuated as appropriate, to provide the required scaling. The multiplexer, under software control, passes the required channel via a low pass filter to the ADC for sampling. The filter is an active 2-pole Bessel type, selected for its fast settling time.

For the ADC, the successive approximation and the dual-slope integration types were considered. The latter has excellent noise rejection, as the integration time can be set so that it is equal to (or a multiple of) the period of the interfering signal eg mains pick-up. However, the ZN448, an 8-bit successive approximation device, was chosen for its low conversion time (9 us) and its low cost. By using the 1 MHz bus and an assembly language routine, sampling rates up to 16k samples/sec are possible.

An 8-bit device was chosen as a compromise between optimum resolution, sampling speed and economy of disc storage space. Each sample is stored as a single 8 bit byte.

The control section is based upon a decoder which produces the ADC and multiplexer control signals by decoding the addresses generated by the software.

Operation

The wear simulator can be operated with either continuous sliding or, to simulate the dwell time between train passes, intermittant contact.

In the continuous sliding mode, multiple sampling/averaging takes place continuously, with an averaged value for each channel stored, for example, every second. The data is also written to the screen after appropriate scaling.

In the intermittant mode the carbon strip is only sliding on the disc for 0.4 s, and is lifted clear for one minute during the intervening periods. The data logger is triggered by the passage of current operating a reed switch, so that sampling is carried out for the duration of the contact only. The ADC samples at its maximum rate, with only a single average value for each channel being recorded.

After completion of the test, the data may be retrieved off the disc, scaled and compensated if required, and then plotted using an X-Y recorder. Figure 2 shows a typical plot for a continuous sliding test, some channels ommitted for clarity. The plot indicates the relationships between the strip temperature (which is affected by short term variations in sliding conditions and the longer term changes in the coolant temperature), the contact voltage, and the drive motor load. Although the latter will be a function of the motor and simulator friction and windage as well as the contact friction, the former terms are approximately constant thus the drive motor load signal can be used as a qualitative guide to the contact friction. The wear rate of the strip can be calculated from the slope of the average strip displacement.

COPPER DISC WEAR MEASUREMENT

These measurements had previously been carried out using an indentation technique (1), where the diameter of a spherical indentation was recorded before and after a wear test, and the wear depth calculated. To improve the accuracy and resolution of wear measurement a dual LVDT system has been developed.

A non-wearing reference shoulder has been cut into the disc adjacent to the wear track. The LVDTs are firmly mounted together in a holder on the simulator frame, and two displacement measurements are carried out simultaneously, one on the reference shoulder, the other on the wear track. The change in the depth of the shoulder below the wear track, taken before and after a wear test, is equal to the worn depth. To improve the resolution of this measurement, and because wear is not completely uniform all the way round the disc, a multiple point sampling/averaging technique is employed. The displacement readings are sampled at several hundred positions around the disc, starting from a relocateable position. To prevent damage to the copper surface and to avoid any non-axial forces on the LVDT stylii and linear bearings, the stylii are retracted whilst the disc is being rotated to the next measuring position by the stepper motor, and also whilst a wear test is in progress. The retraction mechanism was originally a solenoid, but this was modified to a servo motor driven rack and pinion system to avoid the stylii being released onto the copper surface too vigourously. Filtered compressed air is blown onto the disc and onto the stylii whilst they are retracted in order to clear any dust particles, both surfaces having been cleaned beforehand with a soft clean cloth dampened with methylated spirits.

The two LVDT signals are fed via separate pre-amplifiers to a 2-way analogue switch followed by a common amplifier, demodulator and active filter so that any drift in these latter stages will affect both channels equally and thus cancel. OP07 and OP27 op-amps were used throughout. The overall drift introduced by the electronics was found to be negligible. The signal is then fed to the BBC's internal ADC for sampling. The recorded displacement and temperature signals for each disc position are the average of 16 samples; this gives an improvement in resolution by a factor 1/4 (3).

The entire system is under software control via the BBC's User Port to enable automatic operation. A set of measurements for one disc revolution takes about one hour, and to further improve the resolution of the wear measurement, this is repeated for 4 or 5 complete disc revolutions. In practise the resolution is limited by the linearity and repeatability of the LVDTs, and the roughness of the copper surface. Spherical LVDT stylii (3 mm diameter) are used, giving a wear measurement only along the centre line of the wear track. The LVDTs were calibrated in a jig and checked in situ by altering the temperature of the disc, whose radius varies by 4.5 μm/deg.C. Long term drift tests, with the stylii resting undisturbed on the disc, have been carried out lasting several days and over a wide range of ambient temperatures. The drift with temperature was within 0.1 μm/deg.C on the difference signal. In fact, all the measurements are carried out with the room temperature set at 19 +/- 1 deg.C, making temerature compensation unnecessary. An overall wear measurement resolution of better than +/- 1 μm has been obtained. Figure 3 shows a before and after profile for a wear test of 15 hours duration (test conditions: v=180 km/h, L=50 N, I=50 A dc). The traces represent the surface-shoulder difference before (top trace) and after (bottom trace) the wear test, the diffenece between the traces thus representing the worn depth of copper for that test. In this example the aveage worn depth was 9.9 μm, which compares with 6.4 and 8.9 μm measured at two positions on the sliding surface using the old indentation method.

CONCLUSIONS

A low cost computer-based data logger has been developed to enable the identification of the relationships between the parameters of the sliding contact. A more detailed analysis of these relationships is now possible using statistical software routines.

The disc wear measuring system has also been developed at relatively low cost and is capable of measuring the wear along the centre of the sliding track to a resolution of 1 µm, to permit faster and more reliable assessment of copper wear than was previously obtained.

REFERENCES

(1) Klapas D , Benson F A , Hackam R, "Simulation of wear in overhead current collection systems", Rev.Sci.Instrum. 56 (9) Sept.1985, pp1820-1828

(2) Horowitz P, Hill W, "The art of electronics" (Cambridge University Press, 1980)

(3) Beverley P, "How to get full 12-bit value from your ADC", Acorn User, March 1984, pp115-120
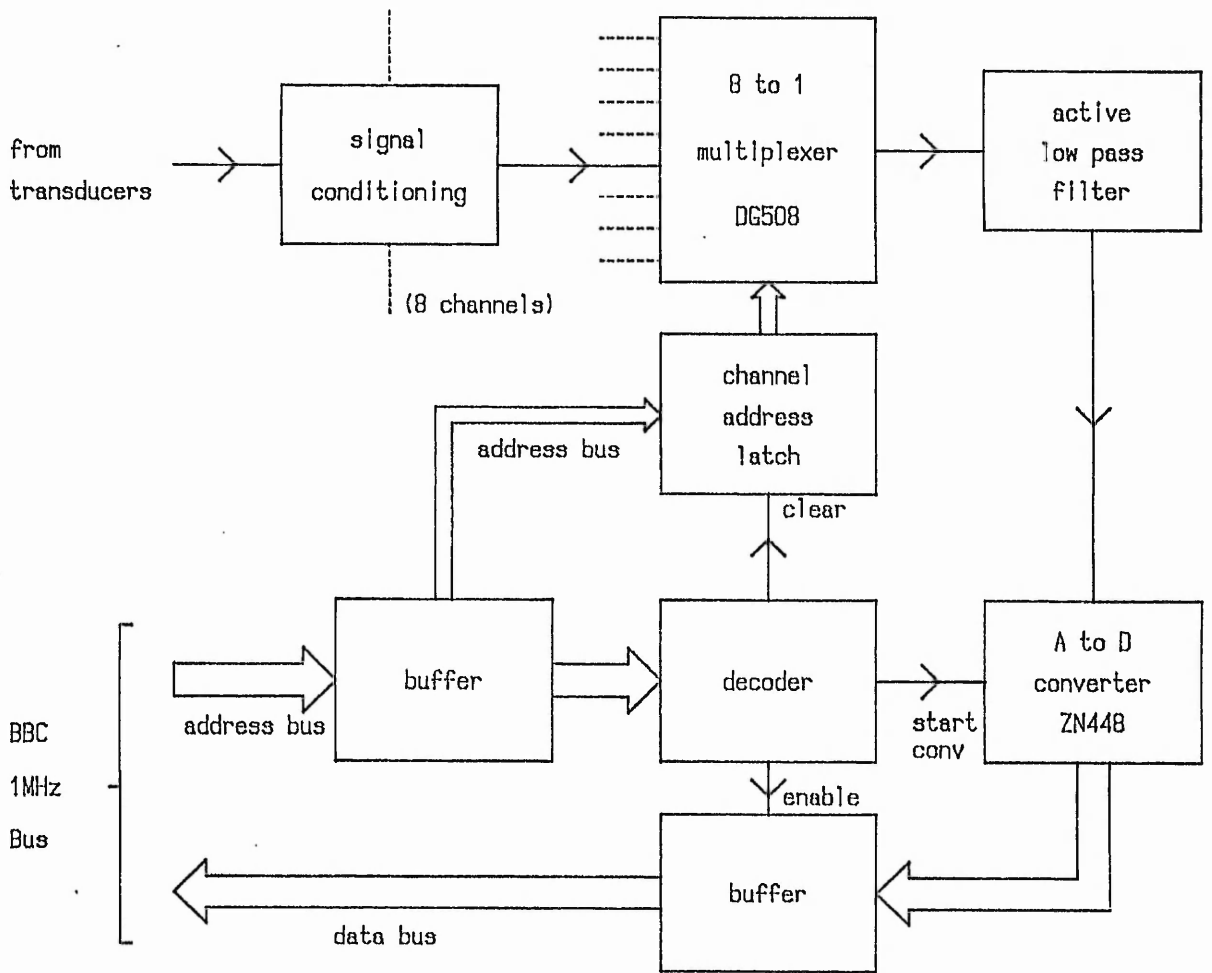
Figure 1.   Data logger block diagram

Speed	60 km/h	Mode	cont.
Load	50 N	T max	34 deg.C
Current	100 A dc	Traverse	off

WEAR TEST 21A1087

50 deg.C
250 deg.C
arb. units
250 μm
1.25 V

2 coolant temp. (deg.C)
3 strip temp. (deg.C)
4 drive motor load
5 strip displacement (um)
6 light emission
7 contact V (V)

5

4

2

7

3
6

0

each graduation = 10 mins

no. of samples = 4500   sample time = 2 secs   Time ⟶

150
mins
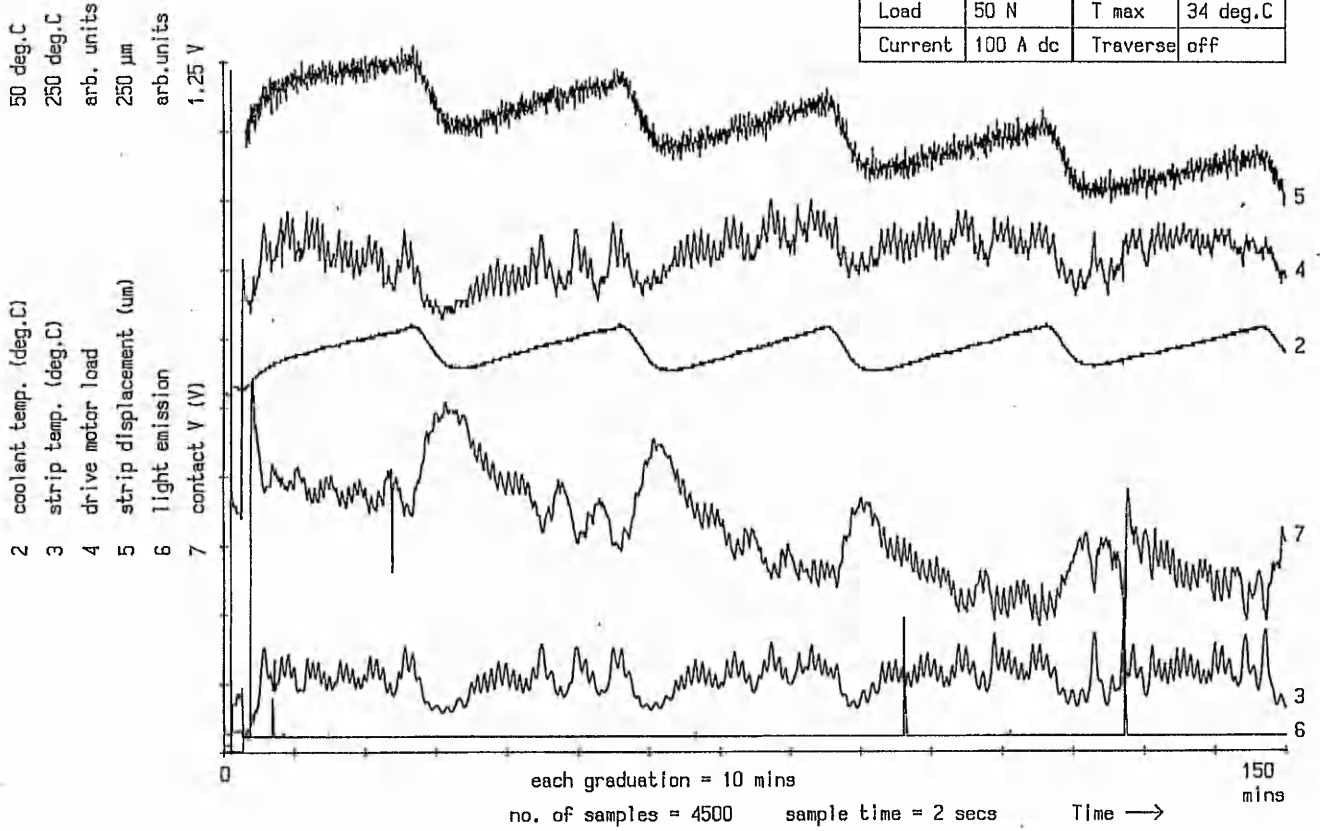
Figure 2.   Example of a wear test plot

rel. displacement (μm)

16

12

8

4

0

-4

-8

-12

-16

1 disc revolution
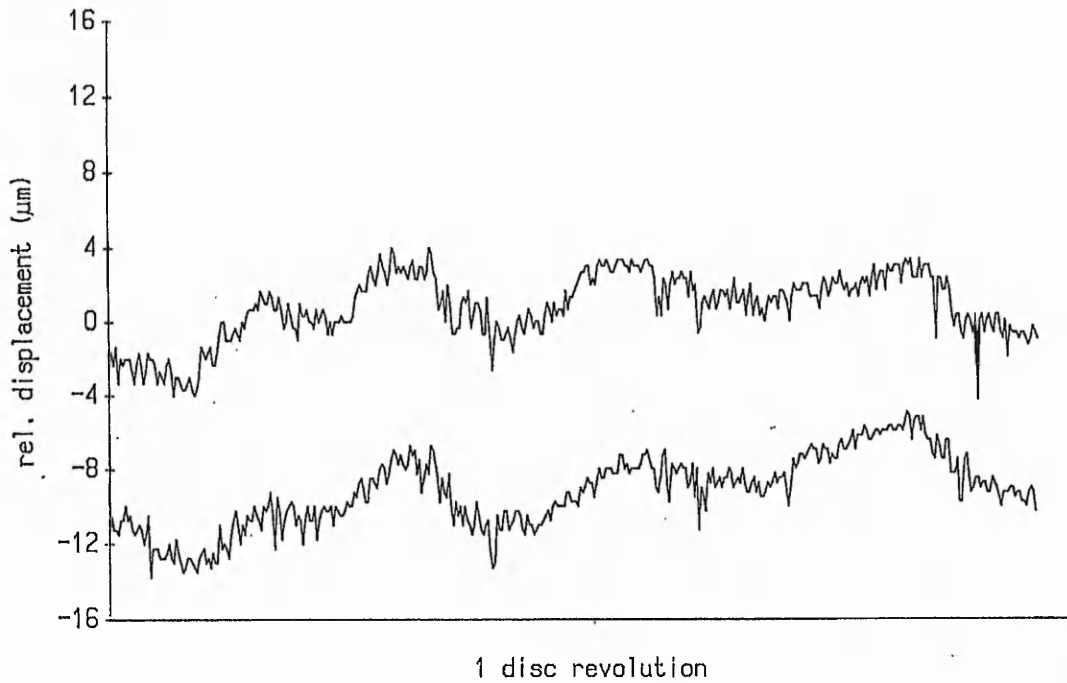
Figure 3.   Example of copper disc profiles